DEVELOPMENT OF ELECTROCHEMICAL BIOSENSORS FOR THE DETECTION OF BIOLOGICAL WARFARE AGENTS

Samuel Bacena Dulay

Dipòsit Legal: T 1237-2014

Samuel Bacena Dulay

Development of electrochemical biosensors for the detection of biological warfare agents

DOCTORAL THESIS

Department of Chemical Engineering

UNIVERSITAT ROVIRA I VIRGILI

Tarragona

2014

Samuel Bacena Dulay

Development of electrochemical biosensors for the detection of biological warfare agents

DOCTORAL THESIS

Supervised by Dr. Ciara K. O'Sullivan

Department of Chemical Engineering

UNIVERSITAT ROVIRA I VIRGILI

Tarragona

2014

Departament d'Enginyeria Quimica
Universitat Rovira i Virgili
Campus Sescelades,
Avda. Països Catalans, 26
43007 Tarragona
Tel: 977 55 96 58
Fax: 977 55 96 67

Dr. Ciara K. O'Sullivan,

CERTIFY:

That the present study, entitled "Development of electrochemical biosensors for the detection of biological warfare agents" presented by Samuel Bacena Dulay for the award of the degree of Doctor, has been carried out under my supervision at the Chemical Engineering Department of the Universitat Rovira I Virgili, and that it fulfils the requirements to obtain the Doctor European Mention.

Tarragona, June 6, 2014,

Dr. Ciara K. O'Sullivan

Acknowledgements

First of all I would like to thank my supervisors, Pablo Lozano Sanchez and Ciara O'Sullivan, for trusting me when I joined the group and for their guidance and encouragement through my Master and PhD studies. I would like to thank as well George Attard and Iris Nandhakumar, for sharing their expertise and knowledge and for giving me the opportunity to work and learn to their laboratory during my stage at the University of Southampton, England. I also appreciate the efforts of Marilena, who is a master graduate student of SOTON, for sharing and helping me in her AFM expertise. I would like to thank the doctoral scholarship from the MultiSense Chip research project funding received from the European Community´s Seventh Framework Programme (FP7/2007-2013) under Grant agreement number 261810 for the economical support. I also extend my thanks to the mobility grant given Universitat Rovira I Virgili. To my former supervisors/professors in Philippines, Dr. Fortunato and Dr. Melfei, thanks for the encouragement and friendship. I also would like to express gratitude to all the people from NBG and BBG group, the present members and the former members. To Mari Carmen, Mary Luz, Josh, Marketa and Miriam Jauset, for helping me always in ELISA/ELONA, conjugation techniques, PCR amplification techniques and other things that are needed in my thesis experiment. Of course to Mabel and Ahmed who were my former mates in the Master's degree in Nanoscience and good friends for life. To Joanne, Gael, and Jonathan who are always present in the lab and killing boredom moments while doing experiments. To Diego dela Cruz, Bernabe Lopez, Juan Carlos Contapay and Maria Luisa Rallos, thanks for the friendship, encouragement and inspirations. To all my friends here in Tarragona, the Filipino community, David Masegosa, Ate Ligaya Ola, Ligaya Liit, Kuya Nicanor, Jenny Bareng, Lorenz Agustin, Jocelyn Jumawan and Marjorie, thank you for being part of my adjustment days and the friendship. You all helped me during my hard times.

I would like to thank as well my parents, Mommy Ibing and Daddy Pilis for their support and unconditional love, thanks for bringing me out in this world Mommy, I love you both. To all my siblings, Manong Deo, Manong Cyrus, Manang Filma, Manong Lawrence, and Ading Meriam, thanks for the encouragements. You all serve my inspiration to push through.

And above all, the Almighty Great Energy. Thanks for the wonderful life I have.

Table of contents

Summary i

List of publications iv

List of abbreviations v

List of figures and schemes vii

List of tables viii

Chapter 1. Introduction 1

1.1 Brief history of biological weapons 1

1.1.1 Biological warfare agents 5

1.1.1.1 *Bacillus anthracis* 6

1.1.1.2 *Brucella species* 8

1.1.1.3 *Francisella tularensis* 9

1.1.1.4 *Yersinia pestis* 10

1.1.1.5 *Coxiella burnettii* 11

1.1.1.6 *Burkholderia mallei and pseudomallei* 12

1.1.1.7 *Bacillus thuringiensis* subsp. *kurstaki* 13

1.1.1.8 Bacteriophages 14

1.2 Antibody: A recognition element in biological assays 15

1.2.1 Structure and classes of immunoglobulins 16

1.2.2 Antibody production 19

1.2.3 Labelling of antibodies 20

1.2.4 Immobilisation of antibodies 23

1.3 Biosensors for biological weapons 26

1.3.1 Electrochemical biosensors 29

1.3.1.1 Potentiometric biosensors 29

1.3.1.2 Impedimetric biosensors 31

1.3.1.3 Amperometric biosensors 31

1.4 Nanostructuring of electrodes: *Electrochemical biosensor enhancement* 33

1.5 Thesis objectives 35

1.7 References 37

Chapter 2 Automated microfluidically controlled electrochemical biosensor for the rapid and highly sensitive detection of *Francisella tularensis* 46

Chapter 3 Development of an immunosensor for the detection of *Francisella tularensis* antibodies 78

Chapter 4 Integrated microsystem for multiplexed genosensor detection of biowarfare agents 97

Chapter 5 Lyotropic liquid crystals as a template for DNA self-assembled monolayers 125

Conclusions 154

Outlook 159

Summary

An early, rapid and reliable detection of the presence of biowarfare agents, pathogens, viruses and toxins is required in different situations which include civil rescue and security units, homeland security, military operations, public transportation securities such as airports, metro and railway stations. There is a global argument about the threat of bioterroristic attacks using high risk pathogens with significant potential impact on humans, plants and animals. Electrochemical biosensors have received important attention for the rapid detection of these pathogens due to simplicity, low cost, portability, multiplexing capability and sensitivity. Moreover, their compatibility with microfabrication technologies makes them attractive for automated immunological and deoxyribonucleic acid (DNA) diagnostics. The first element of the work described in this thesis is the development of an electrochemical immunosensor and DNA biosensor array for the detection of different virulent species. In the development of the immunosensor, the use of whole antibodies and antibody fragments for the detection of *Francisella tularensis* were compared. In the development of the DNA biosensor array, simultaneous detection of eight (8) different virulent species has been explored. The developed immunosensor and DNA biosensor were integrated in a microfluidics and housed in a tester set-up that facilitated complete automation of the assay. The only end-user intervention is sample addition that requires less than one minute hands-on time. The use of the automated microfluidic set-up not only required much lower reagent volumes but also the required incubation time was considerably reduced and a notable increase of sensitivity was achieved. The second element explored was the improvement of biosensor performance by increasing sensitivity and to achieve lower limit of detection. The use of a template using lyotropic liquid crystal was exploited and an improved analytical performance achieved.

This thesis is divided in five chapters. A general introduction covering the different topics of the thesis is presented in Chapter 1. Chapters 2 to 4 describe the development of electrochemical

biosensors for detection of biowarfare agents while chapter 5 covered the developed strategy in improving biosensor performance.

In chapter 2, different surface chemistry using antibody fragments or whole antibodies were explored in the development of an immunosensor for the highly sensitive detection of bacterial cells. The developed biosensor integrated with microfluidics housed in a tester set-up for automated hands-on analysis. Chapter 3, focuses on the development of an immunosensor for the detection of anti-*Francisella tularensis* antibodies in animal serum samples comparing the use of a membrane antigen to bacterial cells to capture the antibodies. Optimal conditions for the best assay format were explored and real samples of sera from animals known to be infected with tularemia were analysed and the results compared to that obtained using ELISA methods, showing an excellent degree of correlation. Chapter 4 discussed the simultaneous detection of eight (8) virulent species using a sensor array. Different designs of capture probes and assay conditions were thoroughly studied in the detection of polymerase chain reaction products. The developed multiplexed biosensor array was again integrated with microfluidics housed in a tester set-up device. Chapter 5 details a nanotemplating method that had the objective of improving probe distribution and an enhanced biosensor performance. In this chapter, different phases of lyotropic liquid crystals of the surfactant octaethylene glycol monohexadecyl ether ($C_{16}EO_8$) were explored for the creation of nanosized pores. Fluorescence and atomic force microscopy as well as electrochemistry were used to evaluate the modified surfaces of gold electrode.

Overall, this work constitutes a complete overview of the development of quantitative electrochemical biosensors for the detection of bacterial cells of *F. tularensis*, anti-*F. tularensis* antibodies as well a highly sensitive and selective multiplexed DNA biosensor array for the detection of PCR products from real samples. The search to improve sensitivity and lower limit of detection

of a DNA biosensor was achieved using a nanotemplating method for a better probe distribution enhancing hybridisation efficiency.

List of Publications

Master Thesis:

1. Dulay, S., Lozano-Sánchez, P., Iwuoha, E., Katakis, I. and O'Sullivan, C. K., Electrochemical detection of celiac disease-related anti-tissue transglutaminase antibodies using thiol based surface chemistry, Biosensors and Bioelectronics (2011) 26, 9, 3852-3856

PhD Thesis:

2. Dulay, S. B., Gransee, R., Julich, S., Tomaso, H. and O'Sullivan, C. K. Automated microfluidically controlled electrochemical biosensor for the rapid and highly sensitive detection of Francisella tularensis, Biosensors and Bioelectronics (2014) 59, 342-349
3. Dulay, S. B., Julich, S., Tomaso, H. and O'Sullivan, C. K. Development of an immunosensor for the detection of Francisella tularensis antibodies. Analytical and Bioanalytical Chemistry- *Manuscript accepted.*
4. Dulay, S., B., Gransee, R., Julich, S., Tomaso, H. and O'Sullivan, C. K. Integrated microsystem for multiplexed genosensor detection of biowarfare agents- *For submission*
5. Dulay, S., B., Lozano-Sanchez, P., Nandhakumar, I. S., Attard, G. S. and O'Sullivan, C. K. Lyotropic liquid crystals as a template for DNA self-assembled monolayers- *For submission*

List of Abbreviations

AFM	Atomic Force Microscopy
ALP	Alkaline phosphatase ALP
ATP	adenosine triphosphate
$C_{16}EO_8$	octaethylene glycol monohexadecyl ether
CFU/mL	colony forming units per mL or number of 'cells/mL'
CV	Cyclic voltammetry
DNA	Deoxyribonucleic acid, single-stranded DNA (ssDNA) or doublestranded DNA (dsDNA)
DT1	10-(3,5-bis((6-mercaptohexyl)oxy)phenyl)-3,6,9-trioxadecanol
DT2	22-(3,5-bis((6-mercaptohexyl)oxy)phenyl)-3,6,9,12,15,18,21-heptaoxadocosanoic acid
EDC	1-Ethyl-3-[3-imethylaminopropyl]carbodiimide hydrochloride
EDTA	Ethylenediaminetetraacetic acid
EIS	Electrochemical impedance spectroscopy
ELISA	Enzyme-linked immunosorbent assay
ELONA	Enzyme-linked oligonucleotide assay
F(ab')	Fragment antibody
Fw	Forward (primer)
HEPES	(4-(2-hydroxyethyl)-1-piperazineethanesulfonic acid
H_I	hexagonal phase
HRP	Horse-radish peroxidase
I g	Immunoglobulin
ICT	immunochromatographic
IFA	immunofluorescence assay
IgG	Immunoglobulin G
ISFETs	ion selective field effect transistors
IUPAC	International Union and Applied Chemistry
L_1	Micellar
LLC	lyotropic liquid crystalline
LOD	Limit of detection

LPS	Lipopolysaccharide
LVS	live vaccine strain
L_{α}	Lamellar
mAb	Monoclonal antibody
MCH	Mercaptohexanol
MHA	6-mercaptohexanoic acid
NHS	*N*-Hydroxysuccinimide
OPM	Optical polarising microscope
PAb (PAb)	Polyclonal antibodies
PCR	Polymerase Chain Reaction
PEG	1-(mercaptoundec-11-yl)tetra (ethyleneglycol)
Rct	Charge transfer resistance
RNA	Ribonucleic acid
RSD	Relative standard deviation
RT	Room temperature
RT-PCR	Real time polymerase chain reaction
Rv	Reverse (primer)
SAM	Self-assembled monolayer
SAS	Step and sweep voltammetry
SATA	succinimidyl acetylthioacetate
SCE	Silver chloride electrode
SPR	Surface Plasmon Resonance
TMB	3,3',5,5'-tetramethylbenzidine
UV	Ultraviolet
VEE	venezuelan equine encephalomyelitis
WW1	World War 1
WWII	World War II

List of Figures and Schemes

		Page
Chapter 1		
Figure 1.1	Typical structure of antibody	16
Figure 1.2	Typical structure of different antibodies	17
Figure 1.3	Conjugation process of Ab with Maleimide activated HRP using SATA	22
Figure 1.4	Typical scheme of immobilising immunoglobulins using SAM of a) protein A, G, or L, b) whole Ab and c) fragment Ab (F(ab)). The metal layer was modified by SAM bipodal through carbodiimide conjugation chemistry for a and b	26
Figure 1.5	Schematic representation of a biosensor	28
Figure 1.6	Typical schematic diagram of a potentiometric biosensor assays	30
Figure 1.7	Schematic diagram of a typical amperometric biosensor. RE: reference electrode, WE: working electrode, CE: counter electrode	32
Chapter 2		
Figure 2.1	Schematic representation of a) sandwich with whole antibody linked to bipodal alkyl thiol (DT2) and whole antibody-HRP conjugate b) sandwich with direct chemisorption of F(ab) fragment and whole antibody-HRP conjugate c) sandwich with direct chemisorption of F(ab) fragment and F(ab)-HRP conjugate	57
Figure 2.2	Amperometric responses of the whole antibodies immobilised via chemical cross-linking to a bipodal alkyl thiol SAM and SAM formed from the direct chemisorption of antibody fragments F(ab) to different LPS and LVS of *F. tularensis* concentrations. Each data point represents the average of three independent measurements.	59
Figure 2.3.	The amperometric immunosensor detection set-up. The set-up contains a peristaltic pump positioned behind the reservoirs to flow the solutions into electrode array mounted within the microfluidics. (a) the electrode array with microfluidics placed in the platform and connected to the potentiostat for amperometric measurement; (b) a sample script-based assay program; (c) the electrode array integrated with microfluidics; (d) a full front view of the tester set-up device; (e) lithographically produced gold electrode array	61

with internal reference electrode and counter electrode.

Figure 2.4. Step and Sweep (SAS) amperometric response of the F(ab) fragment FB11 functionalised electrochemical immunosensor a) to 10 ng/mL LPS sample outside the fluidics and b) to 10 ng/mL LPS sample inside the fluidics at different incubation times of antigen-LPS, c) to 10 ng/mL LPS sample inside the fluidics at different incubation temperatures and d) different incubation times for the secondary labelled antibody T14HRP. Each data point represents the average of nine measurements on three separate electrode arrays. 62

Figure 2.5. Step and Sweep (SAS) amperometric responses of the direct F(ab) fragment FB11 immobilised based electrochemical immunosensor to a fixed concentration (150 bacteria/mL) of *F. tularensis* (LVS). (a) at different incubation times of pre-mixed LVS target and secondary labelled antibody T14HRP; (b) sequential addition of LVS (2 min) and T14-HRP (15 min) with intermittent washing step. Each data point represents the average of nine measurements on three separate microchip array. 63

Figure 2.6. Calibration curve and sensitivity of the electrochemical based-immunosensor detection system for the analysis of inactivated *F. tularensis* LVS subsp. *holarctica* bacteria. Step and Sweep (SAS) amperometric responses are shown for capture antibody on the chip –*F. tularensis* antibody FB11 F(ab) to different bacterial solutions which are flushed into the chip electrodes' surface via microfluidic device. Inset: Specificity of the immunosensor to *F. tularensis* LVS subsp. *holarctica* (F.t (H)Bact.), *F. tularensis* subsp. *novicida* (F.t (N)Bact.), *Yersinia enterocolitica* subsp. *enterocolitica* (YeE Bact.), *Yersinia pseudotuberculosis* (YeP Bact.). Each data point represents the average of three independent measurements. 65

Figure 2.7. Stability of stored Fab-modified sensors over a 45-day period. Sensors were stored at 4 °C and exposed to 10ng/mL LPS every 15 days for 45 days. (n=3, RSD%= 9.6). 66

Figure 2.S1: Scheme planned for ELISA analysis for the characterization of the prepared monoclonal antibody (mAb)-HRP conjugate and for choosing best assay combination 71

Figure 2.S2: ELISA responses of different assay schemes; a) coating probe-FB11, Reporter probe-T14-HRP b) coating probe-T14, Reporter probe-T14-HRP c) coating probe-T14, Reporter probe-FB11-HRP d) coating probe-FB11, Reporter probe-FB11-HRP to different concentrations of LPS varying concentrations of the reporter probes; UV-VIS absorbance at 450 nm. Each data point represents the average of three independent measurements. 73

Figure 2.S3. ELISA responses of a) different assay scheme combinations (10 μg/mL of mAb FB11 or T14 coating) and b) two best assay scheme combinations: (top) coating probe-FB11, secondary labelled antibody-T14-HRP (below) coating antibody-T14, secondary labelled antibody-T14-HRP to different concentrations of LPS with their corresponding detection limit. Each data point represents the average of three independent measurements 74

Figure 2.S4. SDS-PAGE analysis (12% gel; nonreducing conditions) of the full length monoclonal antibodies FB11 and T14 antibody and their $F(ab)_2$ and Fab fragments: (a) lane 1, molecular weight marker; lane 2, full-length monoclonal antibody T14; lane 3, $(Fab')_2$ fragments T14 (obtained by enzymatic bromelain fragmentation); lane 4, cysteine reduction of $(Fab')_2$ T14 to (Fab) fragments T14; lane 5, full-length monoclonal antibody FB11; lane 6, $F(ab)_2$ fragments FB11 (obtained by enzymatic bromelain fragmentation); lane 7, cysteine reduction of $(Fab')_2$ FB11 to (Fab) fragments FB11 74

Figure 2.S5. ELISA result of different concentration of antigen LPS to varied concentration of labelled Fab fragment T14-HRP. On the right side, scheme of the immunoassay. Each data point represents the average of three independent measurements. 75

Figure 2.S6. Typical acid CV (0.5M sulfuric acid) of lithographically produced gold electrodes (3mm and 1mm Ø) with 10 CV cycles at 0.3 V/s scan rate vs. Ag/AgCl reference electrode. (Hoogvliet *et al.* 2000). 75

Chapter 3

Figure 3.1. Schematic of the electrochemical immunosensor architecture. 86

Figure 3.2. ELISA measurement of calibration curve for anti-*F. tularensis* LPS antibody FB11 using a) 15 μg/mL of *F. tularensis* LPS and b) 280 bacteria cells/mL of 87

F. tularensis subsp. *holarctica* as coatings respectively at 0.63 μg/mL of HRP labelled protein A as reporter molecule. Each data points represent the average of six measurements in a plate

Figure 3.3. a) Amperometric response of the electrochemical immunosensor to different mAb FB11concentrations, b) typical amperometric detection of FB11 antibodies present in animal serum samples in red foxes (*Vulpes vulpes)* in different dilution factor using the developed electrochemical sensor and c) summarised table for the calculated concentration of antibodies for ELISA and immunosensor method. Each data point represents the average of three measurements in different separate sensors 89

Figure 3.4. Specificity of the immunosensor to anti-*F. tularensis* antibodies (anti-F. t) from red fox (*Vulpes vulpes*) sera, Brucellosis antibody, and three samples from human serum IgG-positive for *Y. enterocolotica* (anti-Y.e). Sample preparations: D.F 1:1200. Blank – no antibody target. 90

Figure 3.S1: ELISA evaluation of the immunoassay format for the optimum concentration of a) coating label (LPS) at 150 μg/mL of FB11 antibody, b) HRP-Protein A reporter probes at 150 μg/mL of FB11 antibody, c) 6.25 μg/mL of LPS as coating and 2.5 and 0.63 μg/mL of HRP-Protein A reporter probes, d) 15 μg/mL of LPS as coating and 2.5 and 0.63 μg/mL of HRP-Protein A reporter probes and e) typical quantification of concentration of serum sample from red fox (*Vulpes vulpes)* at different dilution factor at 15 μg/mL of LPS as capture antigen and 0.63 μg/mL of HRP-labelled protein A reporter probe 93

Figure 3.S2: ELISA evaluation of the immunoassay format for the optimum concentration of a) coating label (LVS) at 0.63 μg/mL of HRP-Protein A, b) HRP-Protein A reporter probes at 0.63 μg/mL of HRP-Protein A, and c) re-evaluation of the optimum LVS coating concentrations of 188, 375, and 750 Bacteria/mL and d) 280 Bacteria/mL of LVS as coating concentration at 0.63 μg/mL of HRP-Protein A. 95

Chapter 4

Figure 4.1 Schematic representation on the immobilization of thiolated ssDNA and its hybridization process to complete the sandwich assay format illustrating how the electroactive species detected into electrode surface. 108

Figure 4.2. Gel characterisation of dsDNA and ssDNA PCR products produced. 1. *Bacillus anthracis* (BA), 2. *Brucella melitensis* (Bram), 3. *Bacteriophage lambda* (BL), 4. *Francisella tularensis* (FrT), 5. *Burkholderia mallei* (Brum), 6. *Coxiella burnetii* (CB), 7. *Yersinia pestis*(YeP) and 8. *Bacillus thuringiensis var. kurstaki*(BaT). 109

Figure 4.3. Optimum condition for assay development using commercial conjugates and the prepared in-house made conjugates. Each data point represents the average of three measurements on three separate electrode sensors. 110

Figure 4.4. ELONA cross-reactivity and specificity characterisation of designed capture thiolated DNA probes and DNA-HRP labelled reporter probes hybridised with produced PCR products from bacterial cells. Concentrations: capture probe-200nM, target-10nM synthetic target, reporter probe-20nM 111

Figure 4.5. The amperometric immunosensor detection set-up. The set-up contains a peristaltic pump positioned behind the reservoirs to flow the solutions into electrode array mounted within the microfluidics. (a) the electrode array with microfluidics placed in the platform and connected to the potentiostat for amperometric measurement; (b) a sample script-based assay program; (c) the electrode array integrated with microfluidics; (d) a full front view of the tester set-up device; (e) lithographically produced gold electrode array with internal reference electrode and counter electrode 113

Figure 4.6. a) Typical dynamic linear range in the calibration curve obtained for the developed genosensor, b) optimum incubation time of the developed DNA biosensor. Each data point represents the average of three measurements on three separate electrode sensors and c) stability of the immobilised probes into the electrodes. 114

Figure 4.7. Electrochemical based measurement of a) typical single probe co-immobilised with DT1 1:100 (mol/mol) individual assay detection of ssDNA PCR product and b) typical single probe co-immobilised with DT1 1:100 (mol/mol) with only one fixed concentration (5 nM) of 116

complementary target PCR product from real sample specific to one surface thiolated DNA capture probe and label probe. Each data point represents the average of three measurements on three separate electrode array sensors.

Figure 4.S1 Calibration curve of known concentration of the thiolated ssDNA used for conjugation. Inset graph is a typical absorbance of unknown concentration of inhouse conjugated ssDNA with HRP at different dilution factor 122

Figure 4.S2 Comparison of DNA-biotin/strep-HRP, commercial DNA-HRP conjugate, and inhouse made DNA-HRP conjugate as a label 123

Chapter 5

Figure 5.1 Schematic representation on the immobilization of thiolated ssDNA in hexagonal phase (H_I) of $C_{16}EO_8$ and its hybridization process to complete the sandwich assay format illustrating how the electroactive species diffuses to be detected into electrode surface. 129

Figure 5.2. a) Typical cyclic voltammograms of 5mM $Fe^{+3/+2}$ and their b) corresponding oxidation peak current in different mixture conditions, c) Cyclic voltammograms for the reductive desorption of immobilized thiolated DNA in different immobilization condition from the gold electrodes in 50mM of KOH at a scan rate of 0.05 V/s and d) summarized calculated available active area for a and surface coverage of thiols per area cm^2 for c. 135

Figure 5.3. Schematic model of possible orientation of H_I $C_{16}EO_8$ a) vertically and b) horizontally positioned to electrode's surface and obtained graphical representation of relative electrochemically accessible surface area of c) vertically and d) horizontally positioned H_I $C_{16}EO_8$ in the surface of electrode 137

Figure 5.4. Amperometric detection of complementary target DNA hybridized at 5 nM to the immobilized thiolated ssDNA in templated and non templated system at different immobilization time. 138

Figure 5.5. Amperometric responses of the templated and non templated electrochemical DNA biosensor to different complementary target DNA concentrations. Each data point represents the average of three measurements on three separate sensors. 139

Figure 5.6. Fluorescence microscopy imaging for immobilized thiolated DNA hybridized with its complementary target modified with Cy3 in a) aqueous media only (no MCH), b) Sequential backfilling with MCH, c) co-immobilization of SDNA and MCH (1:100 ratio), d) H_I phase of $C_{16}EO_8$ and e) summary table on the estimated total number of molecules hybridized in each conditions 142

Figure 5.7. Atomic Force Microscopy (AFM) imaging for immobilised ssDNA in mica surface a) control, clean mica, b) in HEPES buffer with Ni+ salt only, c) HEPES buffer with Ni+ salt in the presence of H_I template (graph image: cross sectional surface analysis for each surfaces) and fluorescence microscopy imaging for immobilised thiolated DNA modified with Cy3 in: d) aqueous media only, e) H_I phase of $C_{16}EO_8$ (inset: enlarged area-50x50 μm) in Au electrode surface and f) calculated number of molecules for each immobilization method done 145

Figure 5.S1 Optical polarizing microscopy (OPM) Images of different phases of C16EO8 explored in a) different concentration of salt used at H_I $C_{16}EO_8$ b) increasing concentration of $C_{16}EO_8$ at fixed concentration of 0.4 M KH_2PO_4 151

Figure 5.S2. Cyclic voltammograms for the reductive desorption of immobilised MCH monolayers from the gold electrodes in 50mM KOH and their calculated surface coverage (Q=mnF) of thiols per square cm. 151

Figure 5.S3. a) Typical CV scans of the 5mM Fe^{+3}/Fe^{+2} in aqueous solution only and H_I of $C_{16}EO_8$ in different concentration of hexane added at 50mV/s scan rate and its b) Oxidation peak current Inset: oxidation peak current of aqueous 5mM Fe^{+3}/Fe^{+2} only. c) Calculated surface active area of the electrode in different conditions 152

List of Tables

Chapter 1

Table 1.1 Summary of properties for each immunoglobulin 18

Table 1.2	Types of Immuno-experiments and associated labels	20
Table 1.3	Binding characteristics of Protein A, Protein G, and Protein L.	24
Table 1.4	Immunosensors for pathogen detection	33
Chapter 2		
Table 2.S1:	Summary of calculated limit of detection (LOD) of each assay arrangement using prism software statistical analysis, OR-out of range	73
Table 2.S2.	Assay procedure protocol used in the microfluidic set-up for amperometric measurements	76
Table 2.S3.	Comparison with other techniques showing the detection limit obtained on the methods used	76
Chapter 3		
Table 3.S1.	Comparison with other techniques showing the analytical performance obtained on the methods used	95
Chapter 4		
Table 4.S1:	ssDNA sequences	120
Table 4.S2:	Overview about applied bacteria strains and PCR assays	121
Table 4.S2.	Assay procedure protocol used in the microfluidic set-up for amperometric measurements	124
Chapter 5		
Table 5.S1.	Summary of calculated values based on the mathematical model and the data based on actual experiment	153
Table C1	Comparison with other techniques showing the detection limit on the methods used	155

Chapter 1

Introduction

Introduction

1.1 Brief history of biological weapons

Various types of biological weapons have been known and practiced throughout history, including the use of biological agents such as microbes and plants as well as biotoxins and the venoms which can be derived from them. In ancient civilisation, the attempt to infect and kill enemies by throwing cadavers into water wells made by Emperor Barbarossa during the battle of the Italian town, Tortona, in 1155 [1]. Another strategy used by Mongol armies in 1346 was to hurl plague-infected cadavers into the besieged Crimean city of Caffa transmitting the disease to the inhabitants and the fleeing survivors of the siege spread the plague from Caffa to the Mediterranean Basin [2]. In 1495, the Spanish offered wine spiked with the blood of leprosy patients to the French near Naples [3]. In 1797, around the plains of Mantua, Italy suffered floods reportedly spread by Napoleon to enhance the spread of malaria [1].

In the late 19th century, scientists introduced the concept of microorganisms as agents of infectious diseases. Germany was suspected to be the first one to use weapons of mass destruction and sabotage during World War 1 (WW1), both biological and chemical where they employed cholera, anthrax and plague. This kind of sabotage was carried out in the USA, Romania, France and Spain, and later in Argentina and Norway [4, 5]. Due to the exploitation of chemical weapons in WWI and understanding of biowarfare weapon possibilities used by Germany, they were prohibited from storing, and importing or using many types of weapons according to Treaty of Versailles. This move led to the formation of the Geneva Protocol: "Protocol for the prohibition of the use in war of asphyxiating, poisonous or other gases, and of bacteriological methods of warfare" in 1925 and entered into force in February 1928. This protocol aimed to prohibit the use of poisoned weapons. However, although these protocols, including the past treaties, were all agreed to by the League of

Nations, did not guarantee a means of control, and thus failed to prevent interested parties from developing and using biological weapons [4].

Japan and United States of America had (USA) did not ratify the Geneva protocol. Japan started their modern biological arm race in 1932 until the end of World War II (WWII) in which more than 10,000 prisoners were believed to have died as a result of experimental infection during the Japanese program [3]. France ran a similar program in 1936, Canada in 1939 and the United Kingdom (UK) in 1940 [6]. The British secretly developed their own biological warfare program in Porton Down focused on brucellosis, tularemia, venezuelan equine encephalomyelitis (VEE) and vaccinia viruses. Their practical experiments were realized on Gruinard Island near the coast of Scotland. The island remained contaminated until 1986 and successful decontamination was accomplished using formaldehyde [7]. The German effort for obtaining biological weapons was minimal during WW II [5, 8].

USA and Soviet Union has continued their protection activities and was even intensified after WWII. When the Soviet forces captured and interrogated some Japanese members in 1945, they utilized the obtained information in their own biowarfare program and their activities accelerated in 1946. Following this, a series of new biowarfare research and production facilities was constructed in the 1950s. The Soviet biowarfare program included tularemia, anthrax, brucellosis, plague, glanders, marburg virus, smallpox virus, and VEE virus [9]. During the time of the Korean War, it was believed that biowarfare agents were used by the USA against Soviet Union. The USA began their own program in Fort Detrick (former Camp Detrick) in 1943 and a new production facility at Pine Bluff Arsenal in Arkansas was made. USA started producing tons of *Brucella suis* in 1954. In the highest peak of their program, they involved about 3,400 people and a number of agents like *Bacillus anthracis, Francisella tularensis, Brucella suis, Coxiella burnetti, Venezuelan equine encephalitis virus,* yellow fever, botulin*, Staphylococcal enterotoxin,* and the anti-crop agents *Pyricularia*

oryzae and Puccinia graminis [5]. Due to public pressure, the late President Nixon declared disarmament in 1969 to stop biological weapon projects. The only permitted research was defensive, such as diagnostic, vaccines, and chemotherapies tests just like UK where the base in Porton Down was converted into a defence institution.

The most important dates in biological weapons history was in the year 1972 when member nations ratified the biological and toxin weapons convention, that entered into force in March 1975: "The United Nations Convention on the prohibition of the development, production, and stockpiling of bacteriological and toxin weapons and their destruction" [10]. The convention tackled the prohibition of biological weapons after 1975 but the reality was different since Soviet Union continued its' program and taking advantage of the rapid progress in microbiology and biotechnology that led to the formation of special secret organizations, which was named Biopreparat, to develop biowarfare technology and agents. They were accused of supplying mycotoxins to its' Vietnamese and Laotian communist allies for military use against resistance forces in Laos and Cambodia, and of using the same agents in combat operations in Afghanistan in the 1980s [5]. In parallel, Iraq was one of the countries that successfully built industrial biological weapons which was included in their three weapons of mass destruction, i.e nuclear, chemical and biological. Their program in biowarfare started in 1975. They explored and investigated Botulinum toxin*, Bacillus anthracis and Clostridium perfringens* spores, camelpox virus and ricin but their sites were then eventually destroyed during the gulf war [11]. South Africa also initiated a biowarfare program in 1980, and used anthrax for individual assassinations and cholera for contaminating water supplies during attacks against freedom fighters [5].

Acts of bioterrorism have not been controlled in the last decades. In September 1984, Oregon experienced America's first community bioterrorism attack led by the followers of Bhagwan Shree Rajneesh, who established a commune in the county and intentionally infected restaurant

diners in The Dalles as part of a plot to take over county government and at least 750 people became ill with a unique strain of Salmonella (https://www.nwpublichealth.org). In Tokyo, Japan, the attempt to disseminate anthrax in 1993 by the Aum Shrinikyo cult was not successful but the cult was able to recruit many professionals, including those with scientific and medical training and were able to obtain *Bacillus anthracis* through their contacts. Nobody was harmed by the anthrax attack because the source was a non-pathogenic strain and the authorities were not even aware of the release until later when the cult was investigated for the release of Sarin gas on the Tokyo underground [12].

Recently, the threat of bioterrorism attacks has attracted attention once again and threatens the whole world due to the recent chemical attack that has struck Syria [13] which killed hundreds of men, women, and children as well as the *Bacillus anthracis* spore-containing letter attack [14, 15] that happened in United States shortly after the 9/11 attack. The presented history on biological warfare and bioterroristic attacks would highlights the risks associated with biowarfare agents, and how biowarfare could be used for mass destruction in the future, and the associated threats that could bring to humankind.

1.1.1 Biological warfare agents

Considering the general availability of know-how to culture microorganisms in large quantities, there is now a global argument about the possibility of using different pathogens with high risk not only limited to public health safety but also to plants and animals for bioterrorism attacks. There are numerous pathogens, including bacteria, viruses, fungi, toxins among others, which are listed by various agencies as potentially dangerous agents [16]. Critical biological agents based on several criteria have been classified in three categories by the Centers for Disease Control and Prevention (http://www.bt.cdc.gov/agent/agentlist-category.asp). Agents that cause greatest

harm are classified as category A and include *Bacillus anthracis, Yersinia pestis, Variola major, Francisella tularensis,* and viral hemorrhagic fevers. These agents pose a high risk to national security because they can be easily disseminated or transmitted from person to person or potential delivery through weapons which result in high mortality and severe impact on human health, causing public disruption and panic. Category B includes agents that are moderately easy to disseminate, and which result in moderate morbidity rates and lower mortality rates than agents in category A. Agents in this category included *Coxiella burnetti ,* Brucella species*, Burkholderia mallei and pseudomallei,* Alphaviruses*,* Toxins, *Rickettsia prowazekii, Chlamydia psittaci,* Salmonella species*, Shigella dysenteriae, Escherichia coli, Cryptosporidium parvum, and Vibrio cholerae.* Category C includes emerging pathogens that are readily available and easily disseminated such as Nipah virus, Hentavirus, Tickborne hemorrhagic fever viruses, Tickborne Encephalitis virus, Yellow Fever, and multidrug-resistant tuberculosis [17]. Although category C is considered as the lowest risk among the three categories, agents that belong to this category should not be neglected as they are also considered to have potential for high morbidity, mortality rates and major health impact. The following section discusses in details some important high risk pathogens.

1.1.1.1 *Bacillus anthracis*

Anthrax is an acute infectious zoonotic disease caused by the spore-forming, aerobic, Gram positive, non-motile bacterium, *Bacillus anthracis*. The bacteria exists in the environment as a spore and can remain viable in the soil for decades [18]. Anthrax was a major cause of death for animals all over the planet until the end of the 19th century, with occasional, sometimes extensive, contamination to humans [19]. Spores that have been ingested by herbivorous animals can germinate inside the animal to produce the virulent vegetative forms that replicate and eventually kill

the host. Products from infected animals or exposure to dead animals serve as a reservoir for human infections [20].

There are three major clinical forms of anthrax that affect humans; cutaneous, gastrointestinal and inhalational anthrax. Among the three, cutaneous anthrax is globally the most prevalent naturally occurring anthrax infection. This results when any broken skin is exposed to the spores that form ulcer and black eschar. Fever can also occur during the incubation period. Gastrointestinal anthrax is typically related to ingestion of spore contaminated meat and there are two forms of gastrointestinal anthrax: oropharyngeal and intestinal. Spores settle in the pharyngeal area and produce ulcers in oropharyngeal anthrax. The mean incubation of the spores is about 42 hours. In intestinal anthrax, spores are deposited and cause ulcerative lesions anywhere from the jejunum to the cecum. A patient frequently suffers from nonspecific gastrointestinal symptoms, fever and neck swelling. The last form is inhalation or pulmonary anthrax following inhalation of thousands of spores. The first symptoms are similar to influenza and after 2 or 3 days of high fever with haemorrhage there is a rise in systematic infection. Gastrointestinal and inhalation anthrax are fatal when left untreated and undiagnosed and immediate treatment with antibiotics should be employed.

Biological and chemical techniques have been considered in the last decades to be useful in identification and detection of anthrax spores. Identification of *Bacillus anthracis* has been found to be difficult because of its similarity with other strains in its genus. Polymerase chain reaction (PCR) and immunoassays are the two most employed biological methods to detect anthrax spores. PCR-based assays can accurately differentiate pathogenic *Bacillus anthracis* strains from apathogenic *Bacillus anthracis* from non-anthracis Bacillus species [21] while immunoassay is one of the most currently used methods in clinical diagnosis [22]. Recently, specific detection and accurate identification of the

presence of *Bacillus anthracis* in any media including foods has been determined by the use of pyrosequencing technology [23].

1.1.1.2 *Brucella* species

Brucellosis is a widespread zoonotic disease caused by *Brucella* spp. affecting both humans and animals [24]. Human brucellosis remains the most common zoonotic disease worldwide [25]. Domestic animals like cattle, sheep, goats, swine and even dogs, especially sheppard dogs are the natural reservoirs of the organisms. Humans get infected through conjunctiva or skin abrasions when exposed to animal fluids infected with the disease, through ingestion and inhalation [26]. After infecting the host, the pathogen becomes sequestered within cells of the reticuloendothelial system, the mechanism by which brucella enters cells and evades intracellular killing, degrading host's immune system [24]. Brucellosis in human beings is rarely fatal but it can be severely debilitating and disabling. It is a multisystemic disease with a broad spectrum of symptoms, although it can be asymptomatic as well. It begins as a flu-like disease with symptoms such as fever and generalized aches. Gastrointestinal signs, i.e. anorexia, nausea, vomiting, diarrhea, and constipation, coughing, and pleuritic chest pain can also be seen. The most common complications are arthritis, spondylitis, epididymoorchitis, and chronic fatigue. Endocarditis is one of the most serious complications of brucellosis. Some other organs are also affected, resulting in lymphadenopathy, deep vein thrombosis, granulomatous hepatitis, osteomyelitis, anemia, thrombocytopenia, and nephritis [25].

Five species have been recognized in the past, according to relative animal host specificity [27] and additional 5 more species has just been recently added [26]. Pathogenicity of five *Brucella* species for humans has been confirmed. *Brucella melitensis* was isolated in 1887 in Malta (hence called Malta fever) by David Bruce from the spleen of a soldier who died from acute brucellosis. It usually affects sheep and goats whilst *Brucella abortus* causes abortions in cattle. *Brucella suis,* which was also

isolated from wild hares, causes the disease mainly in swine which is also pathogenic for humans. *Brucella canis* isolated from dogs, could be also pathogenic to humans. Finally, *Brucella marina* is found in sea mammals (whales, seals) in the Atlantic Ocean [26, 27]. The disease in humans is mainly due to *Brucella melitensis* as the most pathogenic species followed by *Brucella suis*, while *Brucella abortus* is considered as the mildest type of brucellosis.

Serological and cell culture techniques are the usual diagnostic methods used for both animals and humans. The Wright test or agglutination reaction is still considered the standard method [27] and in recent years, methods of molecular biology have been used increasingly often in the diagnostics of brucellosis, particularly PCR [26].

1.1.1.3 *Francisella tularensis*

Tularemia, also known as rabbit fever, is a highly infectious zoonotic disease caused by the non-motile, non-spore-forming, Gram-negative coccoid rod bacterium, *Francisella tularensis*. It occurs naturally in lagomorphs (rabbits and hares), but many animals have been reported to be infected. Transmission to humans is mostly associated with inhalation of aerosolised bacteria, handling of infected animals, arthropod bites, and ingestion of contaminated foods and water [28, 29]. The usual incubation period is 3-5 days but symptoms can become visible between 1 and 21 days depending on the route of infection. Clinical manifestation of the disease in humans can occur in different forms ranging from skin ulcers to more severe forms such as life threatening-pneumonia [30].

Despite the fact that most of tularemia infections can be treated with antibiotics [31], it is still considered as life-threatening due to its high virulence, transmission and mortality [32]. Identification of *Francisella tularensis* has been achieved using cultivation and molecular techniques including PCR [33] and real time PCR assays [34-36]. Besides the detection of the bacterial cell, the detection of specific antibodies in serum is the most widely used serological analysis technique for

routine laboratory diagnosis of tularemia [37]. Enzyme-linked immunosorbent assay (ELISA) [38], Western blot and other immunological assays can be used to detect seroconversion in patients. However, antibodies only appear 2 weeks or more after infection [39].

1.1.1.4 *Yersinia pestis*

It has been believed that the bacterium *Yersinia pestis,* a nonmotile and slowly growing Gram-negative coccobacillus from the family Enterobacteriaceae, is considered the most likely cause of the most devastating disease outbreaks in human history; the Plague of Justinian and black death in the middle ages [40, 41]. Although some authors debate that the Plague of Justinian was caused by a different pathogen[42]. The natural reservoir of the plague foci are usually rodents that successfully integrate into the host's innate immunity and then propagates to induce bacteremia that is needed in order to constantly circulate and this is then transmitted by infected fleas to a new host through bites [43, 44] that result in the bubonic plague. In this disease, the organisms arrive in lymph nodes and multiply there, after being introduced by the bite of infected fleas. When bubonic plague is left untreated, it progresses to septicemic plague with increasing mortality that may result into pneumonic plague. Aside from the fleas, *Yersinia pestis* infection can also be transmitted by aerosols or contaminated food[45]. Following exposure to the agent, the incubation period takes from 2 to 6 days to appear with some symptoms like fever, malaise, nausea, vomiting and diarrhoea. The flu-like illness rapidly changes into bloody sputum within a very short period between 1 to 3 days after exposure to the agent. Treatment of human plague can be achieved and has been successful using antibiotics like streptomycin, gentamicin, doxycycline, and ciprofloxacin [43].

Several techniques have been developed for efficient detection of *Yersinia pestis,* including molecular techniques including PCR, biosensors, and immunoassay techniques[46]. Although *Yersinia pestis* is unstable in aerosol for longer times which impedes utilisation of this agent as a

biowarfare, The CDC enlisted it into category A due to the high mortality and high virulence and resistance to its' environment as it can live for a long period of time in its' dead host, soil and in water.

1.1.1.5 *Coxiella burnetti*

Coxiella burnetti is an intracellular, Gram-negative pathogenic bacterium which is the causative agent of Q fever (query fever) [47]. It is a zoonotic infection that manifests in humans primarily as an acute flu-like syndrome with potential complications including pneumonia and hepatitis. These signs and symptoms of human Q fever complicate and delay clinical diagnosis. The incubation period varies from a few days to weeks depending on the dose of bacteria and the immune system of the host [48].

The first outbreak of this disease was in Queensland, Australia in 1935. Infection typically occurs by inhalation of the bacterium contained in contaminated dust particles. Sources include barnyards and facilities housing *Coxiella burnetti* research programs. Some rare cases of Q fever have been reported in which a patient has been infected without direct contact with farm animals where the patient came down with Q fever-like symptoms after painting the walls of a science laboratory where a newborn lamb had been dissected. In addition, indirect accidental exposures have occurred with workers in offices near elevators used to transport pregnant sheep that were unknowingly infected with *Coxiella burnetti*. Due to its hazardous consequence, occupational hazards associated with research facilities has largely been eliminated due to implementation of modern biosafety equipment and protocols [49].

Confirmation of the disease normally involves testing for the presence of *Coxiella burnetti* -specific antibodies, which develop in patients 1–2 weeks after infection. The gold standard serological test for Q fever is an indirect immunofluorescence assay (IFA) that relies on serum

reactivity. PCR-based technology is sensitive mainly in the early disease state but as the disease progresses the test sensitivity decrease [49]. The use of mass spectrometry analysis has also been employed for direct detection and identification of the bacterial cells [50].

1.1.1.6 *Burkholderia mallei and pseudomallei*

Burkholderia mallei and *Burkholderia pseudomallei* are facultative intracellular, Gram-negative pathogens and the causative agents of glanders and melioidosis respectively [51], which are highly infectious via the respiratory route, and can cause severe diseases in humans and animals [52].

Glanders is a highly contagious and often fatal zoonotic disease primarily of solipeds such as horses, mules, and donkeys. Over the last 100 years, the occurrence of glanders has decreased due to the reduced economic reliance of using solipeds in terms of transportation. Eventhough glanders has almost been eradicated in most parts of the world, it is still considered as a life-threatening disease agent due to its high mortality. *Burkholderia mallei* was one of the first biological warfare agents used during WWI. Glanders can be transmitted through contact with abraded or lacerated skin, inhalation by bacterial invasion of the nasal, oral, and conjunctival mucous membranes. Depending on the route of infection, symptoms can vary from pulmonary, septicemic, or multi-tissue infection. The general symptoms can be low-grade fever, malaise, fatigue, headache, lymphadenopathy, and chest pain [53].

Melioidosis occurs following exposure to contaminated water or soil, usually through cuts in the skin or via inhalation [54]. *Burkholderia pseudomallei* is commonly found in soil and water in Southeast Asia and Northern Australia. The increasing cases of melioidosis are a serious global threat and clinical manifestations of melioidosis are extremely diverse. Depending on the route of infection, symptoms vary from acute sepsis to chronic localised pathology to latent infections which can reactivate decades later. The lung is the most commonly affected organ when the bacterium is

inhaled resulting in cough and fever that when left untreated and undiagnosed could lead to pneumonia, or secondary to septicaemic spread. The overall mortality rate in individuals infected with B. pseudomallei range from 30-70% resulting in this agent being categorised as one of the biological warfare agents [55].

Detection and identification of both species can be achieved through molecular recognition techniques such as PCR aside from the conventional way of cultures [56].

1.1.1.7 *Bacillus thuringiensis* subsp. *kurstaki*

Bacillus thuringiensis subsp. *kurstaki* is a rod shape and Gram-positive bacterium that produces parasporal crystals during sporulation that are commonly found in soil and plants. It is used as a biological insecticide to control crop-damaging moths and Lymantria dispar. The gypsy moth is a major forest pest that is especially predominant along the eastern seaboard and in the Midwestern USA [57]. Although *Bacillus thuringiensis* subspecies are neither toxic nor pathogenic to mammals, including humans, some cases in animal experimentation has shown that intraperitoneal injection of *Bacillus thuringiensis* can cause death in guinea pigs and that pulmonary infection can result in the deaths of immunocompromised mice [58]. Reports of human disease are uncommon, however, several cases has been reported. An 18-year-old farmer developed corneal cancer after being accidentally splashed with a commercial *Bacillus thuringiensis* product into his eye [59]. Another case was a multiple thigh and knee abscess containing *Bacillus thuringiensis* found in a previously healthy soldier who was severely wounded by a landmine explosion in 1995 [60]. In another case study, it was found that *Bacillus thuringiensis* has been involved in an outbreak of gastroenteritis in four persons [61].

1.1.1.8 Bacteriophages

Bacteriophages were discovered nearly 100 years ago by Frederick Twort (1915) and Felix d'Hérelle (1917) [62]. These small viral entities that specifically infect bacteria exist as nucleic acids (single or double stranded deoxyribonucleic acid/ribonucleic acid (DNA/RNA), circular or linear) wrapped up within a protein capsid protecting the nucleic acids from the environment. After injection of their nucleic acids inside the bacteria, the phage induce: a) lysis of the bacterial host with the release of newly formed viral particles (lytic phages); or b) release of the progeny viruses by extrusion or budding without lysis of the host cell over several generations (filamentous phages); or c) reside as a stable element called prophage inside the host cell as a free plasmid molecule or integrated into the host chromosome (temperate phages) [63].

Bacteriophages are ubiquitous on earth and play a major role in bacterial evolution by serving as a genomic reservoir in the environment and by promoting lateral gene transfer among bacteria through transduction. Bacteriophages, as well as their recombinant derivatives, are now used in a multitude of applications in the biotechnology and medical fields (e.g., as an alternative to antibiotics; tools for screening libraries of proteins, peptides or antibodies; vectors for protein and DNA vaccines; or as gene therapy delivery vehicles). Most phages do not display any risk for human health or the environment, explaining why scientific literature on bacteriophage biosafety is so scarce. However, some phages also play an important role in the evolution and virulence of many pathogens through lysogenic conversion by encoding virulence factors that may negatively impact human health[64]. Some examples of well-known bacteria, such as *Vibrio cholera, Streptococcus pyogenes,* or *Escherichia coli* O157:H7, have gained their pathogenicity through the acquisition of phages in their genomes [63]. Besides of encoding virulence factors, phages can also encode toxins and enhance bacterial resistance to serum and phagocytes (*E. coli* or *Pseudomonas aeruginosa)* or alter bacterial

susceptibility to antibiotics (*Staphylococcus aureus* or *S. pyogenes*) by transferring resistance genes through generalized transduction[65].

The utilisation of the lysogenic bacteriophages that could encode toxins and containing virulence genes and/or broad-spectrum drug-resistance genes could be used as tools to turn non-pathogenic bacteria into pandrug resistant bacteria which are resistant to all known antimicrobial agents. These lysogenic phages are potentials to be used in the manufacture of biological weapons that could be spread in an appropriate environment to produce highly pathogenic drug-resistant bacterial killers. Bioterrorist attacks using these method would be a secret and to detect or prevent dispersal of the biological agents derived from lysogenic bacteriophages would never be easy. Moreover, it would be very difficult to distinguish bacterial agents transformed by lysogenic bacteriophages from naturally occurring bacteria, and tracing them would be problematic. Thus, detection of these organisms is also equally important as a first step to prevent bioterrorist in exploiting these phages that would pose an unexpected biosafety risk [66].

1.2 Antibody: A recognition element in biological assays

An antibody (Ab) also known as immunoglobulin (Ig) is a large Y-shape protein consisting of two heavy chains and two light chains (figure 1) which form a functionally bivalent monomer that is produced by B cells receptor used by the immune system to identify and neutralize foreign objects such as bacteria and viruses [67]. The widely used rapid detection systems exploit antibodies for recognition, identification and quantification of target analytes [68]. Abs played an important role in the advancement of diagnostic assays making it indispensable in diagnostic tests that are currently used routinely in clinics in classical immunological methods such as ELISA, dot blot immunobinding assays, electrochemiluminescence, flow cytometry and several microscopic techniques like fluorescence up to the construction of numerous immunosensors. One of the

parameters that should always be considered in immunoassay methods is sensitivity. Sensitivity of the immunoassay is highly dependent on the affinity of the antibodies involved [69]. However, specificity of these antibodies to the target analyte should also be considered. Specificity is dependent not only on the binding property of the antibody but also on the composition of the sample antigen and its matrix, reagent composition, and immunoassay format. The lack of specificity may lead to false positive or negative results. Another parameter that should not be neglected is the cross-reactivity because it plays an important role in the quality of immunoassays. The ideal antibody exhibits minimal or no cross-reactivity and maximal sensitivity. Cross-reactivity can be defined as an interaction between paratope of antibody and similar epitope or identical epitope presented on different antigens [70].

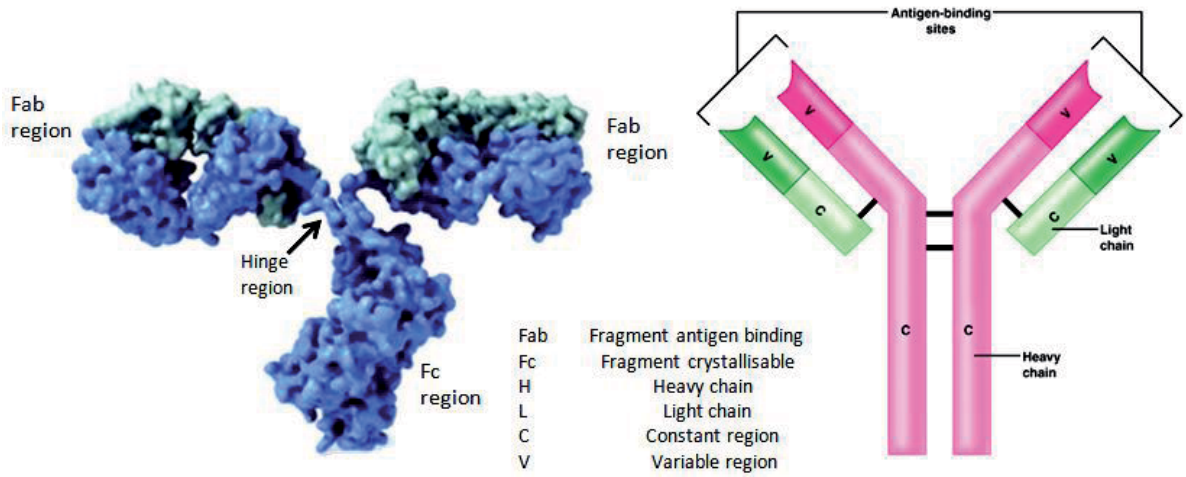

Figure 1.1 Typical structure of antibody.

1.2.1 Structures and classes of immunoglobulins (Ig)

There are five primary classes of Igs: They are IgG, IgM, IgA, IgD and IgE. Each class of Ig are distinguished by the type of heavy chain found in the molecule. The differences in heavy chains polypeptides for each Ig allow them to function differently from each other in specific stages

of immune responses [71]. The Polypeptide protein sequences that are responsible for these differences are found in Fc region. While there are five different types of heavy chains, there are only two main types of light chains: kappa (κ) and lambda (λ) [72]. Antibody classes differ in the number of different Y-like units that joins together (figure 2) to form the complete protein that differentiates them.

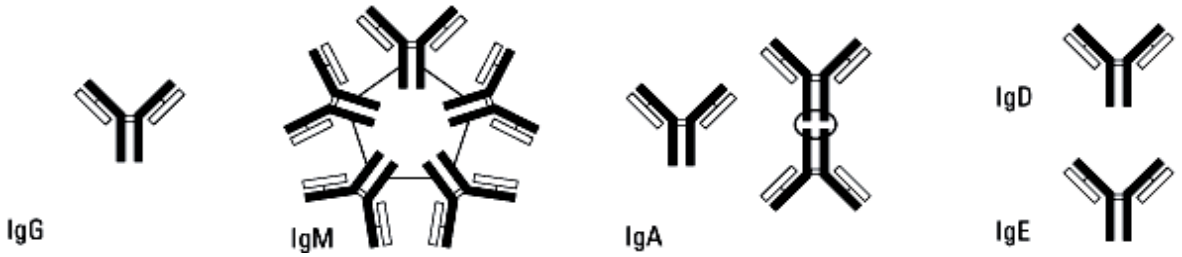

Figure 1.2 Typical structures of different antibodies.

Immunoglobulin G (IgG), a monomer, is the predominant Ig class present in human serum and is principally responsible for the recognition, neutralization, and elimination of pathogens and toxic antigens [73]. Maternal IgG is the only class of Ig that can transport across the placenta in humans to protect the newborn during the first months of life [74]. Because of abundance and excellent specificity toward antigens, IgG is the principle antibody used in immunological research and clinical diagnostics.

Immunoglobulin M (IgM) usually exists as a pentamer in mammals, which predominates in primary immune responses to most antigens and is the most efficient complement fixing immunoglobulin and comprises approximately 10% of normal human serum Ig content. IgM is mainly produced by the immune system for protection against numerous viral, bacterial, fungal and parasitic infections [75].

Immunoglobulin A (IgA) exists as both monomeric and dimeric forms in serum which comprises approximately 15% of the total serum Ig. Secretory IgA, a dimer, provides frontline defense against pathogens borne in aerosols, the environment, and in the diet because of its abundance in mucosal epithelia (e.g., saliva, tears). Although secretory IgA may not destroy totally the antigen, its principal function is to prevent passage of foreign substances into the circulatory system [76].

IgD and IgE are found in serum in much smaller quantities than other Igs. Membrane IgD is a receptor for antigen found mostly on mature B-lymphocytes. The biological function of IgD is still a complete mystery since it has been first discovered in 1965 [77]. IgD molecules do not cross the placenta and are not present in body secretions or urine. IgE antibodies are present in external secretions and to bind to basophils and mast cells to primarily defends against parasitic invasion and is responsible for allergic reactions [78]. Table 1 summarises the properties of each immunoglobulin [72] (http://www.piercenet.com).

Table 1.1 Summary of properties for each immunoglobulin

Classes of Ig	MW (g/mole)	H-chain type, MW (g/mole)	Serum concentration	total Ig (%)	Glycosylation (%weight)	Distribution (vascular)	Function (response)
IgG	150,000	gamma, 50,000	10 – 16 mg/mL	75	3	Intra and extra	Protect against toxic antigens
IgM	900,000	mu, 65,000	0.5 – 2 mg/mL	10	12	Intra	Primary response for toxins and pathogenic species
IgA	320,000	alpha, 55,000	1 – 4 mg/mL	15	10	Intra	protect mucus membranes
IgD	180,000	delta, 70,000	0 – 0.4 mg/mL	0.2	13	lymphocyte surface	Unknown
IgE	200,000	epsilon, 73,000	10 – 400 ng/mL	0.002	12	mast cells in salive and nasal secretions	against parasites

In addition to the five immunoglobulin classes, subclasses of Ig exist in all members of a particular animal species. Antibodies are classified into subclasses based on minor differences in the heavy chain type of each Ig class. In humans there are four subclasses of IgG: IgG1, IgG2, IgG3 and IgG4 (numbered in order of decreasing concentration in serum). Variance among different subclasses is less than the variance among different classes. For example, IgG1 is more closely related to IgG2, 3 or 4 than to IgA, IgM, IgD or IgE. Consequently, antibody-binding proteins (e.g., Protein A or Protein G) and most secondary antibodies used in immunodetection methods cross-react with multiple subclasses but usually not multiple classes of Ig.

1.2.2 Antibody production

Immunological assays rely on the use of antibodies as a capturing and labelling molecule for identifying different targets since Ab binds with biological agents with high affinity and specificity. Current immunological assays utilises the sensitivity and specificity of polyclonal and monoclonal antibodies with respect to their bimolecular antibody–antigen interactions [79]. Polyclonal antibodies (PAb) are produced from different B-lymphocyte lines as a mixture of Ig's. Monoclonal antibody (mAb) is the product of one type of B-lymphocyte.

Polyclonal antibodies are produced by immunization of a host animal such as a rabbit, mice, chicken or goat. Several factors have to be considered in the immunization protocol like the quantity of antigen, the route of injection, number and distribution of injection sites, the frequency of antigen injections, the particular adjuvant which enhance the immune response to an antigen, the quantity of adjuvant, and the ratio of antigen to adjuvant. Harvested Igs are always purified from the sera before being used for bio-detection [80, 81].

Monoclonal antibodies are complex and heteromultimeric glycoproteins. They are used as research reagents for diagnosis as well as for therapy for various human diseases and their demand

has increased substantially [82]. Köhler and Milstein developed methods for the isolation of mAb's from hybridoma cells in 1975. They demonstrated a cell fusion technique to produce hybrids between myeloma cells and antibody producing cells. The resulting hybrid lines were permanently adapted to grow in tissue culture and were capable of inducing antibody production in mice using Jerne's hemolytic plaque assay, which allows direct visualization of antibody-producing B cells [83]. Monoclonal antibodies that are produced in cultured cells should be in sufficient quantities to allow optimization and further refinement of antibody-based assays and development of the nonradioactive detection technologies that are currently used [68].

1.2.3 Labelling of antibodies

Antibodies are widely used in immunoassays to detect and quantify antigens. The antibody that recognizes the antigen is referred to as the 'primary' antibody and confers specificity to the assay. A 'label' is also incorporated into the assay using one of two methods like indirect or direct detection method to provide measurability. The label in an immunoassay provides either 'direct' or 'indirect' detection of the antigen. With direct detection, the label is attached via a covalent bond to the primary antibody. Alternatively, using indirect detection, the label is covalently attached to a secondary antibody, which is allowed to bind to the target (either antibody or antigen) during the immunoassay forming a sandwich assay format. Some commonly used immunoassay techniques are given in Table 2 along with examples of the types of labels that can be employed.

*Table 1.2 Types of Immuno-experiments and associated labels

Immunoassay	Labels
Western Blotting	Enzymes (usually HRP, or alkaline phosphatase)
ELISA	Enzymes, Biotin/Streptavidin
Immunofluorescence	Fluorescent dyes
Flow Cytometry	Fluorescent proteins or dyes, Tandem dyes

*From http://www.biomol.de

Antibodies like all proteins are composed of amino acids, and the side chain of lysine, which terminates in a primary amine (-NH2), is routinely used to link labels covalently to antibody molecules. There are two enzymes that are mostly used for labelling antibodies. They are horseradish peroxidase (HRP) and alkaline phosphatase (ALP).

There are four main chemical approaches for antibody labelling: (i) NHS esters, (ii) heterobifunctional reagents, (iii) carbodiimide and (iv) sodium periodate. The antibody labeling procedure is complicated by the fact that the antibody and label have multiple amines. In this situation it is usual to modify some of the lysines on one molecule (e.g. the antibody) to create a new reactive group (X) and lysines on the label to create another reactive group (Y). A 'heterobifunctional reagent' is used to introduce the Y groups, which subsequently react with X groups when the antibody and label are mixed, thus creating heterodimeric conjugates. A common procedure of this method is the use of succinimidyl acetylthioacetate (SATA). The SATA reacts with the primary amine of the antibody to form a SATA-modified protein. Formation of thiolated protein can be achieved by deprotecting the sulfuhydryl group of the SATA-modified protein. The conjugate can now be reacted with the label that has been also modified with maleimide (Y). Figure 3 summarises the chemical reaction of the conjugation process.

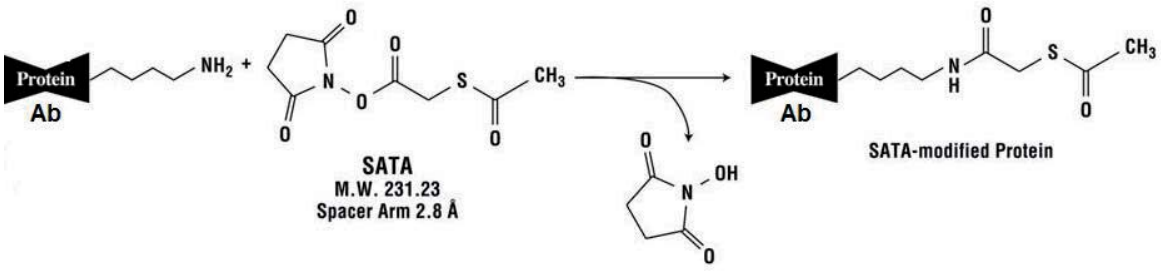

a) Reaction of SATA with a primary amine

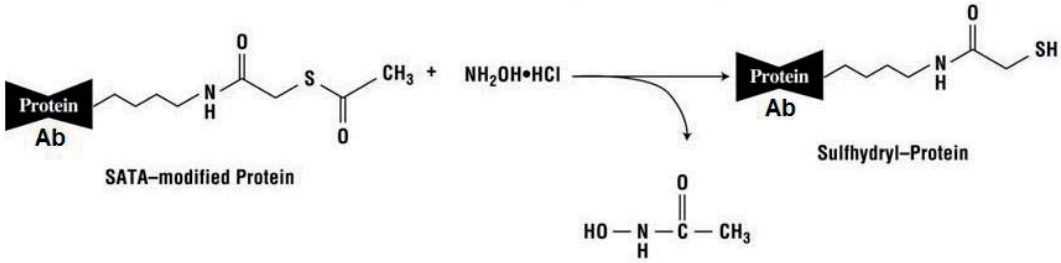

b) Deprotection with hydroxylamine to generate a sulfhydryl

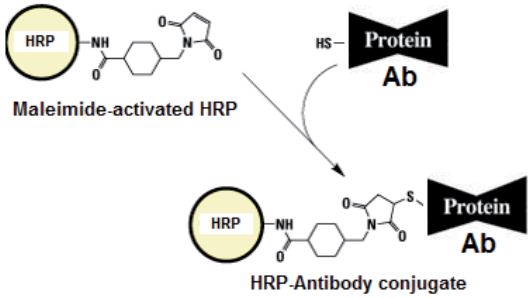

c) Conjugation with maleimide activated HRP

Figure 1.3 Conjugation process of Ab with Maleimide activated HRP using SATA.

In the carbodiimide conjugation method, 1-Ethyl-3-[3-imethylaminopropyl]carbodiimide hydrochloride (EDC or EDAC) is a common crosslinking agent used to create covalent links between amine- and carboxyl-containing molecules. Carbodiimides activate carboxyl groups, and the activated intermediate is then attacked by a primary amine present in the antibody or protein as depicted in Figure 4. Carbodimides are commonly used to conjugate antibodies to carboxylated

particles (e.g. latex particles, magnetic beads), and to other carboxylated surfaces, such as microwell plates or chip surfaces. In the case of sodium periodate, this chemical cannot be employed with the vast majority of labels but is quite an important reagent in that it is applicable to HRP, which is the most popular diagnostic enzyme aside from ALP. Periodate activates carbohydrate chains on the HRP molecule to create aldehyde groups, which are capable of reacting with lysines on antibody molecules. Since HRP itself has very few lysines it is relatively easy to create antibody-HRP conjugates without significant HRP polymerization[84].

1.2.4 Immobilisation of antibodies

Numerous methods are available for the immobilisation of macromolecules that are suitable for the construction of biosensors. Some methods will not be described due to large number of techniques that exceed the scope of this work and only techniques that bear importance to the work presented will be discussed. One of the main issues in the development of an immunosensor is maintaining the immunorecognition capability of the antibody after it has been immobilized on the sensing surface [85]. There are three well-known available methods for attaching antibodies and antigens onto solid surfaces based on interactions [86]: (i) adsorption, i.e physical-chemical adsorption, (ii) covalent attachment and (iii) affinity binding. Covalent methods improve uniformity and reproducibility of the immobilised proteins, i.e antibodies or antigens, onto different solid substrate surfaces by using defined linkages or strong gold (Au)-sulfur (S) bonds to form self-assembled monolayers (SAM) [87]. However, these methods may result in randomly immobilised protein and the binding sites might be partially blocked and this could lead to a decreased binding activity and selectivity of the antibodies resulting in heterogeneous output and false negatives.

Much effort has recently been put in the development of more highly efficient antibody immobilisation methods with regioselectively in a uniform orientation making it more sensitive than

those with random orientations for immunobiosensors [88]. Among the strategies reported is the use of immobilised proteins from *Staphylococcus aureus* (protein A), *Streptococcus C40* (protein G), and *Peptostreptococcus magnus* (protein L) to bind with the antibodies to the surface. Proteins A and G bind to the Fc region in the heavy chains, while protein L binds to κ-light chains outside of the antigen-binding site. They bind in a wide variety of antibodies with different affinities as presented in Table 3.

Table 1.3. Binding characteristics of Protein A, Protein G, and Protein L.

Species	Antibody Class	Protein A	Protein G	*Protein L
Human	Total IgG	S	S	S
	IgG_1, IgG_2	S	S	S
	IgG_3	W	S	S
	IgG_4	S	S	S
	IgM	W	NB	S
	IgD	NB	NB	S
	IgA	W	NB	S
	IgA_1, IgA_2	W	NB	S
	IgE	M	NB	S
	Fab	W	W	S
	ScFv	W	NB	S
Mouse	Total IgG	S	S	S
	IgM	NB	NB	S
	IgG_1	W	M	S
	IgG_{2a}, IgG_{2b}, IgG_3	S	S	S
Goat	Total IgG S6	W	S	NB
	IgG_1	W	S	NB
	IgG_2	S	S	NB
Rabbit	Total IgG	S	S	W
Rat	Total IgG	W	M	S
	IgG_1	W	M	S
	IgG_{2a}	NB	S	S
	IgG_{2b}	NB	W	S
	IgG_{2c}	S	W	S
Pig	Total IgG	S	W	S

W = weak binding, M = medium binding, S = strong binding, NB = no binding-means information not available, *Binding will only occur if the appropriate kappa light chains are present.

The binding affinity only refers to species and subclasses with the correct kappa light chains. Lambda light chains and some kappa light chains will not bind (From Pierce Biotechnology TECH TIP #34 http://www.piercenet.com).

Another method that has gained attention is the direct immobilisation of the antibody itself through its fragment region and thiol modified antibodies. The F(ab') fragment , which is about 50 kDa, can be produced from the reduction of F(ab')2 fragments by using cysteine[87]. The Fab' fragment contains a free sulfhydryl group that may be alkylated or used in conjugation with an enzyme. In contrast, $F(ab')_2$ fragment antibodies are generated by pepsin, papain, ficin or bromelain digestion of whole IgG antibodies to remove most of the Fc region while leaving intact some of the hinge region[89]. $F(ab')_2$ fragments have two antigen-binding F(ab') portions linked together by disulfide bonds, and therefore are divalent with a molecular weight of about 110 kDa.

To date, the use of F(ab') fragment in the field of biosensing has been widely explored such as grapheme field-effect transistor immunosensor [90], SPR-based immunosensors for human growth hormone detection [91] and bovine leukaemia virus [92] and quartz crystal microbalance for the detection of pathogenic Escherichia coli O157:H7 [93]. The antigen-binding activities of immobilized F(ab') fragments gained improved sensitivity of developed biosensors as compared to conventional use of whole antibody having random orientations when immobilised [87].

Figure 4 shows a scheme of typical immobilisation of proteins and antibodies by self-assembled monoloyer (SAM) of thiolated functional group through carbodiimide conjugation chemistry and direct chemisorption of fragments.

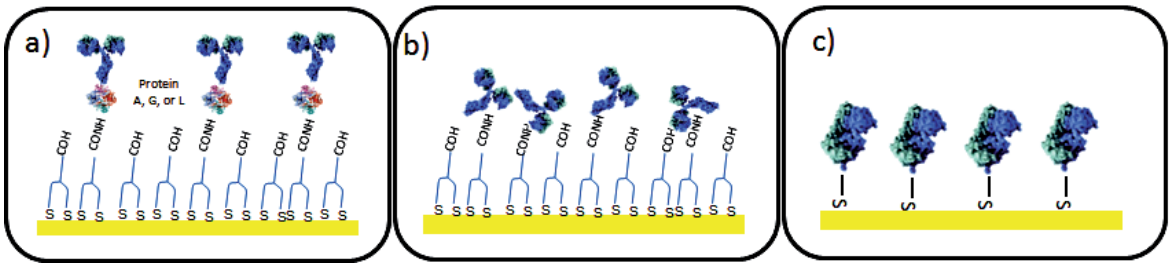

Figure 1.4 Typical scheme of immobilising immunoglobulins using SAM of a) protein A, G, or L, b) whole Ab and c) fragment Ab (F(ab)). The metal layer was modified by SAM bipodal through carbodiimide conjugation chemistry for a and b.

1.3 Biosensors for biowarfare agents

As has been discussed in section 1.1.1, there is a defined need for an immediate detection and identification of the biowarfare agents not only in environmental samples but also in affected individuals. Development of detection systems for biowarfare relies on two purposes: (i) detection of the agents to treat and allow early detection of the disease or (ii) detection of the agent to protect and provide early warning to the site contaminated with dangerous agents to avoid infection [94].

Many methods currently available are being used simultaneously for the detection and identification of several biowarfare agents. The most conventional and widely used method in identifying a certain biowarfare agent is using the biochemical test based assays in which the bacteria are cultured and identification is based on biochemical tests [95]. The presence of adenosine triphosphate (ATP) in all living cells like viruses and bacteria, ATP interaction with luciferin and luciferase, the enzyme, is usually monitored by bioluminescence. The intensity of light produced is proportional to the amount of ATP and therefore the degree of contamination in the presence of any microorganisms can be established [96]. Although this system is cost effective for real time air monitoring to trigger alarm for any unusual rise in the microbial load in the environment, there is always a possibility of ATP contamination from non-microbial sources.

Immunologic detection of antigens and antibodies is widely used for the detection of bacterial and viral biowarfare agents. Enzyme linked immunosorbent assay (ELISA) has been developed to detect not only various diseases associated with biowarfare agents but also the causative agents. Many different formats have been developed trying to mimic ELISA using different substrate labels, like fluorescent, chemiluminescent, electrochemiluminescent and on various platforms like solid support ELISA plates, visual dot and lateral flow formats[97]. Lateral flow system has gained popularity due to rapidity and cost effectiveness when compared to instrument-based detection systems. These tests are based on single use, disposable tests in the form immunochromatographic (ICT) line assays that generate visual lines in the membrane [16], which rapid and easy to perform, but there are high false positive results and normally a confirmative lab-based test is needed.

Recent development in nucleic acid-based diagnostic assays, in particular quantitative polymerase chain reaction (Q-PCR), offers significant advantages over culture-based and immunologic methods for the detection and quantification of biowarfare agents. It is the most researched and developed detection system and have found the greatest use for biowarfare agent analysis because of its' rapidity, sensitivity, and reproducibility, and the reduced risk of human error [98]. In conventional PCR, the bacteria and spores should be disrupted to make the endogenous DNA available for amplifying the specific region of the genome before checking on electrophoresis for the amplification of correct size of product [99]. In Q-PCR assays, the PCR amplification is combined with real time detection based on reporter fluorescence dyes. As the DNA is amplified, the dye is intercalated into the product. In non specific Q-PCR, the amplified DNA is detected based on DNA intercalating fluorescence dyes (SYBR green) [100]. For specific detection, the change in fluorescence relies on the use of dual-labeled fluorogenic probes containing both a reporter fluorescent dye and a quencher dye. An increase in fluorescence indicates that the probe has

hybridized to the target DNA and the quencher dye is no longer able to mask the signal of the fluorescent dye [16]. Q-PCR is used for a variety of applications from quantitative presence or absence tests and rapid confirmation tests to monitor gene expression which is the most commonly used.

Although these standard techniques presented are sensitive in the detection and identification of biowarfare agents, they are rather time consuming, require expensive instrumentation, require trained personnel and the high risk involved in handling samples. The use of biosensors is envisaged to be a valid alternative technology that could be rapid, accurate and unequivocally confirm the presence of these agents not only giving a very low detection limit added to the possibility of detection in varied situations and diverse matrices giving an ideal detection system.

According to the International Union of Pure and Applied Chemistry (IUPAC), a biosensor is a self contained integrated device capable of providing quantitative or semi-quantitative analytical information using a biological recognition element, which is retained in direct spatial contact with a suitable transducer responsible for detecting the biological reaction and converting it into a measurable signal [101](figure 5).

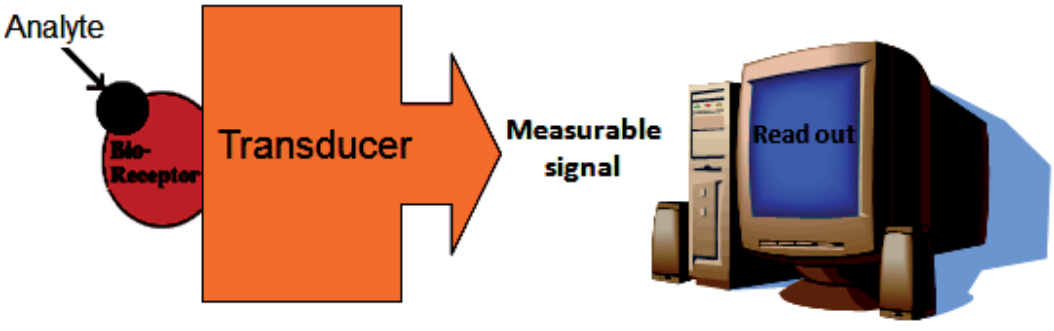

Figure 1.5 Schematic representation of a biosensor.

The biological sensing material or bio-receptor may be a protein such as an enzyme or antibody, antibody fragment, a nucleic acid, a whole microbial cell, or even a plant or animal tissue. Biosensors can be divided into catalytic (enzyme) and affinity (antibodies, lectins, or DNA) sensors. The signal transducer determines the extent of the biorecognition event and converts it into a measurable electronic signal, which can be recorded by the end user [94]. Common transducers include amperometric electrodes, optical waveguides or mass sensitive piezoelectric crystals.

1.3.1 Electrochemical biosensors

Electrochemical biosensors are the most commonly used class of biosensors based on a bio-interaction process. During the bio-interaction process, an electrochemical species is consumed or generated producing an electrochemical signal that is recorded into a measurable signal by an electrochemical detector. Electrochemical biosensors have high sensitivity, selectivity, ability to operate in turbid solutions and rapid analysis, and are amenable to miniaturization [102]. Depending on the electrochemical property to be measured, electrochemical biosensors may be further divided into potentiometric, impedimetric and amperometric biosensors.

1.3.1.1 Potentiometric biosensors

Potentiometric measurement involves the determination of the potential difference between an indicator and a reference electrode [103]. They function under equilibrium conditions and monitor the accumulation of charge, at zero current, created by selective binding at the electrode surface [104]. The electrode surface consists of a perm-selective outer layer and a bioactive material, such as an enzyme, where the enzyme-catalysed reaction generates or consumes a species, which is detected by an ion selective electrode [105]. As can be seen in figure 6 [106], the transducer is an ion-selective electrode (ISE), which is an electrochemical sensor, based on thin films or

selective membranes as recognition elements. ISEs can detect ions such as F^-, I^-, CN^-, Na^+, K^+, Ca^{2+}, H^+, NH_4^-, or gas (CO_2, NH_3) in complex biological matrices by sensing changes in electrode potential when the ions bind to an appropriate ion exchange membrane. The potential difference between these indicator and reference electrodes are proportional to the logarithm of the ion activity or gas fugacity (or concentration), as described by the Nernst equation [102].

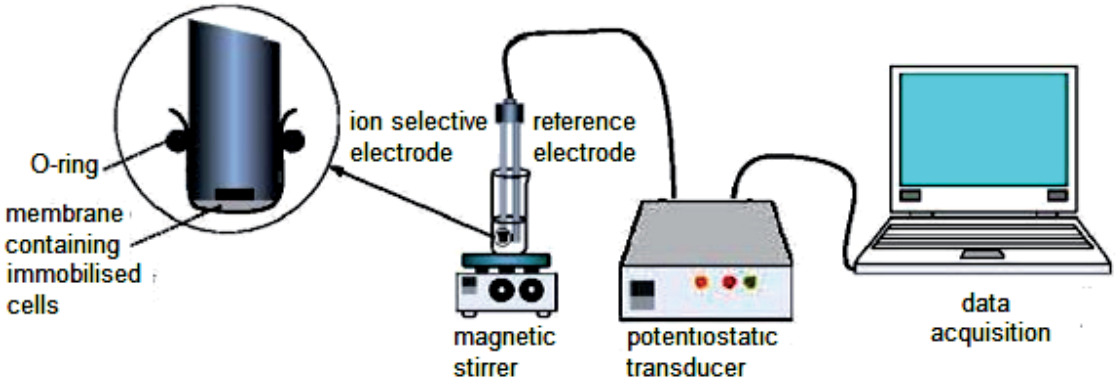

Figure 1.6 Typical schematic diagram of a potentiometric biosensor assays.

Direct potentiometric immunosensor have been reported where using secondary antibody labelled with ALP and addition of substrate p-nitropehnylphosphate to produce corresponding ions for detection [107]. Modified ion selective field effect transistors (ISFETs), which utilise the semiconductor field-effect is another approach for the detection of biological recognition events [108]. ISFETs use an electric field to create regions of excess charge in a semiconductor substrate in order to enhance or decrease local conductivity. The application of these devices in the field of biosensor is not as attractive like as other electrochemical techniques due to problems related to production which include incompatibility of most biomolecule immobilisation methods with the ISFET fabrication technology and difficulty in packaging and encapsulation at wafer level, poor

biosensor performance such as detection limits, linear range and reproducibility and as well as inadequate device stability [109].

1.3.1.2 Impedimetric biosensors

Electrochemical impedance spectroscopy (EIS) is a powerful method for analysing the complex electrical resistance of a system and is sensitive to surface phenomena and changes in bulk properties [110]. It has been demonstrated to be a promising method for pathogenic bacteria detection due to its portability, rapidity, sensitivity, and more importantly it could be used for in-situ detection [111]. Unlike amperometry or potentiometry, labels are no longer necessary making it simpler for sensor preparation. The application of EIS to DNA probe[112] or antibody modified electrodes [113] can be significantly more sensitive than their traditional counterparts such as amperometric, voltammetric, and potentiometric. However, its' detection limits are still poor compared to these methods [109].

Impedance detection technique is classified into two types depending on the presence or absence of specific bio-recognition elements. The first type measures the impedance change caused by the binding of targets to the sensing molecules immobilised in the surface of the electrode. The binding ability of the target, i.e. antigen, antibody, or DNA, and the sensing molecule is then verified through the detection of either a shift in impedance, or change in capacitance or admittance at the bulk of the electrode interface due to the insulating properties. The detection principle of the second type is based on metabolites produced by bacterial cells as a result of growth.

1.3.1.3 Amperometric biosensors

Amperometric biosensors are simpler in comparison to the previously discussed electrochemical biosensors. Amperometric detection of target analytes, i.e. micro-organisms,

antigens, antibodies, or specific complementary target DNA, relies on the measurement of the current generated through electrooxidation/reduction catalysed by their enzymes, or by their involvement in a bioaffinity reaction at the surface of the working electrode. The potential of the working electrode, which could be noble metals, graphite, modified forms of carbon or conducting polymers, is maintained with respect to a reference electrode, usually Ag/AgCl, which is at equilibrium. The current produced is linearly proportional to the concentration of the electroactive product [105, 114]. Figure 7 shows a typical three electrode system in an amperometric biosensor.

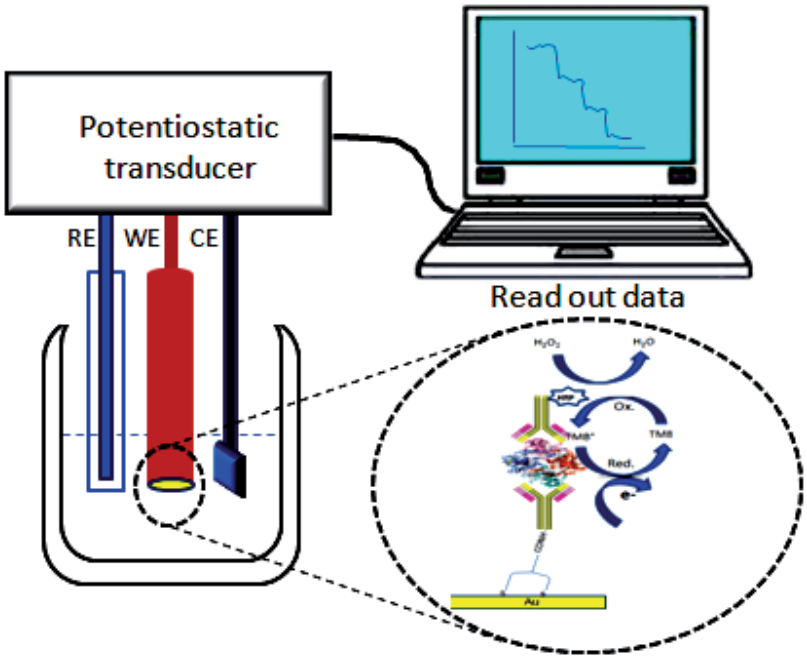

Figure 1.7 Schematic diagram of a typical amperometric biosensor. RE: reference electrode, WE: working electrode, CE: counter electrode.

Amperometric biosensors have the advantage of being highly sensitive, rapid, and inexpensive. The advantage of linear concentration dependence of amperometry makes it well suited for detecting pathogenic species. Amperometric sensors aimed at bacteria detection using antibodies raised against the cell lysate of the bacteria have been developed where the detection range is

normally reported as 'CFU/mL' (colony forming units per mL) or number of 'cells/mL'. Table 4 summarises the recent works on pathogenic detection for biowarfare based on amperometric biosensors with their corresponding obtained limit of detection.

Table 1.4 Immunosensors for pathogen detection

Pathogen detected	Electrode type, immobilisation	Detection limit (cells/mL)	Reference
F. tularensis	Screen-printed gold, adsorption of capture antibody	100	[115]
V. cholera	Screen-printed carbon, adsorption of capture antibody	10^5	[116]
B. anthracis	Lithographic gold, magnetic beads with capture antibody	10^4	[117]
S. penumoniae	Screen-printed gold, magnetic beads-protein A-capture antibody	$1.5x10^4$	[118]
S. typhimurium	Screen-printed gold, adsorption of capture antibody	20	[119]
S. aureus	Screen-printed gold, magnetic beads-protein A-capture antibody	1	[120]
E. coli	Graphite, glutaraldehyde-capture antibody	1000	[121]

1.4 Nanostructuring of electrodes*:* Electrochemical biosensor enhancement

In recent years, there has been an intensive research effort in the field of electrochemical biosensors seeking designs to provide better analytical characteristics in terms of sensitivity, selectivity, reliability, ease of fabrication and use, and lower limits of detection [122]. Electrode nanostructuring is one of the avenue that has been pursued and can be achieved by tailoring the active surface layers of the electrodes by means of advances in nanofabrication providing the electrode with unique properties, due to their enhanced surface area, higher capacitance, higher spatial resolution of measurements, and higher sensitivity that leads in providing enhanced performance characteristics of biosensor devices in comparison to planar substrates [123].

Nanostructured electrodes can be regarded as controlling the architecture of the surface of the electrode at the nanoscale using nanomaterials, templating methods, organic film modification or hybrid modification layers which can be organic monolayers with biomolecules or nanomaterials [122]. Structuring the surface may be achieved by chemical to nanotechnology approaches that involve bottom-up and top down methods to generate nanostructured materials on electrode surfaces [124]. A wide range of electrode surface modification techniques have been reported including electrochemical deposition of metals [125, 126] and polymers [127] or composite films [128] and nanofabrication via different approaches including thermal chemical vapor deposition [129] and lithographic techniques [130] that have been found to improve sensitivity.

More recently, the use of electrochemical methodologies to deposit nanoscale architectures from molecular components has been exploited via incorporation of a template media. The use of liquid and colloidal crystals [131] as templates has been extensively used to produce mesoporous and macroporous nanostructured materials such as metals [132-135] and polymer films [136] or composites [137, 138] resulting in a higher surface area and increased electroactive area that facilitates lower detection limits and enhanced sensitivity.

In addition to electrode surface properties, the orientation of the biosensing molecules is also crucial in the development of electrochemical biosensors. As an example, the performance of a DNA biosensor is dependent on the overall efficiency of hybridization between surface immobilised nucleic acids and target complementary sequences. The formation of self assembled monolayers (SAMs) of short DNA probes on surfaces of metallic electrodes is one of the most straightforward approaches to immobilize a DNA molecule on a metal surface but the main fallback is the formation of highly packed DNA SAMs that affects the overall efficiency of the biosensor due to high DNA probe density [139] whilst direct chemisorption of an antibody onto the surface of the electrode has been reported to have an increased immunosensor performance [87] as immobilisation

of antibodies is crucial as a lack of control of the orientation of antigenic site that can lead to heterogeneous signals. It is well established that the surface chemistry is a critical factor and different immobilisation techniques in immobilising sensing molecules have been explored in the last decade to improve sensor performance. Several strategies have been reported to have controlled surface probe density, including co-immobilisation [140] and backfilling [141], and nanopatterning strategies to ensure a good coverage of sensing molecules whilst maintaining appropriate spacing [142] and in order to avoid probe cluttering and excessive fouling [125] of the electrode surface to achieve better performance characteristics.

1.5 Thesis objectives

Current efforts in the development of biosensors focus on new platforms for the accurate and sensitive analysis of biowarfare agents and the associated disease caused by these pathogens. Considering the general availability of the know-how to culture microorganisms in large quantities, there is a fear about the possibility of using hazardous pathogens for bioterrorism attacks and late detection and diagnosis could lead to high number of infection or even worst like death. Biosensors can play an important role in the early detection of these pathogenic species and early diagnosis of associated disease. In this work, we focused our attention on the development of an electrochemical: (i) immunosensor and (ii) DNA biosensor for the detection of different biowarfare agents.

In the development of the immunosensors, detection of *F. tularensis* bacterial cells and its associated anti-*Francisella tularensis* antibodies has been achieved. Specific objectives for the accomplishment of the developed immunosensor for detecting bacterial cells were to:

- Determine the optimal assay arrangement for the detection of the bacterial cells.
- Study of the optimum method in surface immobilisation of capture antibodies, i.e. using whole and fragment antibodies.

- Analysis of the synthesised secondary antibodies labelled with enzyme HRP.
- Study the incubation time and incubation temperature in the detection of antigens, i.e. LPS and whole bacterial cells.
- Study the specificity of the developed biosensor.
- Stability studies of the immobilised capture antibodies.
- Incorporating the developed immunosensor to microfluidics and automated set-up.

In addition to the immunosensor development, detection of anti-*Francisella tularensis* antibodies has also been explored and developed. A study on the optimum capture probe has been achieved using ELISA. Optimisation of the coating probe and labelling probe concentration was also achieved. Real samples were analysed using the developed immunosensors.

Furthermore, a multiplexed DNA biosensor array for the simultaneous detection of eight (8) virulent species has been developed. To accomplish this, the specific objectives were to:

- Determine the optimal immobilisation approach in order to achieve high sensitivity, stability and occurrence of non-specific interaction.
- Determine the optimum hybridisation conditions and detection strategy.
- Study the cross reactivity of the designed capture probes and the designed labelled probes.
- Study the stability of the biosensor.
- Incorporating the developed DNA biosensor with microfluidics and automated set-up.

Finally, to improve sensitivity and to lower the limit of detection developed DNA biosensor was explored using nanotemplating. The templating system using lyotropic liquid crystals was exploited for immobilisation of thiolated capture probes facilitating optimum spaced-

immobilised probes. To demonstrate an improved surface chemistry, the specific objectives were set to:

- Investigate different phases of lyotropic liquid crystals using the surfactant octaethylene glycol monohexadecyl ether ($C_{16}EO_8$).
- Study the hydrophobic and hydrophilic domains available in the template.
- Study the probe density immobilised in each immobilisation condition.
- The use of imaging techniques to directly visualise the orientation of immobilised probes in the surface of the electrodes.
- Compare the biosensor performance of a conventional immobilisation technique (non-templated) with the templated system.

Overall, this work will contribute in different areas involved in the development of electrochemical quantitative and qualitative sensing platforms methods, from fundamental aspects such as the choice of a better immobilisation technique of sensing probes to the improvement of biosensor performance such as sensitivity and lower limit of detection.

1.6 References

1. Frischknecht, F., *The history of biological warfare.* European Molecular Biology Organization, 2003. 4(Special issue): p. S47-S52.
2. Wheelis, M., *Biological Warfare at the 1346 Siege of Caffa.* Emerging Infectious Diseases, 2002. 8(9): p. 971-975.
3. Riedel, S., *Biological warfare and bioterrorism: a historical review.* Baylor University Medical Center Proceedings, 2004. 17(4): p. 400-406.
4. Metcalfe, N., *A short history of biological warfare.* Medicine, Conflict and Survival, 2002. 18(3): p. 271-282.
5. Roffey, R., Tegnell, A., and Elgh, F., *Biological warfare in a historical perspective.* Clinical Microbiology and Infection, 2002. 8(8): p. 450-454.
6. Pichtel, J., *Terrorism and WMDs: Awareness and Response.* CRC Press, Boca Raton, 2011: p. 127.
7. Willis, E.A., *Seascape with monkeys and guinea-pigs: Britain's biological weapons research programme,1948–54.* Medicine, Conflict and Survival, 2003. 19(4): p. 285-302.
8. Szinicz, L., *History of chemical and biological warfare agents.* Toxicology, 2005. 214: p. 167–181.

9. Roffey, R., Tegnell, A., and Elgh, F., *Biological weapons and bioterrorism preparedness: importance of public-health awareness and international cooperation.* Clinical Microbiology and Infection, 2002. 8(8): p. 522-528.
10. Millet, P.D., *The Biological and Toxin Weapons Convention.* Revue Scientifique Et Technique De L`Office Iinternational Des Epizooties, 2006. 25(1): p. 35-52.
11. Leitenberg, M., *Biological Weapons in the Twentieth Century: A Review and Analysis.* Critical reviews in microbiology, 2001. 27(4): p. 267-320.
12. Gunn, A., and Pitt, S. J., *Microbes as forensic indicators.* Tropical biomedicine, 2012. 29(3): p. 311-330.
13. Enserink, M., and Kaiser, J., *U.N. Taps special labs to investigate syrian attack.* Science, 2013. 341(6150): p. 1050-1051.
14. Bush, L.M., andPerez, M. T., *The Anthrax Attacks 10 Years Later.* Annals of internal medicine, 2012. 156(1): p. 41-44.
15. Sternbach, G., *The history of anthrax.* The Journal of Emergency Medicine, 2003. 24(4): p. 463-467.
16. Lim, D.V., Simpson, J. M., Kearns, E. A., Kramer, M. F., *Current and developing technologies for monitoring agents of bioterrorism and biowarfare.* Clinical Microbiology Reviews, 2005. 18: p. 583-607.
17. Bhalla, D.K., and Warheit, D. B., *Biological agents with potential for misuse: a historical perspective and defensive measures.* Toxicology and Applied Pharmacology, 2004. 199: p. 71-84.
18. Chakraborty, A., Khan, S. U., Hasnat, M. A., Parveen, S., Islam, M. S., Mikolon, A., Chakraborty, R. J., Ahmed, B., Ara, K., Haider, N., Zaki, S. R., Hoffmaster, A. R., Rahman, M., Luby, S. P., and Hossain, M J., *Anthrax Outbreaks in Bangladesh, 2009–2010.* American journal of tropical medicine and hygiene, 2012. 86(4): p. 703-710.
19. Schwartz , M., *Dr. Jekyll and Mr. Hyde: A short history of anthrax.* Molecular Aspects of Medicine, 2009. 30: p. 347–355.
20. Sweeney, D.A., Hicks, C. W., Cui, X., Li, Y., and Eichacker, P Q., *Anthrax infection.* American Journal of Respiratory and Critical Care Medicine, 2011. 184(12): p. 1333-1341.
21. Ågren, J., Hamidjaja, R. A., Hansen, T., Ruuls, R., Thierry, S., Vigre, H., Janse, I., Sundström, A., Segerman, B., Koene, M., Löfström,C., Van Rotterdam, B. and Derzelle, S., *In silico and in vitro evaluation of PCR-based assays for the detection of Bacillus anthracis chromosomal signature sequences.* Virulence, 2013. 4(8): p. 671–685.
22. Tang, S., Moayeri, M., Chen, Z., Harma, H., Zhao, J., Hu, H., Purcell, R. H., Leppla, S. H. and Hewlett, I. K., *Detection of anthrax toxin by an lltrasensitive immunoassay using europium nanoparticles.* Clinical and vaccine immunology, 2009. 16(3): p. 408–413.
23. Amoako, K.K., Janzen, T. W., Shields, M. J., Hahn, K. R., Thomas, M. C., and Goji, N., *Rapid detection and identification of Bacillus anthracis in food using pyrosequencing technology.* International Journal of Food Microbiology 2013. 165: p. 319–325.
24. Franco, M.P., Mulder, M., Gilman, R. H., Smits, H. L., , *Human brucellosis.* Lancet infectious diseases, 2007. 7: p. 775-786.
25. Kose, S., Serin, S., Senger, E., Akkoclu, G., Kuzucu, L., Ulu, Y., Ersan, G., and Oguz, F., *Clinical manifestations, complications, and treatment of brucellosis: evaluation of 72 cases* Turkish journal of medical sciences, 2014. 44: p. 220-223.
26. Galińska, E.M.a.Z., J., *Brucellosis in humans – etiology, diagnostics, clinical forms.* Annals of Agricultural and Environmental Medicine, 2013. 20(2): p. 233–238.
27. Debeaumont, C., Falconnet, P. A. and Maurin, M., *Real-time PCR for detection of Brucella spp. DNA in human serum samples.* European journal of clinical microbiology and infectious dieseases, 2005. 24(12): p. 842-45.
28. Magnarelli, L., Levy, S., and Koski, R., *Detection of antibodies to Francisella tularensis in cats.* Research in vetenerary science, 2007. 82: p. 22-26.

29. Kleo, K., Schafer, D., Klar, S., Jacob, D., Grunow, R., and Lisdat, F., *Immunodetection of inactivated Francisella tularensis bacteria by using a quartz crystal microbalance with dissipation monitoring.* Anal Bioanal Chem, 2012. 404: p. 843-851.
30. Penn, R.L., *Francisella tularensis (tularemia).* Mandell, Douglas and Bennett's principles and practice of infectious diseases, 2005. 2: p. 2927-2937.
31. Dennis, D.T., Inglesby, T.V., Henderson, D. A., Bartlett, J. G., Ascher, M. S., Eitzen, E., Fine, A. D., Friedlander, A. M., Hauer, J., Layton, M., Lillibridge, S. R., McDade, J. E., Osterholm, M. T., O'Toole, E., Parker, G., Perl, T. M., Russel, P. K., and Tonat, K., *Tularemia as a biological weapon.* JAMA: the journal of the American Medical Association, 2001. 285(21): p. 2763-2773.
32. Su, J., Yang, J., Zhao, D., Kawula, T. H., Banas, J. A., and Zhang, JR., *Genome-wide identification of Francisella tularensis virulence determinants.* Infection and immunity, 2007. 75(6): p. 3089-3101.
33. Johansson, A., Ibrahim, A., Göransson, I., Eriksson, U., Gurycova, D., Clarridge, J. E, and Sjöstedt, A., *Evaluation of PCR-Based Methods for Discrimination ofFrancisella Species and Subspecies and Development of a Specific PCR That Distinguishes the Two Major Subspecies of Francisella tularensis.* Journal of clinical microbiology, 2000. 38(11): p. 4180-4185.
34. Bystrom, M., Bocher, S., Magnusson, A., Prag, J., Johansson, A., *Tularemia in Denmark: identification of a Francisella tularensis subsp. holarctica strain by real-time PCR and high-resolution typing by multiple-locus variable-number tandem repeat analysis.* Journal of clinical microbiology 2005. 43(10): p. 5355–5358.
35. Simşek, H., Taner, M., Karadenizli, A., Ertek, M., and Vahaboğlu, H., *Identification of Francisella tularensis by both culture and real-time TaqMan PCR methods from environmental water specimens in outbreak areas where tularemia cases were not previously reported.* Eur J Clin Microbiol Infect Dis., 2012 31(9): p. 2353-2357.
36. Versage, J.L., Severin, D. D., Chu, M.C. and Petersen, J. M., *Development of a multitarget real-time TaqMan PCR assay for enhanced detection of Francisella tularensis in complex specimens.* Journal of clinical microbiology, 2003. 41: p. 5492–5499.
37. Porsch-Ozcürümez, M., Kischel, N., Priebe, H., Splettstösser, W., Finke, EJ., Grunow, R., *Comparison of enzyme-linked immunosorbent assay, Western blotting, microagglutination, indirect immunofluorescence assay, and flow cytometry for serological diagnosis of tularemia.* Clin Diagn Lab Immunol, 2004. 11(6): p. 1008-1015.
38. Pohanka, M., and Skládal, P., *Electrochemical biosensors – principles and applications.* Journal of applied biomedicine, 2008. 6: p. 57-64.
39. Emanuel P. A., B.R., Dang J. L., McClanahan R., David J. C., Burgess R. J., Thompson J., Collins L., and Hadfield T., *Detection of Francisella tularensis within infected mouse tissues by using a hand-held PCR thermocycler.* Journal of Clinical Microbiology, 2003. 41(2): p. 689-693.
40. Bianucci, R., Rahalison, L., Massa, E. R., Peluso A., Ferroglio, E. and Signoli, M., *Technical Note: A Rapid Diagnostic Test Detects Plague in Ancient Human Remains: An Example of the Interaction Between Archeological and Biological Approaches Southeastern France, 16th–18th Centuries).* American journal of physical anthropology, 2008. 136: p. 361-367
41. Didier Raoult, D.M., N., Bitam, I., Piarroux, R., Drancourt, M., *Plague: History and contemporary analysis.* Journal of infection, 2013. 66: p. 18-26.
42. Harbeck, M., Seifert, L., Hansch, S., Wagner, D. M., Birdsell, D., Parise, K. L., Wiechmann, I., Grupe, G., Thomas,A., Keim,P., Zoller, L., Bramanti, B., Riehm, J. M. and Scholz, H. C., *Yersinia pestis DNA from skeletal remains from the 6th century AD reveals insights into justinianic plague.* PLOS Pathogens, 2013. 9(5): p. e1003349.
43. Louie, A., VanScoy, B., Liu, W., Kulawy, R., Brown, D., Heine, H. S. and Drusano, G. L., *Comparative efficacies of candidate antibiotics against Yersinia pestis in an in vitro pharmacodynamic model.* Antimicrobial Agents and Chemotherapy, 2011. 55(6): p. 2623–2628.

44. Dentovskaya, S.V., Kopylov, P. K., Ivanov, S. A., Ageev, S. A. and Anisimov, A. P., *Molecular bases of vaccine prevention of plague.* Molecular Genetics, Microbiology and Virology, 2013. 28(3): p. 87-98.
45. Heine, H.S., Chuvala, L,. Riggins, R., Hurteau, G., Cirz, R., Cass, R., Louie, A., Drusanoa, G. L., *Natural History of Yersinia pestis Pneumonia in Aerosol-Challenged BALB/c Mice.* Antimicrobial Agents and Chemotherapy, 2013. 57(5): p. 2010 -2015.
46. Simon, S., Demeure, C., Lamourette, P., Filali, S., Plaisance, M., Creminon, C., Volland, H. and Carniel, E., *Fast and simple detection of Yersinia pestis applicable to field investigation of plague foci.* PLOS ONE, 2013. 8(1): p. e54947.
47. Maurin, M.a.R., D., *Q Fever.* Clinical Microbiology Reviews, 1999. 12(4): p. 518–553.
48. Wielders, C., Morroy, G., Wever, P. C., Coutinho, R. A., Schneeberger, P. M. and Van der Hoek, W., *Strategies for early detection of chronic Q-fever: a systematic review.* European Journal of Clinical Investigation, 2013. 43(6): p. 616–639.
49. Hechemy, K.E., *History and Prospects of Coxiella burnetii Research* Advances in experimental medicine and biology, 2012. 984: p. 1-11.
50. Hernychova, L., Toman, R., Ciampor, F., Hubalek, M., Vackova, J., Macela, A. and Skultety, L., *Detection and identification of Coxiella burnetii based on the mass spectrometric analyses of the extracted proteins.* Analytical Chemistry, 2008. 80(18): p. 7097–7104.
51. Thibault, F.M., Hernandez, E., Vidal, D. R., Girardet,M. and Cavallo, J. D., *Antibiotic susceptibility of 65 isolates of Burkholderia pseudomallei and Burkholderia mallei to 35 antimicrobial agents.* Journal of Antimicrobial Chemotherapy 2004. 54: p. 1134-1138.
52. Heiss, C., Burtnick, M. N., Roberts, R. A., Black, I., Azadi, P. and Brett, P. J., *Revised structures for the predominant O-polysaccharides expressed by Burkholderia pseudomallei and Burkholderia mallei.* Carbohydrate research, 2013. 381: p. 6-11.
53. Van Zandt, K.E., Greer, M. T. and Gelhaus, H. C., *Glanders: an overview of infection in humans.* Orphanet Journal of Rare Diseases, 2013. 8: p. 131.
54. Dowling, A.J., *Novel gain of function approaches for vaccine candidate identification in Burkholderia pseudomallei.* Frontiers in cellular and infection microbiology, 2013. 2: p. 139.
55. Hara, Y., Chin, C. Y., Mohamed, R., Puthucheary, S. D. and Nathan, S., *Multiple-antigen ELISA for melioidosis - a novel approach to the improved serodiagnosis of melioidosis.* BMC infectious diseases, 2013. 13: p. 165.
56. Limmathurotsakul D, D.D.A.B., Wuthiekanun V., Kaestli M., Mayo M, et al., *Systematic Review and Consensus Guidelines for Environmental Sampling of Burkholderia pseudomallei.* PLOS Neglected Tropical Diseases, 2013. 7(3): p. e2105.
57. Van Cuyk, S., Deshpande, A., Hollander, A., Duval, N., Ticknor, L., Layshock, J., Gallegos-Graves, L. and Omberg,K. M., *Persistence of Bacillus thuringiensis subsp. kurstaki in Urban Environments following Spraying.* Applied and environmental microbiology, 2011. 77(22): p. 7954–7961.
58. Valadares de Amorim, G., Whittome, B., Shore, B. and B. Levin, D. B., *Identification of Bacillus thuringiensis Columbia, Canada, with Foray 48B after Aerial Spraying of Victoria, British from Environmental and Human Samples subsp. kurstaki Strain HD1-Like Bacteria I.* Applied and environmental microbiology, 2001. 67(3): p. 1035-1043.
59. Samples J. R., B.H.J.I.D., *Ocular infection caused by a biological insecticide.* Journal of infectious diseases, 1983. 148(3).
60. Hernandez E., R.F., Cruel T., Ducoureau J. P., Alonso J. M., Cavallo J. D., *Bacillus thuringiensis serovar H34-konkurkian superinfection: report of one case and experimental evidence of pathogenicity in immunosupressed mice.* Journal of clinical microbiology, 1998. 36(7): p. 2138–2139.

61. Hendriksen, N.B.a.H., B. M., *Detection of Bacillus thuringiensis kurstaki HD1on cabbage for human consumption.* FEMS microbiology letters, 2006. 257(1): p. 106–111.
62. Duckworth, D.H., *"Who Discovered Bacteriophage?".* Bacteriological reviews, 1976. 40(4): p. 793-802.
63. Verheust, C., Pauwels, K., Mahillon, J., Helinski, D. R. and Herman, P., *Contained Use of Bacteriophages: Risk Assessment and Biosafety Recommendations.* Applied biosafety, 2010. 15(1): p. 32-44.
64. Brussow, H., Canchaya, C. and Hardt, W., *Phages and the Evolution of Bacterial Pathogens: from Genomic Rearrangements to Lysogenic Conversion.* Microbiology and molecular biology reviews, 2004. 68(3): p. 560–602.
65. Wagner, P.L.a.W., M. K., *Bacteriophage control of bacterial virulence.* Infection and Immunity, 2002. 70(8): p. 3985-3993.
66. Fan, H.a.T., Y., *Potential Duel-Use of Bacteriophage Related Technologies in Bioterrorism and Biodefense.* Journal of bioterrorism and biodefense, 2012. 3(121): p. 4 pages.
67. Litman, G.W., Rast, J. P., Shamblott, M. J., Haire, R. N., Hulst, M., Roess, W., Litman, R. T., Hinds-Frey, K. R., Zilch, A. and Amemiyag, C. T., *Phylogenetic Diversification of Immunoglobulin Genes and the Antibody Repertoire'.* Molecular biology and evolution, 1993. 10(1): p. 60-72.
68. Jayasena, S.D., *Aptamers: An emerging class of molecules that rival antibodies in diagnostics.* Clinical Chemistry, 1999. 45: p. 1628-1650.
69. Khor, S.M., Thordarson, P. and Gooding, J. J., *The impact of antibody/epitope affinity strength on the sensitivity of electrochemical immunosensors for detecting small molecules.* Analytical and Bioanalytical Chemistry, 2013. 405: p. 3889–3898.
70. Tate, J.a.W., G., *Interferences in Immunoassay.* The clinical biochemist reviews, 2004. 25(2): p. 105–120.
71. Alberts B, J.A., Lewis J, et al., *Molecular Biology of the Cell, 4th edition, New York.* Garland Science, 2002.
72. Wang, W., Singh, S., Zeng, D. L., King, K. and Nema, S., *Antibody Structure, Instability, and Formulation.* Journal of pharmaceutical science, 2007. 96(1): p. 1-26.
73. Kaneko, Y., Nimmerjahn, F. and Ravetch, J. V, *Anti-Inflammatory Activity of Immunoglobulin G Resulting from Fc Sialylation.* Science, 2006. 313(5787): p. 670-673.
74. Simister, N.E., *Placental transport of immunoglobulin G.* Vaccine, 2003. 21: p. 3365–3369.
75. Ehrenstein, M.R.a.N., C. A., *The importance of natural IgM: scavenger, protector and regulator.* Nature Reviews Immunology, 2010. 10: p. 778-786.
76. Underdown, B.J., *Immunoglobulin A: Strategic Defense Initiative at the Mucosal Surface* Annual reviews of immunology, 1986. 4: p. 389-417.
77. Vladutiu, A.O., *Immunoglobulin D: Properties, Measurement, and Clinical Relevance.* Clinical and vaccine immunology, 2000. 7(2): p. 131-140.
78. Buckley, R.H.a.F., S. A., *Serum IgD and IgE Concentrations.* The Journal of Clinical Investigation Volume 1975. 55: p. 157-165.
79. Chambers, J.P., Arulanandam,B. P., Matta, L. L., Weis, A. and Valdes, J. J, *Biosensor recognition element.* Current Issues in Molecular Biology, 2008. 10(1-12).
80. Emanuel, P.A., Dang, J., Gebhard, J. S., Aldrich, J., Garber, E., Kulaga, H., Stopa, P., Valdes, J. J. and Schultz, A. D., *Recombinant antibodies: a new reagent for biological agent detection.* Biosensors and Bioelectronics, 2000. 14: p. 751-759.
81. Carey Hanly, W., Artwohl, J. E. and Bennett, B., *Review of Polyclonal Antibody Production Procedures in Mammals and Poultry.* ILAR journal, 1995. 37(3): p. 94-118.

82. Khoudi, H., Laberge, S., Ferullo, J.M., Bazin, R., Darveau,A., Castonguay, Y., Allard, G., Lemieux, R. and Vezina, L. P., *Production of a Diagnostic Monoclonal Antibody in Perennial Alfalfa Plants*. Biotechnology and Bioengineering, 1999. 64(2): p. 135–143.
83. Yamada, T., *Therapeutic Monoclonal Antibodies*. Keio Journal of Medicine, 2011. 60(2): p. 37-46.
84. Hermanson, G.T., *Bioconjugate techniques*. Academic press, 2008. 2nd edition(Oxford, UK.).
85. Liaoa, W.C.a.H., J. A., *Improved activity of immobilized antibody by paratope orientation controller: Probing paratope orientation by electrochemical strategy and surface plasmon resonance spectroscopy*. Biosensors and Bioelectronics, 2014. 55: p. 32-38.
86. Yoon, M., Hwang, H. J. and Kim, J. H., *Immobilization of antibodies on the self-assembled monolayer by antigen-binding site protection and immobilization kinetic control*. Journal of biomedical science andenginering, 2011. 4: p. 242-247.
87. Nassef, H.M., Civit, L., Fragoso, A., and O'Sullivan, C. K., *Amperometric Immunosensor for Detection of Celiac Disease Toxic Gliadin Based on Fab Fragments*. Anal. Chem., 2009. 81: p. 5299-5307.
88. Seo, J., Lee, S. and Poulter, C. D., *Regioselective covalent immobilization of recombinant antibody-binding proteins A, G, and L for construction of antibody arrays*. Journal of the american chemical society, 2013. 135: p. 8973−8980.
89. Zou, Y., Bian, M., Yiang, Z., Lian, L., Liu, W. and Xu, X., *Comparison of four methods to generate immunoreactive fragments of a murine monoclonal antibody OC859 against human ovarian epithelial cancer antigen*. Chinese medical sciences journal, 1995. 10(2): p. 78-81.
90. Okamoto, S.O., Y., Maehashi, K., Inoue, K. and Matsumoto, K., *Immunosensors based on graphene field-effect transistors fabricated using antigen-binding fragment*. Japanese journal of applied physics, 2012. 51(6): p. 06FD08.
91. Kausaite-Minkstimiene, A., Ramanavicius, A., Ruksnaitea, J. and Ramanaviciene, A., *A surface plasmon resonance immunosensor for human growth hormone based on fragmented antibodies*. Analytical methods, 2013. 5 (18): p. 4757-4763.
92. Baniukevic, J., Kirlyte, J., Ramanavicius, A., Ramanaviciene, A., *Application of oriented and random antibody immobilization methods in immunosensor design*. Sensors and Actuators B: Chemical, 2013. 189: p. 217–223.
93. Sharma, H.a.M., R., *Half Antibody Fragments Improve Biosensor Sensitivity without Loss of Selectivity*. Analytical Chemistry, 2013. 85(4): p. 2472-2477.
94. Gooding, J.J., *Biosensor technology for detecting biological warfare agents: Recent progress and future trends*. Analytica Chimica Acta, 2006. 559 p. 137-151.
95. Buchan, B.W., Ginocchio, C. C., Manii, R., Cavagnolo, R., Pancholi, P., Swyers, L., Thomson Jr, R. B., Anderson, C., Kaul, K. and Ledeboer, N. A., *Multiplex Identification of Gram-Positive Bacteria and Resistance Determinants Directly from Positive Blood Culture Broths: Evaluation of an Automated Microarray-Based Nucleic Acid Test*. PLOS medicine, 2013. 10(7): p. e1001478.
96. Davidson, C.A., Griffith, C. J., Peters, A. C. and Fielding, L. M., *Evaluation of two methods for monitoring surface cleanliness-ATP bioluminescence and traditional hygiene swabbing*. Luminiscence, 1999. 14: p. 33–38.
97. Peruski, A.H.a.P.J., L. F, *Immunological Methods for Detection and Identification of Infectious Disease and Biological Warfare Agents*. Clinical and vaccine immunology, 2003. 10(4): p. 506-513.
98. Ivnitski, D., O'Neil, D. J., Gattuso, A., Schlicht, R., Calidonna, M., and Fisher, R., *Nucleic acid approaches for detection and identification of biological warfare and infectious disease agents*. BioTechniques, 2003. 35(4): p. 862-869.
99. Dorsch, M.R., *Rapid detection of bacterial antibiotic resistance: Preliminary evaluation of PCR assays targeting Tetracycline resistance genes*. Human protection and performance division, 2007.

100. Saikaly, P.E., Barlaz, M. A. and de los Reyes, F. L., *Development of Quantitative Real-Time PCR Assays for Detection and Quantification of Surrogate Biological Warfare Agents in Building Debris and Leachate.* Applied and environmental microbiology, 2007. 73(20): p. 6557–6565.
101. Thévenot, D.R., Toth, K., Durst, R. A. and Wilson, G. S., *Electrochemical biosensors: Recommended definitions and classifications (Technical Report).* Pure and applied chemistry, 1999. 71(12): p. 2333-2348.
102. Shah, J.a.W., E., *Electrochemical Biosensors for Detection of Biological Warfare Agents.* Electroanalysis, 2002. 15(3): p. 157-167.
103. Karyakin, A.A., Bobrova, O. A., Lukachova, L. V. and Karyakina, E. E., *Potentiometric biosensors based on polyaniline semiconductor films.* Sensors and actuators B, 1996. 33: p. 34-38.
104. Koncki, R., Radomska, A. and Glab, S., *Potentiometric determination of dialysate urea nitrogen.* Talanta, 2000. 52: p. 13-17.
105. Leonard, P., Hearty, S., Brennan, J., Dunne, L., Quinn, J., Chakraborty, T. and O'Kennedy, R., *Advances in biosensors for detection of pathogens in food and water.* Enzyme and Microbial Technology 2003. 32 p. 3-13.
106. Silva, N., Matos, M. J., Karmali, A. and Rocha, M. M., *An Electrochemical Biosensor for Acrylamide Determination: Merits and Limitations.* Portugaliae Electrochimica Acta, 2011. 29(5): p. 361-373.
107. Pfeifer, P.a.B., W. , *Direct potentiometric immunoelectrodes. I. Immobilization of proteins on titanium wire electrodes* Fresenius Journal o f Analytical Chemistry, 1992. 343: p. 541 -549
108. Bergveld, P., *Thirty years of ISFETOLOGY What happened in the past 30 years and what may happen in the next 30 years.* Sensors and actuators B, 2003. 88: p. 1-20.
109. Lazcka, O., Javier Del Campo, F., Xavier Munoz, F., *Pathogen detection: A perspective of traditional methods and biosensors.* Biosensors and Bioelectronics, 2007. 22 p. 1205-1217.
110. Lisdat, F.a.S., D., *The use of electrochemical impedance spectroscopy for biosensing.* Analytical and Bioanalytical Chemistry, 2008. 391: p. 1555–1567.
111. Wang, Y., Ye, Z. and Ying, Y., *New Trends in Impedimetric Biosensors for the Detection of Foodborne Pathogenic Bacteria.* Sensors, 2012. 12(3449-3471).
112. Park, J.Y.a.P., S. M., *DNA hybridization sensors based on electrochemical impedance spectroscopy as a detection tool* Sensors, 2009. 9(12): p. 9513-9532.
113. Mirsky, V.M., Riepl, M., Wolfbeis, O.S., . , *Capacitive monitoring of protein immobilization and antigen-antibody reactions on monomolecular alkylthiol films on gold electrodes.* Biosensors and Bioelectronics, 1997. 12(9): p. 977-989.
114. Palchetti, I.a.M., M., *Amperometric Biosensor for Pathogenic Bacteria Detection.* Principles of Bacterial Detection: Biosensors, Recognition Receptors and Microsystems, 2008: p. 299-312.
115. Skladal, P., Symerska, Y., Pohanka, M., Safar, B., and Macela, A., *Electrochemical immunosensor for detection of Francisella tularensis.* Defense against Bioterror: Detection Technologies, Implementation Strategies and Commercial Opportunities, 2005: p. 221-232.
116. Rao, V.K., Sharma, M. K., Goel, A. K., Singh, L. and Sekhar, K., *Amperometric Immunosensor for the Detection of Vibrio cholerae O1 Using Disposable Screen-printed Electrodes.* Analytical sciences: The Japan society for analytical chemistry, 2006. 22(9): p. 1207-1211.
117. Peckham, G.D., Hew, B. E., Waller, D. F., Holdaway, C. and Jen, M., *Amperometric Detection of Bacillus anthracis Spores: A Portable, Low-Cost Approach to the ELISA.* International Journal of Electrochemistry, 2013. 2013(Article ID 803485): p. 6 pages.
118. Campuzano, S., de Ávila, B.E.-F., Yuste, J., Pedrero, M., García, J.L., García, P., García, E. and Pingarrón, J. M., *Disposable amperometric magnetoimmunosensors for the specific detection of Streptococcus pneumoniae.* Biosensors and Bioelectronics, 2010. 26(4): p. 1225-1230.

119. Salam, F.a.T., I. E., *Detection of Salmonella typhimurium using an electrochemical immunosensor.* Biosensors and Bioelectronics, 2009. 24(8): p. 2630-2636.
120. Esteban-Fernández de Ávila, B., Pedrero, M., Campuzano, S., Escamilla-Gómez, V. and Pingarrón, J. M., *Sensitive and rapid amperometric magnetoimmunosensor for the determination of Staphylococcus aureus.* Analytical and Bioanalytical Chemistry, 2012. 403(4): p. 917-925.
121. Mittelmann, A.S., Ron, E. Z. and Rishpon, J., *Amperometric Quantification of Total Coliforms and Specific Detection of Escherichia coli.* Analytical Chemistry, 2002. 74(4): p. 903–907.
122. Gooding, J.J., Lai, L. M. H., and Goon, I. Y., *Nanostructured electrodes with unique properties for biological and other applications.* Advances in electrochemical science and engineering, 2009. 11 Chemically modified electrodes.
123. Schroper, F., Bruggemann, D., Mourzina, Y., Wolfrum, B., Offenhausser, A., Mayer, D., *Analyzing the electroactive surface of gold nanopillars by electrochemical methods for electrode miniaturization.* Electrochimica acta, 2008. 53: p. 6265 - 6272.
124. Walcarius, A., and Kuhn, A., *Ordered porous thin films in electrochemical analysis.* Trends in analytical chemistry, 2008. 27(7): p. 593-603.
125. Soreta, T.R., Henry, O. Y.F, and O'Sullivan, C. K., *Electrode surface nanostructuring via nanoparticle electronucleation for signal enhancement in electrochemical genosensors.* Biosensors and Bioelectronics, 2011. 26: p. 3962 - 3966.
126. Li, F., Han, X., and Liu, S., *Development of an electrochemical DNA biosensor with a high sensitivity of fM by dendritic gold nanostructure modified electrode.* Biosensors and Bioelectronics, 2011. 26: p. 2619 - 2625.
127. Dhand, C., Das, M., Datta, M., Malhotra, B. D., *Recent advances in polyaniline biosensors.* Biosensors and Bioelectronics, 2011. 26: p. 2811 - 2821.
128. Zeng, G., Li, Z., Tang, L., Wu, M., Lei, X., Liu, Y., Liu, C., Pang, Y, and Zhang, Y. , *Gold nanoparticles/water-soluble carbon nanotubes/aromatic diamine polymer composite films for highly sensitive detection of cellobiose dehydrogenase gene.* Electrochimica acta, 2010. doi:10.1016/j.electacta.2011.03.035.
129. Cook, I., Sheel D. W., and Hodgkinson, J. L., *Surface nanostructuring via combined all atmospheric pressure processing, coating, patterning and ecthing.* Surface and coatings technology, 2011. doi:10.1016/j.surfcoat.2011.03.059.
130. Sugimura, H., Takai, O., and Nakagiri, N., *Scanning probe lithography for electrode surface modification.* Journal of Electroanalytical Chemistry, 1999. 473: p. 230-234.
131. Li, Y., Cai, W., and Duan, G., *Ordered micro/nanostructured arrays based on the monolayer colloidal crystals.* Chem. Mater., 2008. 20: p. 615 - 624.
132. Ben-Ali, S., Cook, D. A., Bartlett, P. N., and Kuhn, A., *Bioelectrocatalysis with modified higly ordered macroporous electrodes.* Journal of electroanalytical chemistry, 2005. 579(181 - 187).
133. Han. J. H., B., H., Park, S., Chung, T. D., *Electrochemical oxidation of hydrogen peroxide at nanoporous platinum electrodes and the application to glutamate microsensor.* Electrochimica acta, 2006. 52: p. 1788 - 1791.
134. Foyet, A., Hauser, A., and Schafer, W., *Template electrochemical deposition and characterization of zinc-nickel alloy nanomaterial.* Journal of electroanalytical chemistry, 2007. 604: p. 137 - 143.
135. Guo, R., Zhang, B., and Liu, X., *Electrodeposition of nanostructured Pt films from lyotropic liquid crystalline phases on alpha-Al2O3 supported dense Pd membranes.* Applied surface science, 2007. 254: p. 538 - 543.
136. Xu, Q., Zhu, JL., and Hu, XY., *Ordered mesoporous polyaniline filmm as a new matrix for enzyme immobilization and biosensor construction.* Analytica Chimica Acta, 2007. 597: p. 151 - 156.

137. Li, J., and Lin, X. Q., *Electrodeposition of gold nanoclusters on overoxidized polypyrrole film modified glassy carbonelectrode and its application for the simultaneous determination of epinephrine and uric acid under coexistence of ascorbic acid.* Analytica Chimica Acta, 2007. 596: p. 222 - 230.
138. Rapecki, T., Donten, M., and Stojek, Z., *Electrodeposition of polypyrrole–Au nanoparticles composite from one solution containing gold salt and monomer.* Electrochemistry Communications, 2010. 12 p. 624-627.
139. Henry, O.Y.F., Gutierrrez Pereza, J., Sanchez, J. L. A. and O'Sullivan, C. K., *Electrochemcial characterisation and hybridisation efficiency of co-assembled monolayers of PEGylated ssDNA and mercaptohexanol on planar gold electrodes.* Biosensors and Bioelectronics, 2010. 25(5): p. 978–983.
140. Henry, O., Y. F., Perez, J. G., Sanchez, J. L. A., and O'Sullivan, C. K, *Electrochemcial characterisation and hybridisation efficiency of co-assembled monolayers of PEGylated ssDNA and mercaptohexanol on planar gold electrodes* Biosensors and Bioelectronics, 2010. 25(5): p. 978 - 983.
141. H.Nasef, V.B., V.C. Ozalp, C.K. O'Sullivan, Analytical and Bioanalytical Chemistry, 2010. 396: p. 2565.
142. Beni, V., Gelaw, T. K., and O'Sullivan, C. K., *Study of the combination of the deposition/stripping of sacrificial metal nano-structures and alkanethiol as a route for genosensor surface preparation.* Electrochemistry Communications, 2011. 13: p. 325-327.

Chapter 2

Automated microfluidically controlled electrochemical biosensor for the rapid and highly sensitive detection of *Francisella tularensis*

Biosensors and Bioelectronics (2014) 59, 342-349. *Available online 12 April 2014*

(http://dx.doi.org/10.1016/j.bios.2014.03.024)

Automated microfluidically controlled electrochemical biosensor for the rapid and highly sensitive detection of *Francisella tularensis*

Samuel B. Dulay[a*], Rainer Gransee[b], Sandra Julich[c], Herbert Tomaso[c], and Ciara K. O'Sullivan[a,d*]

[a] Nanobiotechnology and Bioanalysis Group, INTERFIBIO, Departament d'Enginyeria Quimica, Universitat Rovira i Virgili, Avinguda Països Catalans 26, 43007 Tarragona, Spain

[b]Fraunhofer ICT-IMM, Carl-Zeiss-Strasse 18-20, 55129, Mainz, Germany

[c]Institute of Bacterial Infections and Zoonoses, Friedrich-Loeffler-Institut, Naumburger Strasse 96 a, Jena, 07743, Germany

[d]Institució Catalana de Recerca i Estudis Avancats,Passeig Lluís Companys, 23, 08010 Barcelona, Spain

*Corresponding author.

E-mail addresses: samuelbacena.dulay@estudiants.urv.cat (S.B.Dulay), ciara.osullivan@urv.cat (C.K.O'Sullivan).

ABSTRACT

Tularemia is a highly infectious zoonotic disease caused by a Gram-negative coccoid rod bacterium, *Francisella tularensis*. Tularemia can be treated with antibiotics, but it is still considered as a life-threatening potential biological warfare agent due to its high virulence, transmission, mortality and simplicity of cultivation. In the work reported here, different electrochemical immunosensor formats for the detection of whole *F.tularensis* bacteria were developed and their performance

compared. An anti-*Francisella* antibody (FB11) was used for the detection that recognises the lipopolysaccharide found in the outer membrane of the bacteria. In the first approach, gold-supported self-assembled monolayers of a carboxyl terminated bipodal alkanethiol were used to covalently cross-link with the FB11 antibody. In an alternative second approach F(ab) fragments of the FB11 antibody were generated and directly chemisorbed onto the gold electrode surface. The second approach resulted in an increased capture efficiency and higher sensitivity. Detection limits of 4.5 ng/mL for the lipopolysaccharide antigen and 31 bacteria/mL for the *F.tularensis* bacteria were achieved. Having demonstrated the functionality of the immunosensor, an electrode array was functionalised with the antibody fragment and integrated with microfluidics and housed in a tester set-up that facilitated complete automation of the assay. The only end-user intervention is sample addition, requiring less than one-minute hands-on time. The use of the automated microfluidic set-up not only required much lower reagent volumes but also the required incubation time was considerably reduced and a notable increase of 3-fold in assay sensitivity was achieved with a total assay time from sample addition to read-out of less than 20 min.

Keywords: Electrochemical immunosensors, *Francisella tularensis*, Self-assembled monolayer (SAM), Lab-on-a-chip

2.1 INTRODUCTION

In the last decades, there has been increased interest in developing new methods for the rapid detection of microorganisms including toxigenic and pathogenic organisms (Grunow *et al.* 2000; Magnarelli *et al.* 2007; Savitt *et al.* 2009). Tularemia, also known as rabbit fever, is a highly infectious zoonotic disease caused by the non-motile, non-spore-forming, Gram-negative coccoid rod bacterium, *Francisella tularensis*. It occurs naturally in lagomorphs (rabbits and hares), but many animals have been reported to be infected. Transmission to humans is mostly associated with inhalation of aerosolised bacteria, handling of infected animals, arthropod bites, and ingestion of contaminated foods and water (Kleo *et al.* 2012; Magnarelli *et al.* 2007). The usual incubation period is 3-5 days but symptoms can become visible between 1 and 21 days following exposure depending on the route of infection. Clinical manifestation of the disease in humans can occur in different forms ranging from skin ulcers to more severe forms such as life threatening-pneumonia (Penn *et al.* 2005).

Despite the fact that most of tularemia infections can be treated with antibiotics (Dennis *et al.* 2001), it is still considered as life-threatening due to its high virulence, transmission and mortality (Su *et al.* 2007). *F. tularensis* could be used as a potential biological warfare agent or in terrorist attacks. Identification of *F. tularensis* has been achieved using cultivation and molecular techniques including polymerase chain reaction (PCR) (Johansson *et al.* 2000) and real time PCR assays (Bystrom *et al.* 2005; Simşek *et al.* 2012 ; Versage *et al.* 2003). Besides the detection of the bacterial cell, the detection of specific antibodies in serum is the most widely used serological analysis technique for routine laboratory diagnosis of tularemia (Porsch-Ozcürümez *et al.* 2004). Enzyme-linked immunosorbent assay (ELISA) (Pohanka *et al.* 2008a), Western blot and other immunological assays can be used to detect seroconversion in patients. However, antibodies to *F.tularensis* appear only 2 weeks or more after infection (Emanuel *et al.* 2003). An early identification of the pathogen is

important and serological diagnosis is not useful as a rapid diagnostic approach (Grunow *et al.* 2000). Although these standard techniques are sensitive, they are rather time consuming and require intensive hands-on-time.

The detection of *F. tularensis* is required in different situations which include civil rescue and security units, homeland security, military operations, public transportation securities such as airports, metro and railway stations due to its harmful effect on the human population (Skládal *et al.* 2010). Therefore, there is a need for a specific detection system which could be portable, rapid and cost-effective.

Electrochemical biosensors are renowned for their excellent sensitivity, selectivity, versatility, and simplicity, (Lazcka *et al.* 2007; Pividori *et al.* 2009). There is a continual interest in the development of these technologies for application in clinical diagnostics, food quality control and environmental monitoring (Warsinke *et al.* 2000), as promising alternatives to traditional methods in detecting pathogens (Pohanka *et al.* 2007). Many of the electrochemical immunosensor format architectures try to mimic that found in standard ELISA where different strategies in immobilisation of the biocomponent on the transducer's surface have been developed. The use of self-assembled monolayers (SAM) has garnered increased interest due to the possibility of avoiding random orientation of the biocomponents (antibody/antigen) on the surface, good surface coverage and the possibility of incorporating efficient surface protection moieties to eliminate non-specific binding. Specifically targeting *F. tularensis*, Kleo and co-workers (Kleo *et al.* 2012) successfully demonstrated the immobilisation of an antibody using a carboxy-terminated thiol layer onto a gold surface and *F. tularensis* bacterial cells were directly detected by frequency change using quartz crystal microbalance technique, achieving a detection limit of 4 x 10^3 CFU/mL. Skladal and co-workers (Skladal *et al.* 2005) used a sandwich format for the amperometric detection of inactivated *F. tularensis* bacterial cells obtaining a detection limit of 100 CFU/mL in 30 min.

In this work, we report a biosensor for the detection of whole inactivated *Francisella tularensis* live vaccine strain (LVS) bacterial cells comparing the use of whole antibodies immobilised via chemical cross-linking to a bipodal alkyl thiol self-assembled monolayer (SAM) and a SAM formed from the direct chemisorption of F(ab) antibody fragments through their free sulfhydryl group which inherently correctly orients the antibody. The biosensor was housed within a microfluidic set-up and the assay was automated via the use of a peristaltic pump, with the only required end-user intervention being sample addition. Parameters such as incubation time and temperature were optimised and applied to the detection of both the lipopolysaccharide (LPS) antigen and whole *F. tularensis* bacterial cells.

2.2 EXPERIMENTAL

All the starting materials were obtained from commercial suppliers and used without further purification. Monoclonal antibodies (mAb) FB11 and T14 were purchased from Hytest Ltd. Company, Finland. Lipopolysaccharide (LPS) from *Francisella tularensis* was purchased from MICROMUN Privates Institut fűr Mikrobiologische Forschung GmbH, Germany. Whole cell bacteria of *Francisella tularensis* LVS subsp. *holarctica*, *F. tularensis* subsp. *novicida, Yersinia enterocolitica* subsp. *enterocolitica,* and *Yersinia pseudotuberculosis* were kindly provided by the Friedrich-Loeffler-Institut, Institut für bakterielle Infektionen und Zoonosen, Germany. 1-(mercaptoundec-11-yl)tetra (ethyleneglycol) (PEG) was purchased from Sigma-Aldrich Co., sulfuric acid, strontium nitrate, phosphate-buffered saline (PBS) (dry powder), PBS-Tween-20, hydrogen peroxide 30% v/v, ethanolamine, acetone and ethanol (synthetic grade), N-(3-dimethylaminopropyl) – N – ethylcarbodiimide (EDC), N-hydroxysuccinimide (NHS), and acetic acid were purchased from Scharlau (Spain); (22-(3,5-bis((6 mercaptohexyl)oxy)phenyl)-3,6,9,12,15,18,21- heptaoxadocosanoic acid dithiol PEG-6 carboxylate (DT2) was purchased from SensoPath Technologies (USA) and

3,3,5,5-Tetramethylbenzidine (TMB) Liquid Substrate System for ELISA was obtained from Sigma. Aqueous solutions were prepared with Milli-Q water Millipore (18mΩ.cm) and all reagents were used as received.

2.2.1 Instrumentation

Electrochemical studies were carried out using an Autolab PGSTAT 10 potentiostat with measurements performed using either a conventional three-electrode cell for 3 mm-diameter lithographically produced gold electrodes (for developmental work) or 1 mm-diameter electrodes. An array of 24 gold electrodes with internal reference and counter electrodes was used for the final format with the biosensor integrated within the microfluidic set-up. The lithographically produced gold electrodes were provided by Fraunhofer ICT-IMM (IMM), Germany, and were produced as previously reported (Fragoso *et al.* 2011). In the developmental work, a standard silver/sliver chloride (sat. KCl) was used as a reference electrode (CHI 111 CH Instruments) and platinum gauze as the counter electrode. All sonication procedures were conducted with an ultrasonic bath (Branson ultrasonic corporation, model 2510E-MT, USA). Enzyme-linked immunosorbent assay (ELISA) studies were performed using bioNOVA cientifica, S.L. (Madrid, Spain) and HydroFlex 3-in-1 well washer, TECAN (Spain).

The microfluidic set-up for incubation of analytes and flushing/washing with built in peristaltic pump was designed together with and provided by IMM, Germany and the polymeric microfluidics were supplied by microfluidic ChipShop GmbH, Germany.

2.2.2 Preparation and characterisation of fragment antibodies

Preparation of $(Fab)_2$ Fragments

Anti-*Francisella tularensis* antibodies (FB11 and T14), were purified using YM100 KDa microcon and washed four times with 0.15 M NaCl. Fifty microlitres of 0.5 M Tris buffer containing 50 mM EDTA (pH 7) was added to 500 μL of the purified antibodies (1 mg/mL), followed by 50 μL (10 mg/mL) of bromelain solution in PBS (pH 7.2, 0.01 M). The mixture was incubated at 37 °C overnight. The produced $F(ab')_2$ fragments were separated with a Sephacryl S-100 column using 0.15 M NaCl as the eluting agent. The fractions with maximum absorbance at 280 nm were concentrated using a YM10 KDa microcon, washed several times with PBS (pH 7.4, 0.01 M), and stored at −20 °C (Nassef *et al.* 2009).

Preparation and Characterization of F(ab) Fragments (F(ab)FB11 and F(ab)T14)

The F(ab) fragments were always prepared freshly from $F(ab)_2$ fragments before use. 1500 μL of 10 mM cysteine in PBS (pH 10.3) was added to 60 μL (0.483 mg/mL) of $F(ab)_2$ fragments. The mixture was incubated for 2 h at room temperature under gentle shaking and the excess of cysteine was removed using a YM10 KDa microcon. The obtained fragments were washed with PBS (pH 7.4, 0.01 M) four times and quantified spectrochemically at 280 nm (Nassef *et al.* 2009). The fragments were characterised by non-reducing sodium dodecyl sulphate-polyacryamide gel electrophoresis analysis (SDS-PAGE, 12% acrylamide in tris-glycine gel) (Riddles 1983). A precision protein standard marker (Bio-Rad, Nazareth Eke, Belgium was used as a molecular weight reference. Coomasie brilliant blue R250 (Sigma, Spain) was used to stain the proteins.

Preparation of whole-antibody and F(ab)-horseradish peroxidase conjugates

Whole antibodies (FB11 and T14) were purified prior to conjugation to eliminate any preservatives present that would affect the efficiency. The purified whole antibodies were dissolved in 0.1 M MES, 0.15 mM NaCl solution at pH 7.2 to a final volume of 1500 μL and subsequently 10 μL of SATA (*N*-Succinimidyl S-Acetylthioacetate) in DMSO was added (15:1 Ab:SATA). The mixture was then gently stirred in a thermomixer for 30 min at room temperature, protected from light. To deprotect the sulphydryl groups formed, 100 μL of 0.5 M hydroxylamine hydrochloride in 0.15 mM NaCl adjusted to pH to 7.2 was added and were reacted for 2 hours at room temperature, again protected from light. Maleimide activated horse radish peroxidase (Maleimide HRP) was then added to the previous mixture to a final concentration of 4:1 (Maleimide HRP:Ab ratio) and incubated for 90 min at 37 °C, after which 2-mercapto ethanol was added to a final concentration of 0.0015 M to stop the reaction. The final products were purified using a YM100 KDa cut-off microcon and were washed with buffer and stored at -20°C.

ELISA evaluation of optimum antibody combination for sandwich assay

Monoclonal Antibody (mAb) FB11 and T14 (10 μg/mL in carbonate buffer, pH 9.5) were prepared separately and added to each well of a NUNC immunosorp microtiter plate and incubated for 30 min at 37 °C. Following thorough washing with PBS-Tween 20 (pH 7.4, 0.01 M), the plate was then blocked by addition of 200 μL of PBS-Tween 20 (pH 7.4, 0.01 M) and incubated for 1 h at 37 °C, followed by thorough washing of the plate. In the immunorecognition step, 50 μL each of a range of concentrations of *F. tularensis* LPS antigen in PBS-Tween 20 (pH 7.4, 0.01 M) were added to each well coated with mAb FB11 or T14. The plate was again incubated, under shaking conditions for 30 min at 37 °C, and subsequently thoroughly washed with PBS-Tween 20, prior to

exposure to different concentrations of mAb-HRP conjugates as a secondary labelled antibody, i.e. FB11-HRP and T14-HRP, and again left to incubate under shaking conditions for 30 min at 37 °C. After a final wash, 50 μL of TMB for ELISA substrate was added to each well and product formation allowed to proceed for at least 15 min at room temperature. The reaction was finally stopped by addition of 1 M H_2SO_4, and the absorbance read at 450 nm. Analysis was carried out in triplicate.

2.2.3 Cultivation and inactivation of *Francisella tularensis* bacteria suspension

Francisella tularensis LVS was cultivated on cysteine heart agar (Becton Dickinson GmbH, Heidelberg, Germany) supplemented with 10 % chocolatized sheep blood. Incubation was carried out for 3 days at 37 °C in an atmosphere with 5 % CO_2. Heat assisted inactivation was carried out for 10 min at 95 °C (Thermomixer Compact, Eppendorf AG, Hamburg, Germany). To check sterility, the suspension was plated on agar plates and incubated for 7 days and no growth was observed.

2.2.4 Electrode modification and electrochemical detection

Prior to modification of the lithographic gold electrodes, a three-step cleaning protocol was applied. Initially, in order to remove the protective resist used during storage, the electrodes were sonicated for 5 min in acetone (2 times), 5 min in isopropanol (3 times) and rinsed with water and dried with compressed air. In a second step, the electrodes were then further treated with cold Piranha's solution (*Warning: Piranha's solution is highly corrosive and violently reacts with organic materials; this solution is potentially explosive and must be used with extreme caution*) for 30s and subsequently washed with Milli-Q water before use. In the last step, electrochemical cleaning was performed in 0.5 M H_2SO_4 by application of a constant potential of 1.6 V for 10s followed by 10 voltammetric cycles in the

potential range −0.2 to 1.6 V at a scan rate of 0.3 V/s. Finally, the electrodes were rinsed with Milli-Q water and dried with nitrogen.

Modification of the cleaned electrodes was carried out in two ways; 1) formation of a SAM of the bipodal alkanethiol DT2 followed by covalent linking of whole anti-*F. tularensis* antibody and 2) direct chemisorption of F(ab) fragments. In the DT2 immobilisation, electrodes were immersed in an ethanolic solution of 1 μM DT2 for 3 hours, then rinsed with ethanol and dried with argon. To activate the carboxylic acids of the DT2, the electrodes were then immersed in a mixture 50% (v/v) EDC (0.2M) and 50% (v/v) NHS (0.05M) for 30 min and then rinsed with Milli-Q water. Subsequently, 100 μg/mL of monoclonal antibody (mAb) FB11 in PBS (pH 7.4, 0.01 M) was added to the electrodes modified with the activated DT2 for 30min and then rinsed with Milli-Q water. Finally, any unreacted activated carboxylic acid groups remaining were blocked by immersion of the electrodes for 15 min in ethanolamine pH 8.5, followed by a final rinse with Milli-Q water.

For the immobilisation of F(ab) fragments, the fragments were prepared as previously reported (Nassef *et al.* 2009). SAM formation of the F(ab) fragments into gold electrode was carried out by overnight immobilisation of 100 μg/mL F(ab) prepared in PBS (pH 7.4, 0.01 M) solution at room temperature. Blocking with 1 mM poly(ethylene)glycol (PEG) was carried out for 30 min, and the modified surfaces were incubated in PBS-Tween-20 (pH 7.4, 0.05M) for another 30 min to avoid non-specific adsorption.

The electrodes were then exposed to different concentration of LPS or *F. tularensis* LVS in PBS (pH 7.4, 0.01 M) for a specified period of time (2-20 min) and then incubated for a defined period of time (2-20 min) with the corresponding horseradish peroxidase labelled monoclonal antibody. Amperometric measurement was carried out at 0.15V vs. Ag/AgCl. All the electrochemical measurements were performed at room temperature. The overall immobilization process and detection mechanism can be seen in Figure 2.1.

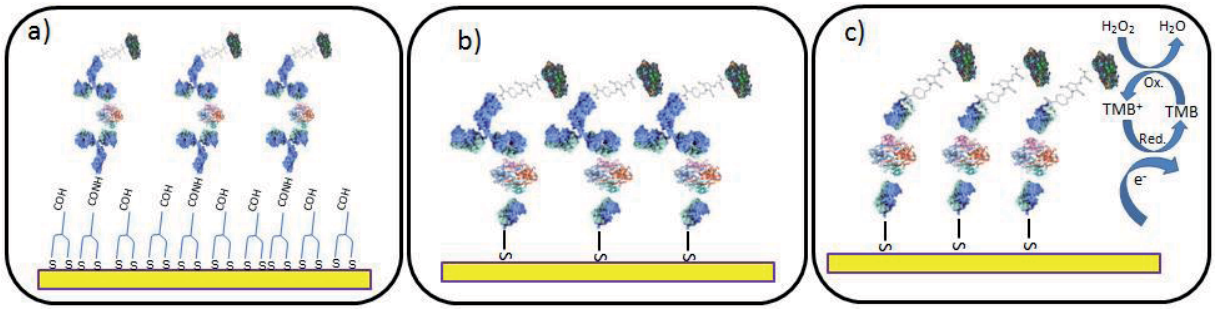

Figure 2.1 Schematic representation of a) sandwich with whole antibody linked to bipodal alkyl thiol (DT2) and whole antibody-HRP conjugate b) sandwich with direct chemisorption of F(ab) fragment and whole antibody-HRP conjugate c) sandwich with direct chemisorption of F(ab) fragment and F(ab)-HRP conjugate.

2.3. RESULTS AND DISCUSSION

2.3.1 ELISA optimisation on assay combination

Monoclonal antibodies (mAb) FB11 and T14 can both recognise and react with the LPS antigen of *Francisella tularensis* and these antibodies were compared in terms of their performance for the detection of the bacteria using ELISA technique. Four different assay constructions combining both antibodies at different concentration conditions of the secondary labelled antibody were evaluated to find the optimum conditions for the best assay format (Supplementary Information Figure 2.S1-2.S3). It was observed that FB11-LPS-T14HRP and T14-LPS-T14HRP assay combinations gave best results, achieving limits of detection of 10 and 21 ng/mL, respectively. As the FB11-LPS-T14HRP assay format was more sensitive (Supplementary Information Figure 2.S3b), this format was used for the construction of the electrochemical immunosensor.

2.3.2 Preparation and characterisation of fragment antibodies

Whole mAbs (FB11 and T14) were first digested with bromelain to obtain their corresponding $(Fab)_2$ fragment following chromatographic purification. The fragmentation of whole monoclonal antibodies to $(Fab)_2$ fragment and the subsequent chemical reduction using cysteine to F(ab) fragments was successfully achieved. The obtained fragments were characterised using non

reducing gel electrophoresis. The gel characterisation showed bands confirming for the successful generation of fragments from whole antibody (See Supplementary Information Figure 2.S4 for more details).

Both whole antibodies and antibody fragments modified with horseradish peroxidise (HRP) were used as secondary labelled antibodies in combination with immobilised F(ab) fragments by modification with maleimide activated horseradish peroxidise (HRP) (Hermanson *et al.* 2008). The conjugates were evaluated using ELISA.

The F(ab)FB11 fragment was used as a capture antibody and F(ab)T14 fragment modified with HRP and T14-HRP served as secondary HRP labelled antibody. The results obtained from the ELISA demonstrated that the produced fragments were still active after fragmentation and chemical reduction, and, in the case of the labelled antibody, after chemical linkage to HRP (Supplementary Information Figure 2.S5). The optimum concentrations were elucidated, achieving limits of detection of 6.2 and 5.8 μg /mL, for the labelled F(ab)T14 and labelled whole T14 antibody, respectively.

2.3.3 Development of Electrochemical immunosensor

For development and testing of the immunosensor, a conventional three-electrode cell was used, where 3 mm-diameter macro lithographically produced gold electrodes were used as working electrodes with a Ag/AgCl reference and Pt counter electrode. The electrochemical immunosensor was constructed using the FB11 whole antibody/F(ab) fragments as capture antibody and whole T14/F(ab) T14 fragments as secondary labelled antibodies. This sensor was used to detect different concentrations of the LPS antigen isolated from *F. tularensis* as well as for the detection of whole (inactivated) bacterial cells of *F. tularensis* LVS.

The immunosensor exploiting a F(ab)FB11 fragment SAM was more sensitive, with >2 times fold higher signal observed for the detection of whole bacterial cells. This can be attributed to a better orientation of the fragment on the surface directly exposing the antigen binding site, facilitating more efficient antigen binding, combined with the antibody enzyme label being closer to the electrode interface, thus giving a better response (Figure 2.2b). The use of labelled antibody fragment as secondary antibody was not observed to be significantly different to that of the use of the whole labelled antibody.

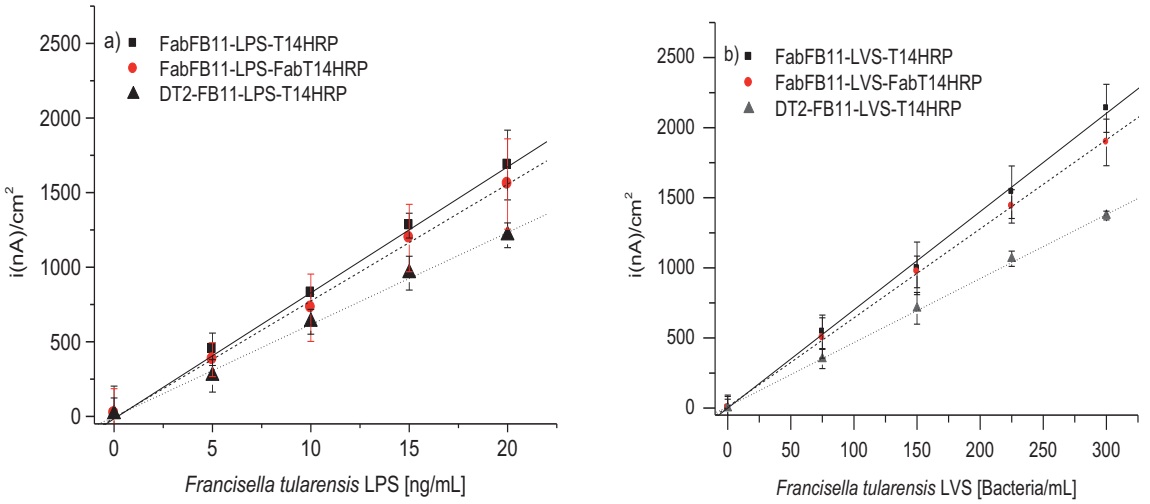

Immunosensor format	L.O.D *F. tularensis*				Sensitivity	
	LPS (ng/mL)	RSD (%)	LVS (bacteria/mL)	RSD (%)	LPS (nA.mL/ng.cm²)	LVS (nA.mL/bacteria.cm²)
DT2- FB11 T14-HRP	5.3	9.9	37	9.8	62	4
F(ab)FB11 T14-HRP	4.5	9.5	31	9.4	83	8
F(ab)T14 F(ab)-HRP	6.5	9.7	42	9.6	79	6

Figure 2.2 Amperometric responses of the whole antibodies immobilised via chemical cross-linking to a bipodal alkyl thiol SAM and SAM formed from the direct chemisorption of antibody fragments F(ab) to different LPS and LVS of *F. tularensis* concentrations. Each data point represents the average of three independent measurements.

2.3.4 Fluidics and set-up

Following demonstration of the functionality of the developed immunosensor for the detection of both the LPS antigen as well as the inactivated bacterial cells, an electrode array was functionalised and housed within microfluidics (Figure 2.3), within a tester set-up consisting of several reservoirs for analytes and buffers, silicone tubes, waste tanks, fluidics, and controlled by a script-based assay programme. The whole set-up enabled complete automation of the immunosensor as well as facilitating the use of smaller quantities of reagents. Electrode functionalisation with the optimum surface platform, i.e. F(ab)FB11 fragment was carried out outside the microfluidics set-up. Following the modification process, the electrode array was housed in the microfluidic set-up (Figure 2.3c) using an adhesive gasket which acts as spacer between the polycarbonate microfluidic chip and the glass electrode. This generates a flow cell above the electrode area with a width of 4.5 mm, a height of 0.1 mm and a total length of 24 mm, housing 24 individual working electrodes (which could be separately functionalized, allowing multiplex detection and/or the incorporation of controls). The flow cell has an inlet resp. outlet with a diameter of 1 mm that is connected with a feeding channel with a width of 0.8 mm and a height of 0.3 mm leading to tube inlets resp. a waste outlet. The silicone tubes connected to the reservoirs were connected to the tube inlets of the microfluidic set-up via Mini-Luer adapters (supplied by microfluidic ChipShop GmbH), allowing flowing of different liquid samples as required throughout the assay. The four reservoirs available were used to store pre-mixed LVS and T14-HRP labelled antibody, PBS, TMB substrate, and Milli-Q water for washing. The flowing of liquids over the electrode was carried out automatically using the script based assay programme, which was also used to process the data obtained.

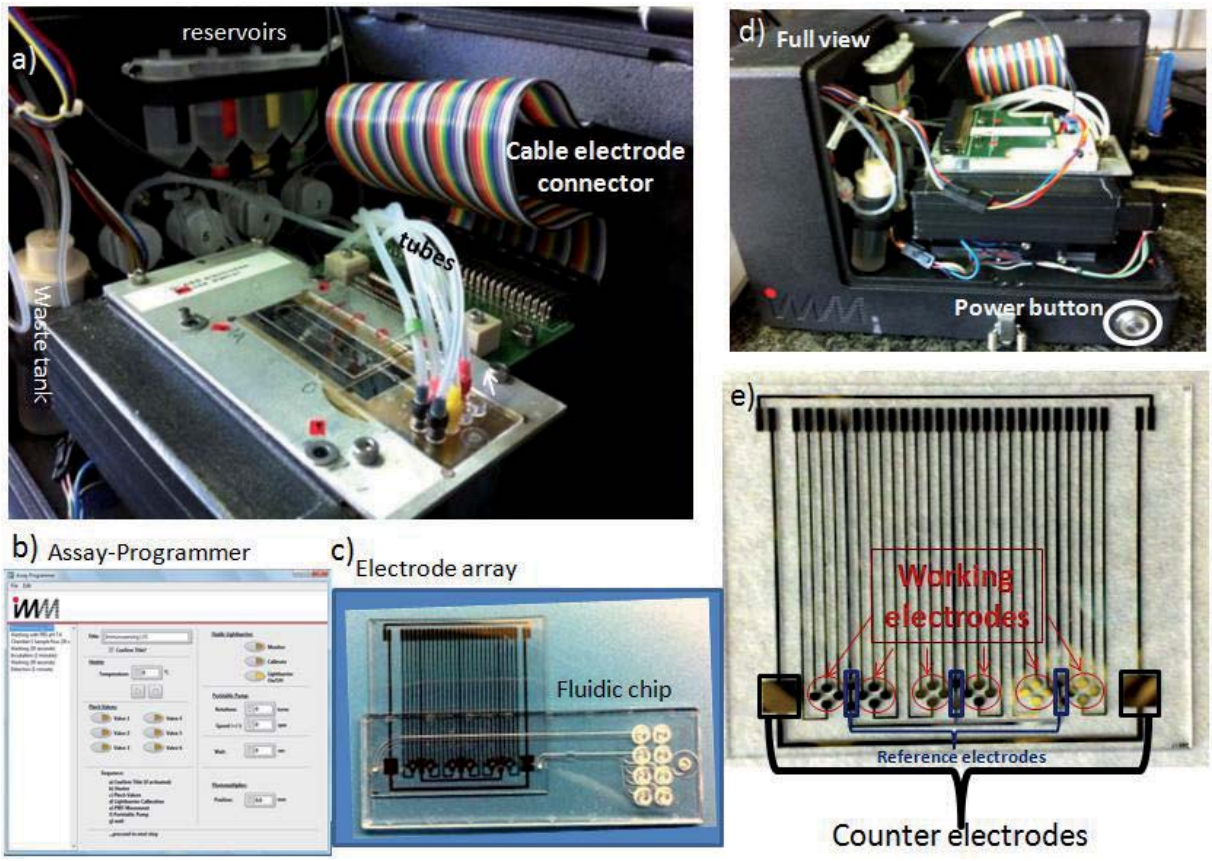

Figure 2.3. The amperometric immunosensor detection set-up. The set-up contains a peristaltic pump positioned behind the reservoirs to flow the solutions into electrode array mounted within the microfluidics. (a) the electrode array with microfluidics placed in the platform and connected to the potentiostat for amperometric measurement; (b) a sample script-based assay program; (c) the electrode array integrated with microfluidics; (d) a full front view of the tester set-up device; (e) lithographically produced gold electrode array with internal reference electrode and counter electrode.

An optimisation of the incubation time outside and inside the microfluidic set-up was carried out. Interestingly, incubation of the target inside the fluidic cell resulted in an increased current response, even though smaller electrodes are used. This is due to the fact that incubation of antigen sample inside the fluidic cell is more favourable to the formation of the immunocomplex. This can be explained by an easy direction of the antigen towards the binding site of the immobilised capture antibody sensing probe which is confined to a very small channel and not the large volume used outside the microfluidics in the developmental work. Furthermore, the required incubation

time was vastly reduced when the immunosensor was housed within the fluidics (Figure 2.4b), and just 2 min incubation was required, as compared to a 10 min incubation outside the fluidics (Figure 2.4a). The microfluidic set-up also allowed a tight control of temperature during the assay and to this end, the effect of temperature on sensor performance was evaluated and no great differences were observed at the temperatures studied (Figure 2.4c).

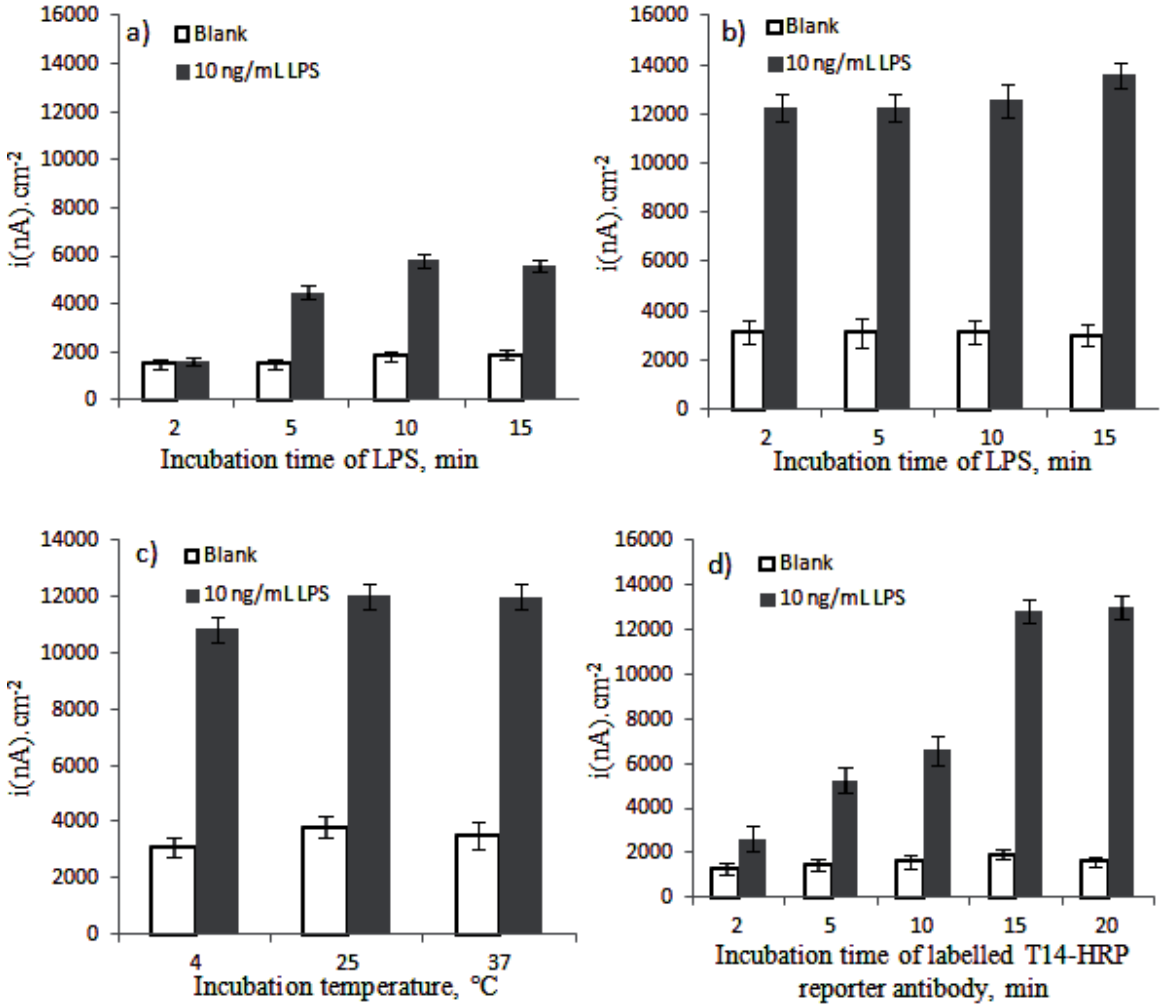

Figure 2.4. Step and Sweep (SAS) amperometric response of the F(ab) fragment FB11 functionalised electrochemical immunosensor a) to 10 ng/mL LPS sample outside the fluidics and b) to 10 ng/mL LPS sample inside the fluidics at different incubation times of antigen-LPS, c) to 10 ng/mL LPS sample inside the fluidics at different incubation temperatures and d) different incubation times for the secondary labelled antibody T14HRP. Each data point represents the average of nine measurements on three separate electrode arrays.

The incubation time was also optimised for the detection of the *F. tularensis* bacterial cells, and similar results were obtained and again 2 min exposure was observed to be adequate. A 15 min incubation was required for the labelled secondary antibody (Figure 2.4d), and together with the automated washing steps after each incubation as well as automated substrate addition and measurement, the duration for performance of the overall assay was 22 min.

In order to further shorten the length of the assay, the target bacterial cells and the labelled secondary antibody were mixed together at different pre-incubation times before exposure to the immunosensor. A 15 minute pre-incubation of the bacterial cells and HRP-labelled mAb gave equivalent response to that obtained when the antigen and labelled antibody were added sequentially with an intermittent washing step. The length of exposure of this pre-mixed solution on the electrochemical sensor was 2 min, resulting in a total assay time of ca.18 min, with only one required washing step, thus simplifying the fluidic requirements.

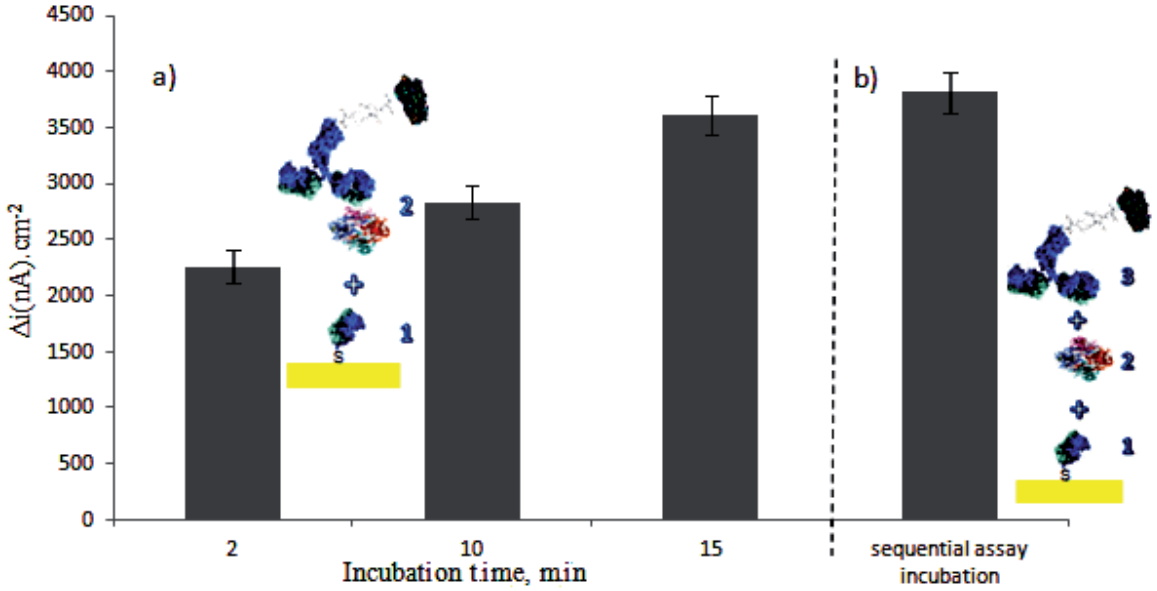

Figure 2.5. Step and Sweep (SAS) amperometric responses of the direct F(ab) fragment FB11 immobilised based electrochemical immunosensor to a fixed concentration (150 bacteria/mL) of *F. tularensis* (LVS). (a) at different incubation times of pre-mixed LVS target and secondary labelled antibody T14HRP; (b) sequential addition of LVS (2 min) and T14-HRP (15 min) with intermittent

washing step. Each data point represents the average of nine measurements on three separate microchip array.

Finally, using the optimised incubation time and temperature, and pre-mixing the bacterial cells and the labelled reporter antibody, different concentrations of whole bacterial cells were detected using the developed automated set-up with fragment F(ab)FB11 as capture antibody and whole mAb T14-HRP as secondary labelled antibody. The instrumentation used for detection was fully automated using script-based programming after insertion of the immunosensor array (1mm Ø). The buffer solutions for washing and the sample mixed with T14-HRP were stored in each of the reservoirs and the solutions the array was exposed to the different solutions through microfluidics via the peristaltic pump. The whole *F. tularensis* LVS bacteria can be detected up to 1 x 10^3 bacteria/mL with a very low limit of detection of 38 bacteria/mL. This detection limit is far lower compared to previously reported immunosensors (Anderson *et al.* 2000; Kleo *et al.* 2012; Skladal *et al.* 2005) and even with reported ELISA results (Pohanka *et al.* 2008b). In order to evaluate the sensitivity of the immunosensor using the whole set-up, the amperometric response was normalised taking into consideration the surface active area of the electrodes used, and a 3 fold increase in sensitivity as compared to the signal obtained outside the fluidics was observed (Figure 2.2b). This highlights the important role microfluidics play in improving the sensitivity of the biosensor. The analysis time is approximately 18 min, comprising pre-incubation (15 min), automated addition of this pre-mixed solution to the housed electrode array and 2 min incubation, washing steps with buffer solution (<30s) before automated substrate addition and electrochemical detection. The output signal was measured in less than 1 min. This short analysis time is advantageous in real situations such as bioterrorism events, and is far shorter than the analysis time required for ELISA (Vivekananda *et al.* 2006) or PCR (Sjostedt *et al.* 1997). Furthermore, the actual operator's hands-on time is less than a minute and simply requires rapid mixing of the sample

containing the target with the labelled antibody in a reaction vessel e.g. Eppendorf tube and addition to the appropriate reservoir within the tester set-up.

To demonstrate the specificity of the immunosensor, control measurements were performed by exposing the modified electrode array with three different species (Figure 2.6 inset). It was observed that F(ab)FB11 modified electrodes only obtained a specific sensor response when exposed to *F. tularensis* LVS subsp. *holarctica* bacteria. Other bacterial species, i.e. *Yersinia enterocolitica* subsp. *enterocolitica* and *Yersinia pseudotuberculosis,* including *F. tularensis* subsp. *novicida* did not give any response, highlighting the specificity of the developed immunosensor.

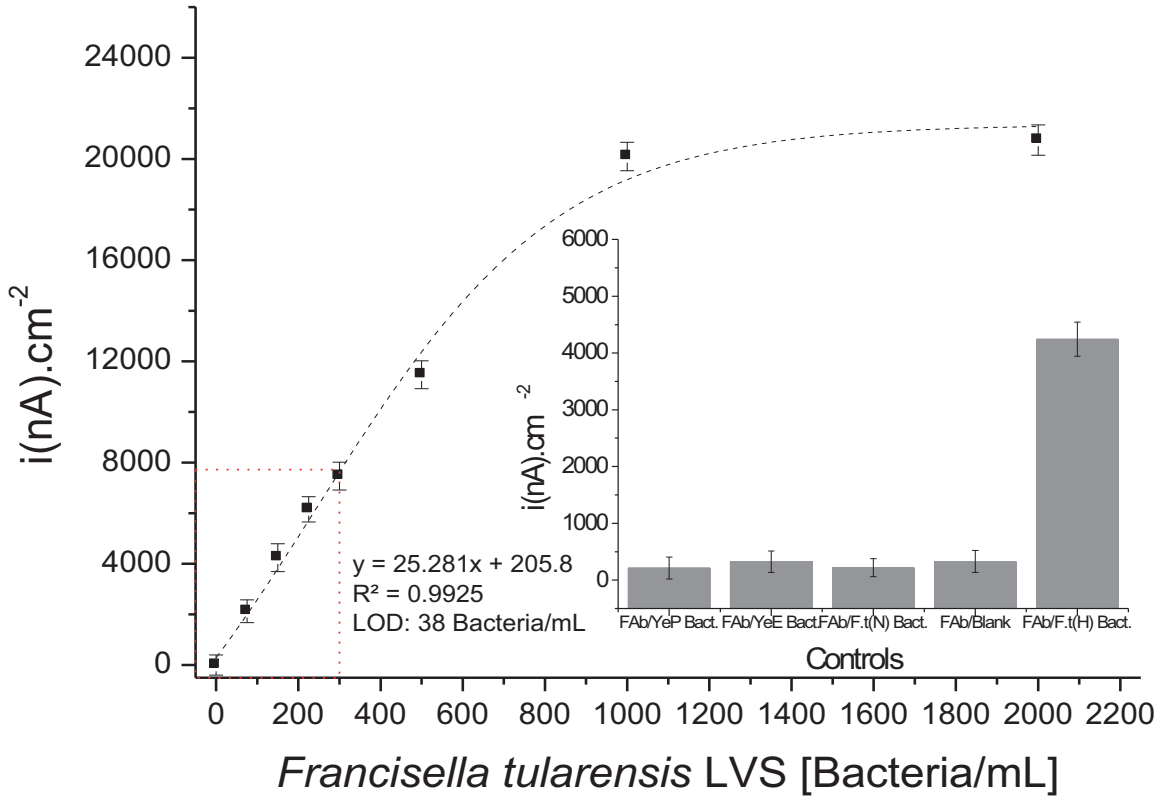

Figure 2.6. Calibration curve and sensitivity of the electrochemical based-immunosensor detection system for the analysis of inactivated *F. tularensis* LVS subsp. *holarctica* bacteria. Step and Sweep (SAS) amperometric responses are shown for capture antibody on the chip –*F. tularensis* antibody FB11 F(ab) to different bacterial solutions which are flushed into the chip electrodes' surface via microfluidic device. Inset: Specificity of the immunosensor to *F. tularensis* LVS subsp. *holarctica* (F.t

(H)Bact.), *F. tularensis* subsp. *novicida* (F.t (N)Bact.), *Yersinia enterocolitica* subsp. *enterocolitica* (YeE Bact.), *Yersinia pseudotuberculosis* (YeP Bact.). Each data point represents the average of three independent measurements.

In order to show the true application of the immunosensor as an alarm sensor that would be integrated within a temperature controlled, automated microsystem linked, for example, to an automated air sampler, the stability of the immobilised F(ab) fragments on the gold electrode array was evaluated over a 45-day period. Electrode arrays were stored at at 4 °C. As can be seen in Figure 2.7, the electrodes modified with the Fab fragments showed a practically constant amperometric response to fixed concentration of 10 ng/mL of LPS target over 30 days, with only a slight loss of antigen recognition activity observed after 45 days, indicating the high stability of the immobilized Fab fragments. It can thus easily be envisaged that the sensor arrays could be replaced on a monthly basis from an automated sampling site.

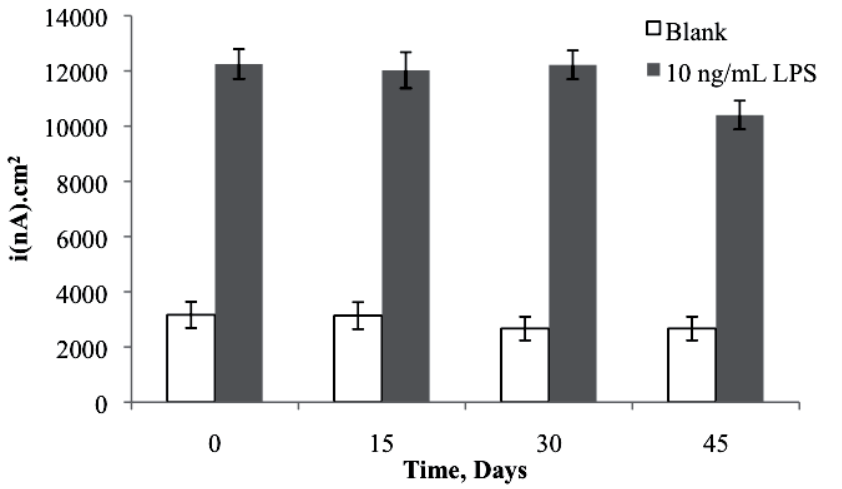

Figure 2.7. Stability of stored Fab-modified sensors over a 45-day period. Sensors were stored at 4 °C and exposed to 10ng/mL LPS every 15 days for 45 days. (n=3, RSD%= 9.6).

2.4. CONCLUSIONS

This report details the development of an electrochemical immunosensor for the automated detection of *F. tularensis* LVS subsp. *holarctica* based on F(ab) fragments on Au surfaces as it gave better sensitivity compared to chemisorbed self-assembled monolayer cross-linked whole antibody. Antibody-enzyme conjugates were prepared in-house using whole antibody as well as antibody fragments, and similar results obtained in both cases. The immunosensor was used for the detection of the lipopolysaccharide antigen as well as *F. tularensis* LVS bacterial cells. The F(ab) fragments retained ~85% of antigen recognition ability after 45 days of storage at 4 °C. The developed electrochemical immunosensor was then transferred to an automated microfluidic set-up housed within a tester set-up and the assay parameters were optimised and the required incubation time within the fluidic set-up was reduced from 10 to 2 min for the target and 15 min for the labelled secondary antibody. Washing steps were reduced by mixing the bacterial cells sample with the labelled antibody and incubated in one of the reservoirs for 15 minutes before being introduced to the electrode array for signal read-out. The specificity of the immunosensor has been clearly determined and no cross-reactivity has been found.

This report is the first stage of development of a platform for the multiplexed detection of a range of bioterrorism agents (i. e, *Bacillus anthracis, Brucella abortis and melitensis, Bacteriophage lambda, Burkholderia mallei and pseudomallei, Coxiella burnetii, Yersinia pestis, and Bacillus thuringiensis*) and the electrode arrays used in this work has been designed to allow incorporation of multiple antibodies immobilised on individual electrodes for the simultaneous detection of the listed bioterrorism agents

and work is ongoing to achieve this goal. The applicability of the developed system to real situations such as an early detection of bioterrorism events is very promising as the obtained LOD was very low and the assay time quite short. This facilitates a rapid alarm based detection of *F. tularensis* when linked e.g. to an air-sampling system. Ongoing and future work will focus on attempting to further reduce the sampling time, to increase the stability of the Fab functionalised sensors using stabilising agents and to apply to the analysis of real samples within specialised regulatory laboratories.

ACKNOWLEDGMENTS

The research leading to these results has received funding from the European Community's Seventh Framework Programme "The lab-free CBRN detection device for the identification of biological pathogens on nucleic acid and immunological level as lab-on-a-chip system applying multisensor technologies", MultisenseChip [FP7/2007-2013]. The authors thank microfluidic ChipShop (http://www.microfluidic-chipshop.com/) for provision of the microfluidics.

APPENDIX A. SUPPLEMENTARY DATA

REFERENCES

Anderson, G.P., King, K.D., Gaffney, K.L. and Johnson, L.H., 2000. *Biosensors and Bioelectronics* 14 (10-11), 771-777.

Bystrom, M., Bocher, S., Magnusson, A., Prag, J., Johansson, A., 2005. J*ournal of Clinical Microbiology* 43(10), 5355–5358.

Dennis, D.T., Inglesby, T.V., Henderson, D. A., Bartlett, J. G., Ascher, M. S., Eitzen, E., Fine, A. D., Friedlander, A. M., Hauer, J., Layton, M., Lillibridge, S. R., McDade, J. E., Osterholm, M. T., O'Toole, E., Parker, G., Perl, T. M., Russel, P. K., and Tonat, K., 2001. *The Journal of the American Medical Association* 285(21), 2763-2773.

Emanuel P. A., B.R., Dang J. L., McClanahan R., David J. C., Burgess R. J., Thompson J., Collins L., and Hadfield T., 2003. *Journal of Clinical Microbiology* 41(2), 689-693.

Fragoso, A., Latta, D., Laboria, N., von Germar, F., Hansen-Hagge, T. E, Kemmner, W, Gärtner, C., Klemm, R., Dreseb, K. S., and O'Sullivan, C. K, 2011. *Lab on a Chip* 11, 625-631.

Grunow, R., Splettstoesser, W., McDonnald, S., Otterbein, C., O'Brien, T., Morgan, C., Aldrich, J., Hofer, E., Finke, EJ., and Meyer, H., 2000. *Clinical and Diagnostic Laboratory Immunology* 7(1), 86-90.

Hermanson, G.T., 2008. Bioconjugate techniques. Academic press 2nd edition(Oxford, UK.).
Johansson, A., Ibrahim, A., Göransson, I., Eriksson, U., Gurycova, D., Clarridge, J. E, and Sjöstedt, A., 2000. *Journal of Clinical Microbiology* 38(11), 4180-4185.

Kleo, K., Schafer, D., Klar, S., Jacob, D., Grunow, R., and Lisdat, F., 2012. *Analytical and Bioanalytical Chemistry* 404, 843-851.

Lazcka, O., Javier Del Campo, F., Xavier Munoz, F., 2007. *Biosensors and Bioelectronics* 22 1205-1217.

Magnarelli, L., Levy, S., and Koski, R., 2007. *Research in Vetenerary Science* 82, 22-26.

Nassef, H.M., Civit, L., Fragoso, A., and O'Sullivan, C. K., 2009. *Analytical Chemistry* 81, 5299-5307.

Penn, R.L., 2005. *Mandell, Douglas and Bennett's Principles and Practice of Infectious Diseases* 2, 2927-2937.

Pividori, M.I., Lermo, A., Bonanni, A., Alegret, S., del Valle, M., 2009. *Analytical Biochemistry* 388, 229 - 234.

Pohanka, M., and Skládal, P., 2008a. *Journal of Applied Biomedicine* 6, 57-64.

Pohanka, M., Pavlis, O., Kroca, M., 2008b. *Defence Science Journal* 58 (5), 698-702

Pohanka, M., Skládal, P., and Kroèa, M., 2007. *Defence Science Journal* 57(3), 185-193.

Porsch-Ozcürümez, M., Kischel, N., Priebe, H., Splettstösser, W., Finke, EJ., Grunow, R., 2004. *Clinical Diagnostic Laboratory Immunology* 11(6), 1008-1015.

Riddles, P.W., 1983. *Methods in Enzymology* 91, 49-60.

Savitt, A.G., Mena-Taboada, P., Monsalve, G., and Benach, J. L., 2009. *Clinical and Vaccine Immunology* 16(3), 414-422.

Simşek, H., Taner, M., Karadenizli, A., Ertek, M., and Vahaboğlu, H., 2012. *European Journal of Clinical Microbiology & Infectious Diseases* 31(9), 2353-2357.

Sjöstedt, A., Eriksson, U., Berglund, L., and Tarnvik, A., 1997. *Journal of Clinical Microbiology*, 35(5), 1045–1048.

Skládal, P., Pohanka, M., Kupská, E., and Šafář, B., 2010. *In: Biosensors, INTECH, Vienna,* 115-126.

Skladal, P., Symerska, Y., Pohanka, M., Safar, B., and Macela, A., 2005. *Defense against Bioterror: Detection Technologies, Implementation Strategies and Commercial Opportunities,* 221-232.

Su, J., Yang, J., Zhao, D., Kawula, T. H., Banas, J. A., and Zhang, JR., 2007. *Infection and Immunity* 75(6), 3089-3101.

Versage JL, S.D., Chu MC, Petersen JM, 2003. *Journal of Clinical Microbiology* 41, 5492–5499.

Vivekananda, J.a.K., J. L., 2006. *Laboratory Investigation* 86, 610-618.

Warsinke, A., Benkert, A., Scheller, F. W., 2000. *Journal of Analytical Chemistry* 366(6-7), 622-634.

Chapter 2: Supplementary information

Automated microfluidically controlled electrochemical biosensor for the rapid and highly sensitive detection of *Francisella tularensis*

Samuel B. Dulay*, Rainer Gransee, Sandra Julich, Herbert Tomaso, and Ciara K. O'Sullivan*

This supporting information material includes:

1. Materials used in Enzyme Linked Immunosorbent Assay (ELISA) characterisation of the prepared monoclonal antibody (mAb)-HRP conjugate and for choosing best assay combination
2. Results and Figures
3. References

2.1 MATERIALS AND METHODS

Materials

All the starting materials were obtained from commercial suppliers and used without further purification. NUNC-immunoplates (Thermo scientific) were purchased from Nunc A/S, Kamstrupvej 90, Denmark. Monoclonal antibodies FB11 and T14 were purchased from Hytest Ltd. Company, Finland. Lipopolysaccharide (LPS) from *Francisella tularensis* subsp. *holarctica* was purchased from MICROMUN Privates Institut fűr Mikrobiologische Forschung GmbH, Germany. Phosphate-buffered saline and Phosphate-buffered saline with Tween 20 were purchased from Scharlau (Spain). 3,3',5,5'-Tetramethylbenzidine (TMB) liquid substrate system for ELISA was purchased from Sigma. Aqueous solutions were prepared with Milli-Q water Millipore (18mΩ.cm) and all reagents were used as received.

Methods

Conjugation synthesis

Preparation of horseradish peroxidase – labelled monoclonal antibody (mAb), i.e FB11-HRP, T14-HRP, and fragment FabT14-HRP were prepared according to the procedure of bioconjugate techniques by Hermanson (Hermanson 2008).

1. RESULTS AND FIGURES

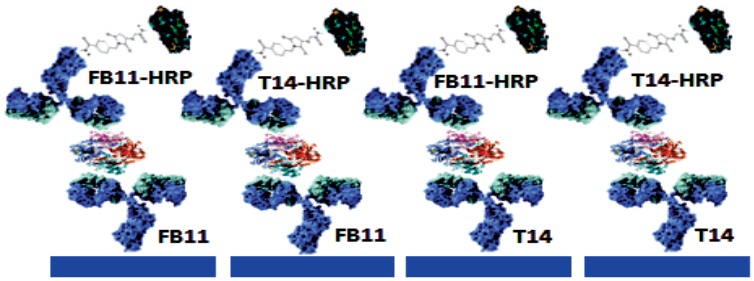

Figure 2.S1: Scheme planned for ELISA analysis for the characterization of the prepared monoclonal antibody (mAb)-HRP conjugate and for choosing best assay combination

Immobilization of Antibody and detection of antigen

The concentration of the coating used was 10 μg/mL, which is more than enough to completely coat the surface of the plate. The reporter probe concentration was varied (0-10μg/mL) to evaluate and determine the optimum condition of each assay for detection of different concentrations of antigen LPS (0-20 μg/mL).

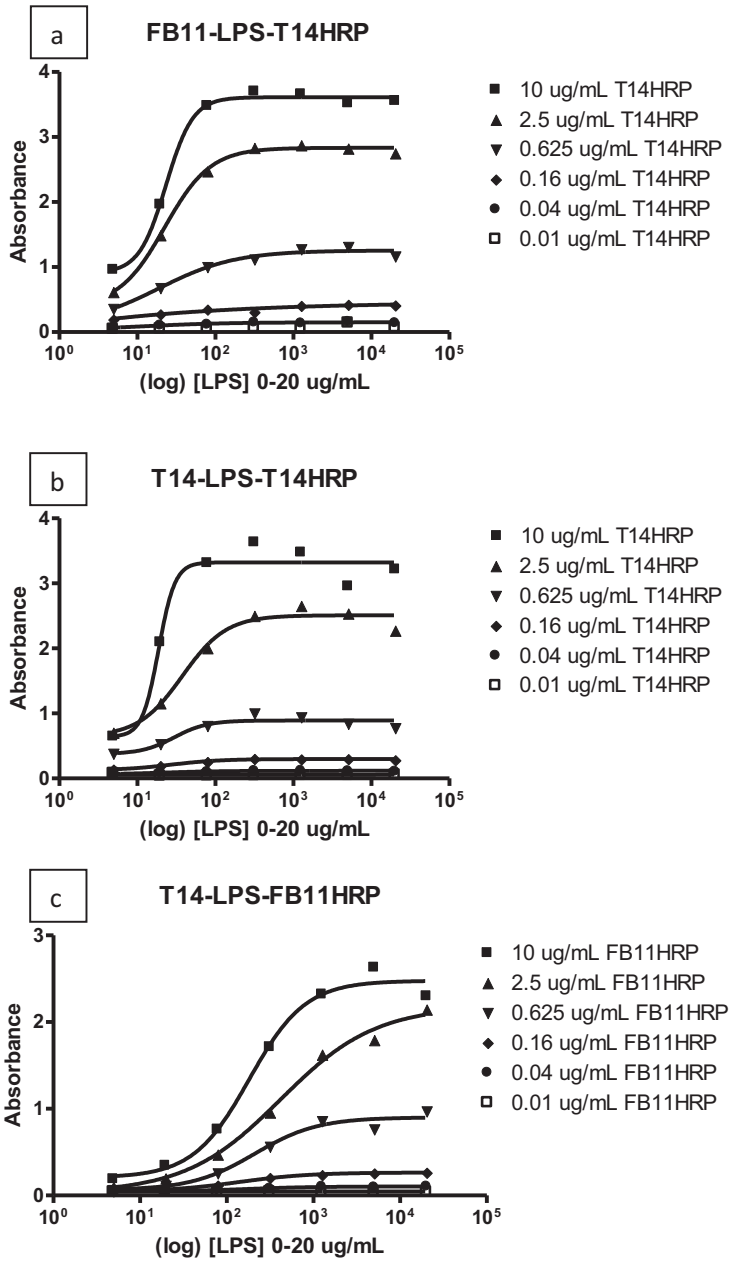

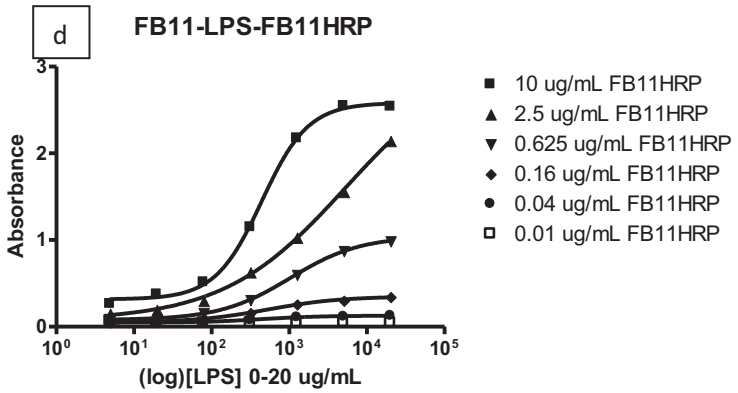

Figure 2.S2: ELISA responses of different assay schemes; a) coating probe-FB11, Reporter probe-T14-HRP b) coating probe-T14, Reporter probe-T14-HRP c) coating probe-T14, Reporter probe-FB11-HRP d) coating probe-FB11, Reporter probe-FB11-HRP to different concentrations of LPS varying concentrations of the reporter probes; UV-VIS absorbance at 450 nm. Each data point represents the average of three independent measurements.

Table 2.S1: Summary of calculated limit of detection (LOD) of each assay arrangement using prism software statistical analysis, OR-out of range

Reporter probe [AbHRP] µg/mL	Assay arrangement			
	T14-LPS-FB11HRP	**T14-LPS-T14HRP**	**FB11-LPS-T14HRP**	**FB11LPS-FB11HRP**
	LOD (ng/mL)			
10	59	21	10	56
2.5	57	30	8	24
0.625	107	49	OR	18
0.16	19	19	OR	42
0.04	99	OR	OR	82
0.01	OR	OR	OR	OR

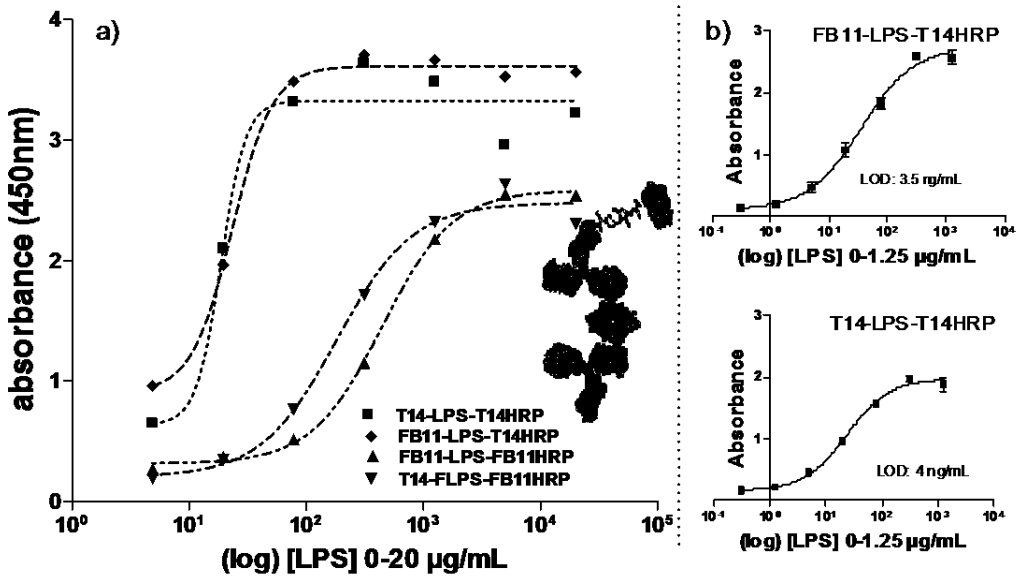

Fig. 2.S3. ELISA responses of a) different assay scheme combinations (10 µg/mL of mAb FB11 or T14 coating) and b) two best assay scheme combinations: (top) coating probe-FB11, secondary labelled antibody-T14-HRP (below) coating antibody-T14, secondary labelled antibody-T14-HRP to different concentrations of LPS with their corresponding detection limit. Each data point represents the average of three independent measurements.

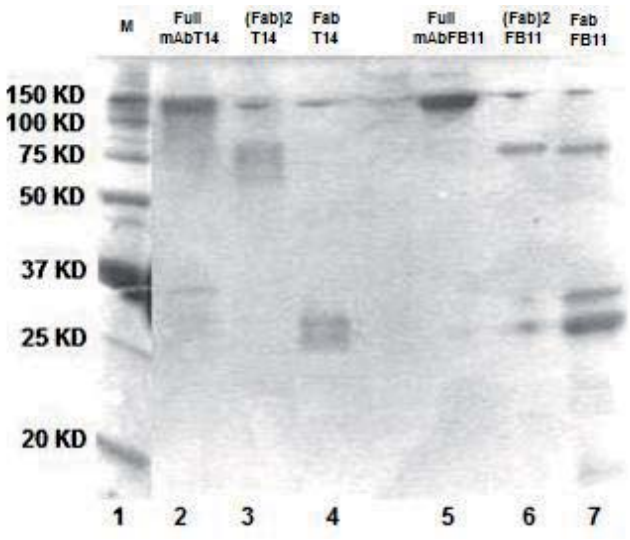

Fig. 2.S4. SDS-PAGE analysis (12% gel; nonreducing conditions) of the full length monoclonal antibodies FB11 and T14 antibody and their $F(ab)_2$ and Fab fragments: (a) lane 1, molecular weight marker; lane 2, full-length monoclonal antibody T14; lane 3, $(Fab')_2$ fragments T14 (obtained by enzymatic bromelain fragmentation); lane 4, cysteine reduction of $(Fab')_2$ T14 to (Fab) fragments T14; lane 5, full-length monoclonal antibody FB11; lane 6, $F(ab)_2$ fragments FB11 (obtained by enzymatic bromelain fragmentation); lane 7, cysteine reduction of $(Fab')_2$ FB11 to (Fab) fragments FB11.

Figure 2.S4 illustrates the SDS-PAGE (12%) analysis of the full length monoclonal antibodies FB11 and T14 and their corresponding $(Fab')_2$ and (Fab) fragments under non-reducing conditions. Lane 4 and 7 of Figure 2.S4 clearly show bands around 30 kDa indicating that a significant amount of Fab fragments was generated from both the T14 and FB11 antibodies. Lane 3 and 6 presents a major band around 75 kDa which can be attributed to the produced $(Fab')_2$ fragments for both mAb. As expected in Lane 3 and 6, few bands were observed around 60 and 30 kDa respectively, indicating that further reduction of $(FAb')_2$ fragment to (FAb) fragment was achieved.

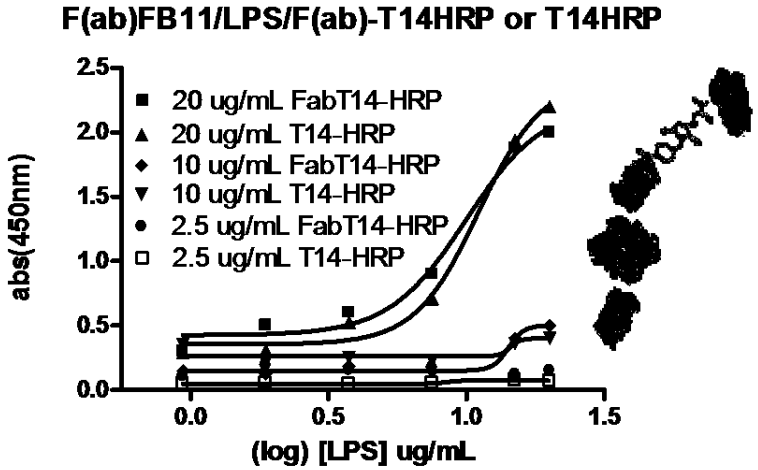

Fig. 2.S5. ELISA result of different concentration of antigen LPS to varied concentration of labelled Fab fragment T14-HRP. On the right side, scheme of the immunoassay. Each data point represents the average of three independent measurements.

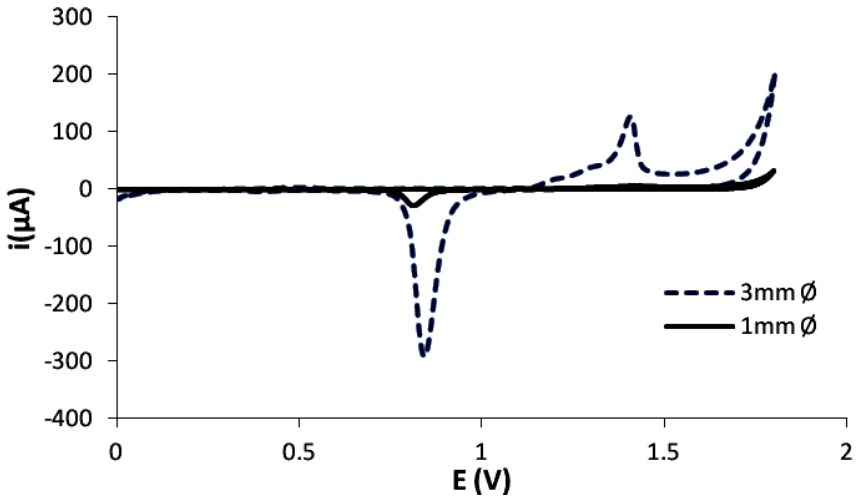

Fig. 2.S6. Typical acid CV (0.5M sulfuric acid) of lithographically produced gold electrodes (3mm and 1mm Ø) with 10 CV cycles at 0.3 V/s scan rate vs. Ag/AgCl reference electrode. (Hoogvliet *et al.* 2000).

Protocol for assay measurement within microfluidics:

To avoid build up of bubbles within the microfluidics, the speed of the liquid flow was optimised and a 70 rotation per minute (rpm) was found to be the optimum speed to avoid bubble formation. Turning valves with minileur connections to 4 inlet ports were used with one outlet and one venting port, where simple rotational turning of the valve aligns specific inlet-outlet channels that connect individual reservoirs with microchannels for introduction of each of the reagents to the microsystem and the electrode array. A syringe pump was used to drive the fluids, and the rotation and syringe pump speed, as well as the incubation times are given in Table 2.S2.

Table 2.S2. Assay procedure protocol used in the microfluidic set-up for amperometric measurements

Protocol	Rotation (turn)	Speed (rpm)	Waiting (s)
1. Incubation of pre-mixed LVS target and secondary labelled antibody (T14-HRP)	70	70	900
2. Venting (vacuum sucking)	150	1000	5
3. Washing with PBS, pH 7.4	200	100	10
4. Venting (vacuum sucking)	150	1000	5
5. Amperometric measurement, TMB substrate	50	20	160
		Total assay time	1080

Table 2.S3. Comparison with other techniques showing the detection limit obtained on the methods used

Techniques	Limit of detection (CFU/mL)	References
Fab - EC sensor in microfluidics	38	Current work
Electrochemical biosensor	100	(Skladal *et al.* 2005)
Piezoelectric immunosensor	105	(Pohanka *et al.* 2007)
Quartz crystal microbalance with	$4x10^3$	(Kleo *et al.*2012)

dissipation monitoring		
Fiber optic biosensor	$5x10^5$	(Anderson *et al.* 2000)
ELISA	$6.9x10^6$	(Pohanka *et al.* 2008)

References:

Anderson, G.P., King, K.D., Gaffney, K.L. and Johnson, L.H., 2000. *Biosensors and Bioelectronics* 14, 771-777.

Hermanson, G.T., 2008. Bioconjugate techniques. Academic press 2nd edition(Oxford, UK.)

Hoogvliet, J.C., Dijksma, M., Kamp, B., and Van Bennekom, W.P., 2000. *Analytical Chemistry* 72(9), 2016-2021.

Kleo, K., Schafer, D., Klar, S., Jacob, D., Grunow, R., and Lisdat, F., 2012. *Analytical Bioanalytical Chemistry 404*, 843-851.

Pohanka, M., Pavlis, O., Kroca, M., 2008. *Defence Science Journal* 58 (5), 698-702

Pohanka, M.a.S., P., 2007. *Folia microbiologica* 52(4), 325-330.

Skladal, P., Symerska, Y., Pohanka, M., Safar, B., and Macela, A., 2005. *Defense against Bioterror: Detection Technologies, Implementation Strategies and Commercial Opportunities*, 221-232.

Chapter 3

Development of an immunosensor for the detection of *Francisella tularensis* antibodies

Analytical and Bioanalytical Chemistry, *Manuscript accepted*

Development of an immunosensor for the detection of *Francisella tularensis* antibodies

Samuel B. Dulay[a*], Sandra Julich[b], Herbert Tomaso[b], and Ciara K. O'Sullivan[a,c*]

[a]Departament d'Enginyeria Quimica, Universitat Rovira i Virgili, Avinguda Països Catalans 26, 43007 Tarragona, Spain

[b]Institute of Bacterial Infections and Zoonoses, Friedrich-Loeffler-Institut, Naumburger Strasse 96 a, Jena, 07743, Germany

[c]Institució Catalana de Recerca i Estudis Avancats,Passeig Lluís Companys, 23, 08010 Barcelona, Spain

*Corresponding author.

E-mail addresses: samuelbacena.dulay@estudiants.urv.cat (S.B.Dulay), ciara.osullivan@urv.cat (C.K.O'Sullivan).

ABSTRACT

Tularemia, also known as rabbit fever, is a highly infectious zoonotic disease caused by a non-motile and non-spore-forming Gram-negative coccoid rod bacterium, *Francisella tularensis*. It occurs naturally in lagomorphs (rabbits and hares), but many animals have been reported to be susceptible. Transmission to humans is mostly caused by inhalation of aerosolised bacteria, handling of infected animals, arthropod stings, and ingestion of contaminated foods and water. At present, pathogenic isolation, molecular detection, and serology are the most commonly used methods to

confirm the diagnosis of tularemia. In this work, an electrochemical immunosensor for the detection of anti-*F. tularensis* antibodies was developed, consisting of gold-based self-assembled monolayers of a carboxylic group terminated bipodal alkanethiol that is covalently linked to lipopolysacharride (LPS) that can be found in the outer membrane of the bacteria *F. tularensis*. The presence of anti-*F. tularensis* antibodies was measured using horseradish peroxidase-labelled protein A (HRP-Protein A) from *Staphylococcus aureus*, and the developed immunosensor gave a stable quantitative response to different anti-*F. tularensis* FB11 antibodies concentrations after 30 min with a limit of detection of **15** ng/mL, RSD of 9%, n = 3. The developed immunosensor was tested with serum from animals infected with tularemia and was compared to the results obtained using ELISA showing an excellent degree of correlation.

Keywords: Electrochemical immunosensors, Francisella tularensis, Self-assembled monolayer (SAM)

3.1. INTRODUCTION

Tularemia is a highly contagious and infectious zoonotic disease caused by *Francisella tularensis*. This non-motile and non-spore-forming Gram-negative coccoid rod bacterium occurs naturally in lagomorphs (rabbits and hares), but many animals have been reported to be infected. Transmission to humans is often associated with inhalation of aerosolised bacteria, handling of infected animals, arthropod stings, and ingestion of contaminated foods and water [1, 2]. Clinical manifestation of the disease in humans can occur in different forms ranging from skin ulcers to more severe forms such as life-threatening pneumonia [3] due to its high virulence, transmission and mortality [4]. *F. tularensis* could be used as a potential biological warfare agent or in terrorist attacks and has been classified as category A (http://emergency.cdc.gov/agent/agentlist-category.asp). To date, identification of *F. tularensis* has been achieved using cultivation and molecular techniques

including polymerase chain reaction (PCR) [5] and real time PCR assays [6-8]. Besides the detection of the bacterial cell, the detection of specific antibodies in serum is the most widely used serological analysis technique for routine laboratory diagnosis of tularemia [9]. In veterinary medicine, serology is used mainly for tularemia surveillance in rodents, hares, or surrogate animals such as boars or predators, including wolves or bears[10]. Detection of antibodies against *F. tularensis* is also useful to confirm successful vaccination after immunization with live or subunit vaccines. It is advantageous as well to do serology to detect *F. tularensis* antibodies, which appears 6-10 days after infection[11], when tularemia has not yet been diagnosed since bacterial culture is difficult and poses a high risk of laboratory infection. Several techniques like Enzyme-linked immunosorbent assays (ELISA) [12, 13], Western blot and other immunological assays can be used to detect the status of seroconversion in patients. Although these standard techniques are sensitive, they are inherently laboratory based, rather time consuming requiring intensive hands-on-time as well as specialised instrumentation.

Electrochemical biosensors are an interesting alternative for in situ detection due to their excellent sensitivity, selectivity, versatility, and simplicity [14, 15]. The development of these technologies has garnered a continual interest for application in clinical diagnostics, food quality control and environmental monitoring [16] as promising alternatives to traditional methods in detecting pathogens [17]. The architecture of most electrochemical sensors attempt to mimic that found in standard ELISA where different strategies for immobilisation of the biocomponent on the transducer's surface have been developed. The use of self-assembled monolayers (SAM) has gained increased interest due to the possibility of avoiding random orientation of the biocomponents (antibody/antigen) on the surface, good surface coverage and the possibility of incorporating efficient surface protection moieties to eliminate non-specific binding.

In this work, we demonstrate the development of an electrochemical immunosensor for rapid detection of anti-*F. tularensis* antibodies and apply it to the analysis of serum taken from an

infected red fox (*Vulpes vulpes*). The sensor surface chemistry exploits gold-based self-assembled monolayers of a carboxylic group terminated bipodal alkanethiol that is covalently linked to lipopolysaccharide (LPS) that can be found in the outer membrane of the bacteria *F. tularensis*. The presence of anti-*F. tularensis* antibodies was measured using HRP-Protein A from *Staphylococcus aureus* as a reporter molecule.

3.2. MATERIALS AND METHODS

All the starting materials were used without further purification. Monoclonal antibody (mAb) FB11 (isotype IgG2a) was purchased from Hytest Ltd., Finland. Lipopolysaccharide (LPS) from *Francisella tularensis* subsp. *holarctica,* whole cell bacteria of *Francisella tularensis* LVS subsp. *holarctica*, red fox serum samples, Brucellosis control serum and three human serum samples-IgG positive for *Yersinia enterocolotica* were kindly provided by the Friedrich-Loeffler-Institut, Institut für bakterielle Infektionen und Zoonosen, Germany. NUNC-immunoplates (Thermo scientific) were purchased from Nunc A/S, Kamstrupvej 90, Denmark. Sulphuric acid, strontium nitrate, phosphate-buffered saline (PBS) (dry powder), PBS-Tween-20, hydrogen peroxide 30%, ethanolamine, acetone and ethanol (synthetic grade), Phosphate-buffered saline, Phosphate-buffered saline with Tween 20, N-(3-dimethylaminopropyl) – N – ethylcarbodiimide (EDC), N-hydroxysuccinimide (NHS), and acetic acid were purchased from Scharlau (Spain); (22-(3,5-bis((6 mercaptohexyl)oxy)phenyl)-3,6,9,12,15,18,21- heptaoxadocosanoic acid dithiol PEG-6 carboxylate (DT2) was purchased from SensoPath Technologies (USA) and 3,3,5,5-Tetramethylbenzidine (TMB) Liquid Substrate System for ELISA was obtained from Sigma. Aqueous solutions were prepared with Milli-Q water Millipore (18 MΩ·cm) and all reagents were used as received.

3.2.1 Instrumentation

Electrochemical studies were carried out using an Autolab PGSTAT 10 potentiostat and measurements were performed using a conventional three-electrode cell. 3 mm-diameter lithographically produced gold electrodes were used as working electrode, a standard silver/sliver chloride (sat. KCl) as a reference electrode (CHI 111 CH Instruments) and a platinum gauze as the counter electrode. The lithographically produced gold electrodes were provided by Fraunhofer ICT-IMM (IMM), Germany, and were produced as previously reported [18]. All sonication procedures were conducted with an ultrasonic bath (Branson ultrasonic corporation, model 2510E-MT, USA). Enzyme-linked immunosorbent assay (ELISA) studies were performed using a microtitre plate reader (bioNOVA cientifica, S.L. Madrid, Spain) and a HydroFlex 3-in-1 well washer, TECAN (Spain).

3.2.2 Preparation and characterisation of immunoassay format

Sample collection

Previous studies demonstrated, that foxes such as wild boars can be used as indicator animals for investigation on the circulation of *F. tularensis* in the environment [10]. Blood samples obtained from red foxes were collected in 2011 in Saxony-Anhalt. Blood cells were separated from serum by centrifugation.

Cultivation and inactivation of Francisella tularensis bacteria suspension

F. tularensis LVS subsp. *holarctica* was cultivated on cysteine heart agar (Becton Dickinson GmbH, Heidelberg, Germany) supplemented with 10 % chocolatized sheep blood. Incubation was carried out for 3 days at 37 °C in an atmosphere with 5 % CO_2. Heat assisted inactivation was carried out for 10 min at 95 °C (Thermomixer Compact, Eppendorf AG, Hamburg, Germany). To

check sterility, the suspension was plated on agar plates and incubated for 7 days and no growth was observed.

ELISA evaluation of optimum capture probe antigen and labelled reporter molecule for sandwich assay

F. tularensis LPS and inactivated whole bacterial cells of *F. tularensis* LVS subsp. *holarctica* of 0.02 - 100 μg/mL and 47 – 3000 bacterial cells in carbonate buffer, pH 9.5, respectively were prepared separately and were added to each well of a NUNC immunosorp microtiter plate and incubated for 30 min at 37 °C. Following thorough washing with PBS-Tween 20 (pH 7.4, 0.01 M), the plate was then blocked by addition of 200 μL of PBS-Tween 20 (pH 7.4, 0.01 M) and incubated for 1 h at 37 °C, followed by thorough washing of the plate. In the immunorecognition step, 50 μL each of a range of concentrations of anti-*F. tularensis* antibody FB11or 50 μL of animal serum samples (diluted 1:1 – 1:1500) prepared in PBS-Tween 20 (pH 7.4, 0.01 M) were added to each well coated with LPS of *F. tularensis* subsp. *holarctica* or inactivated whole bacterial cells of *F. tularensis* LVS subsp. *holarctica*. The plate was again incubated, under shaking conditions for 30 min at 37 °C, and subsequently thoroughly washed with PBS-Tween 20, prior to exposure to different concentrations of HRP-Protein A (0-2.5 μg/mL) as reporter molecule and again left to incubate under shaking conditions for 30 min at 37 °C. After a final wash, 50 μL of TMB for ELISA substrate was added to each well and product formation was allowed to proceed for at least 15 min at room temperature. The reaction was finally stopped by addition of 1 M H_2SO_4, and the absorbance read at 450 nm. Analysis was carried out in triplicate.

3.2.3 Electrode modification and electrochemical detection

Prior to modification of the lithographic gold electrodes, a two-step cleaning protocol was applied. Initially in order to remove the protective resist used during storage, the electrodes were sonicated for 5 min in acetone (2 times), 5 min in isopropanol (3 times) and rinsed with water and dried with compressed air. In a second step, electrochemical cleaning was performed in 0.5 M H_2SO_4 by application of a constant potential of 1.6 V for 10s followed by 10 voltammetric cycles in the potential range −0.2 to 1.6 V at a scan rate of 0.3 V/s. Finally, the electrodes were rinsed with Milli-Q water and dried with nitrogen.

Modification of the cleaned electrodes was carried by formation of a SAM of the bipodal alkanethiol DT2 followed by covalent linking of *F. tularensis* LPS. In the DT2 immobilisation, electrodes were immersed in an ethanolic solution of 1 μM DT2 for 3 hours, then rinsed with ethanol and dried with argon. To activate the carboxylic acids of the DT2, the electrodes were then immersed in a mixture of 50% (v/v) EDC (0.2M) and 50% (v/v) NHS (0.05M) for 30 min and then rinsed with Milli-Q water. Subsequently, 100 μg/mL of *F. tularensis* LPS in PBS (pH 7.4, 0.01 M) was added to the electrodes modified with the activated DT2 for 30 min and then rinsed with Milli-Q water. Finally, any unreacted activated carboxylic acid groups remaining were blocked by immersion of the electrodes for 15 min in ethanolamine pH 8.5, followed by a final rinse with Milli-Q water.

The electrodes were then exposed to different concentration of anti-*F. tularensis* antibody FB11 in PBS (pH 7.4, 0.01 M) for 15 min and then incubated for another 15 min with HRP-Protein A. Subsequently, the electrodes were gently washed with PBS (pH 7.4, 0.01 M) for 30 sec. Amperometric measurement was carried out at 0.15 V vs. Ag/AgCl in an electrochemical cell for less than 2 minutes upon addition of TMB solution. All electrochemical measurements were performed at room temperature. The overall immobilization process and detection mechanism is depicted in Figure 3.1.

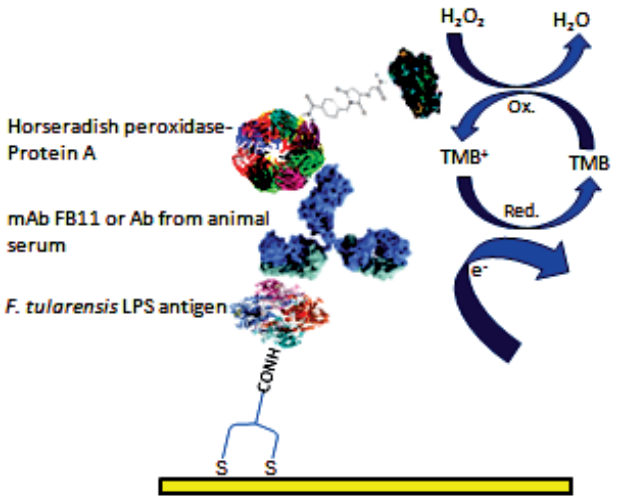

Fig. 3.1. Schematic of the electrochemical immunosensor architecture.

3.3. RESULTS AND DISCUSSIONS

3.3.1 ELISA evaluation of optimum capture probe antigen and labelled reporter molecule for sandwich assay

ELISA was developed to optimise the conditions to be used in the electrochemical immunosensor, and to this end two different coating antigens were compared to probe which provided better levels of sensitivity for the detection of anti-*F. tularensis* antibodies. The antigens compared were LPS that can be found in the outer membrane of *F. tularensis* subsp. *holarctica* and inactivated whole bacterial cells of *F. tularensis* subs. *holarctica* live vaccine strain (LVS). Using checkerboard type assays, different concentrations of coating antigens and HRP-Protein A as reporter molecule were evaluated to elucidate the optimum conditions for each assay format at a fixed concentration of 150 μg/mL mAb FB11 (Supplementary Information Figure 3.S1-3.S2). mAb FB11 has been derived from hybridization of Sp2/0 myeloma cells with spleen cells of Balb/c mice immunized with *F. tularensis* (http://www.hytest.fi). As can be seen in Figure 3.2, it was observed

that LPS gave a better limit of detection and sensitivity, presumably due to higher density of binding sites attributable to the higher number of LPS immobilised as compared to that of the use of whole bacterial cells. The optimum concentrations of LPS coating antigen and HRP-Protein A was found to be 15 μg/mL and 0.63 μg/mL respectively, with a detection limit of 27 ng/mL, a linear range extending from 0.1 to 25 μg/mL.

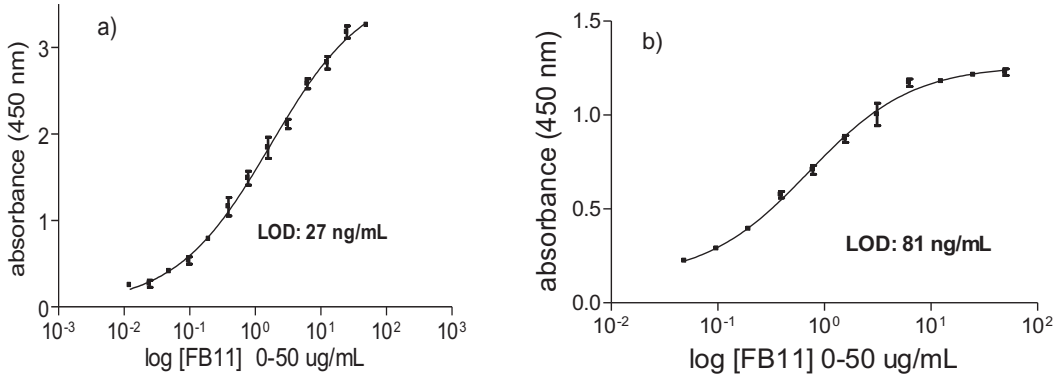

Fig. 3.2. ELISA measurement of calibration curve for anti-*F. tularensis* LPS antibody FB11 using a) 15 μg/mL of *F. tularensis* LPS and b) 280 bacteria cells/mL of *F. tularensis* subsp. *holarctica* as coatings respectively at 0.63 μg/mL of HRP labelled protein A as reporter molecule. Each data points represent the average of six measurements in a plate.

3.3.2 Development of electrochemical immunosensor

For development and testing of the immunosensor, a conventional three-electrode cell was used, where 3 mm-diameter macro lithographic gold electrodes were used as working electrodes with a Ag/AgCl reference and Pt counter electrode. The electrochemical immunosensor was constructed using the LPS covalently linked to bipodal alkanethiol DT2 as capture probe antigen and HRP-Protein A as reporter molecule. This sensor was used to detect different concentrations of mAb FB11 as well as the anti-*F. tularensis* antibody in infected animal serum samples from red foxes

(*Vulpes vulpes*). The signal of the zero concentration value plus three times its standard deviation was used to estimate a limit of detection of 15 ng/mL of the anti-*F. tularensis* antibody FB11 (Fig. 3.3a) slightly better than that obtained with ELISA (Figure 3.2a) and significantly comparable to some methods reported that have detected the *F. tularensis* antibodies qualitatively (see Supplementary Information Table 3.S1). The linear range obtained with the immunosensor was smaller than that obtainable with ELISA, due to the number of capture-molecules immobilised on the electrode surface as they have different surface properties where ELISA plate surfaces directly absorbs more antigen probes compared to the immobilised antigens in immunosensor that is controlled by the number of immobilised DT2 as an anchor for the antigen capture probe.

Real animal serum samples were tested using the same electrochemical immunosensor. Sera did not affect the performance of the electrodes, due to the presence of the polyethylene glycol moiety present in the bipodal dithiol, which effectively eliminates non-specific binding of any sample matrix components, whilst its' bipodal structure facilitated optimal spacing on the electrode surface and consequently, good electron transfer.

Different real animal serum samples from red foxes (*Vulpes vulpes*) were evaluated using the developed immunosensor and the currents obtained extrapolated to the calibration plot (Fig. 3.3a) As the concentration of the antibodies in the animal samples is unknown, a range of dilutions of the samples were tested (Figure 3.3b), and a dilution factor of between 1 in 320 and 1 in 1200 used for ELISA and immunosensor respectively. As can be seen in the table in Figure 3.3, the comparison of the results obtained using the electrochemical immunosensor showed an excellent degree of correlation with the results obtained using ELISA .

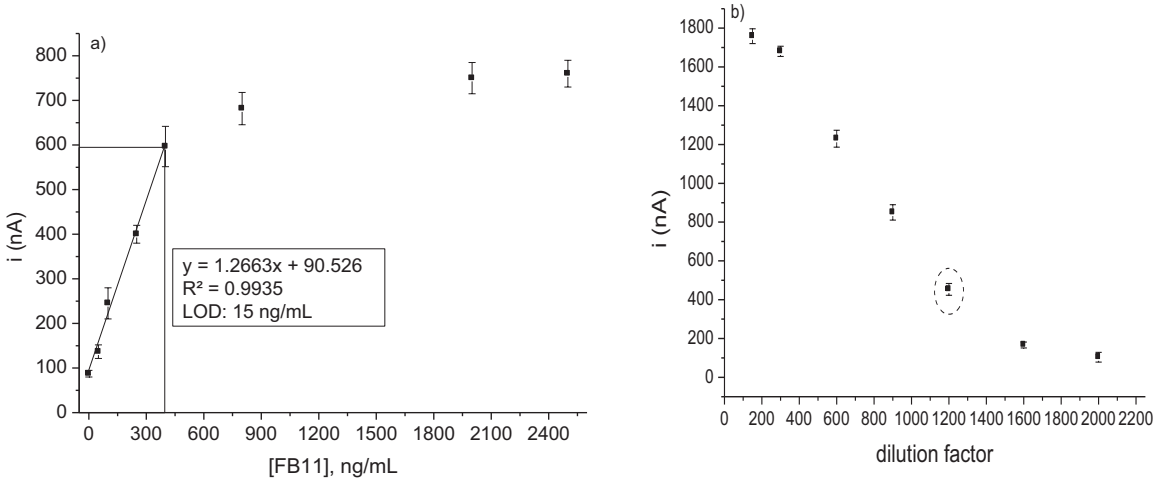

c) Fox serum sample	ELISA (D.F. 1:320)	Immunosensor (D.F. 1:1200)	
	mAb FB11, ng/mL	i (nA)	mAb FB11, ng/mL
Fox serum 1	300±26	454±25	287±20
Fox serum 2	200±18	299±20	165±15
Fox serum 3	380±27	589±26	394±20

Fig. 3.3. a) Amperometric response of the electrochemical immunosensor to different mAb FB11concentrations, b) typical amperometric detection of FB11 antibodies present in animal serum samples in red foxes (*Vulpes vulpes)* in different dilution factor using the developed electrochemical sensor and c) summarised table for the calculated concentration of antibodies for ELISA and immunosensor method. Each data point represents the average of three measurements in different separate sensors.

To demonstrate the specificity of the immunosensor, control measurements were performed by exposing the modified electrode array with two different antibodies (Figure 3.4). It was observed that LPS modified electrodes only obtained a specific sensor response when exposed to anti-*F. tularensis* antibodies present in animal serum samples in red foxes. Other types of

antibodies, i.e antibodies against Brucellosis and anti-*Y. enterocolotica* antibodies, did not give any response, highlighting the specificity of the developed immunosensor.

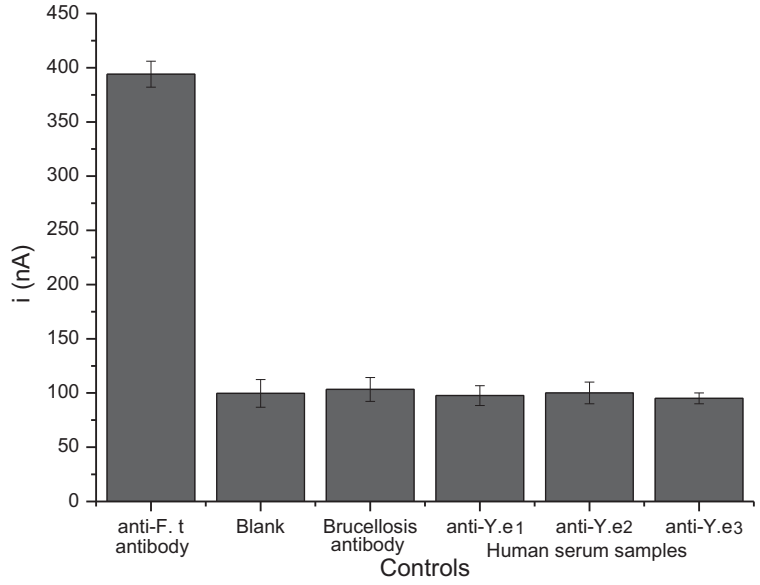

Fig. 3.4. Specificity of the immunosensor to anti-*F. tularensis* antibodies (anti-F. t) from red fox (*Vulpes vulpes*) sera, Brucellosis antibody, and three samples from human serum IgG-positive for *Y. enterocolotica* (anti-Y.e). Sample preparations: D.F 1:1200. Blank – no antibody target.

3.4 CONCLUSIONS

This report details the development of an electrochemical immunosensor for the detection of anti-*F. tularensis* antibodies. Using ELISA, the use of whole *Francisella tularensis* cells and the liopolysaccharide antigen found on the cell membrane were compared as coating antigens, and the latter found to result in much higher sensitivity. The cross-linking of LPS from *F. tularensis* to a chemisorbed self-assembled monolayer of bipodal alkane thiol was thus used as the biocomponent capture layer in the electrochemical immunosenosr. HRP-Protein A from *Staphylococcus aureus* was exploited as a reporter molecule, facilitating the sensitive quantification of anti-*F. tularensis*

antibodies, achieving a lower limit of detection than that obtained using ELISA. The immunosensor was applied to real serum samples and an excellent correlation in the results obatined with the more laborious and time-consuming ELISA procedure was observed. The specificity of the immunosensor has been clearly determined and no cross-reactivity has been found. The developed platform is a promising alternative for the rapid, reliable, portable and low cost detection of antibodies related to bacterial infections such as tularemia.

ACKNOWLEDGEMENT

The research leading to these results has received funding from the European Union's Seventh Programme for research, technological development and demonstration under grant agreement number FP7/2007-2013-Multisense Chip: "The lab-free CBRN detection device for the identification of biological pathogens on nucleic acid and immunological level as lab-on-a-chip system applying multisensor technologies". Blood samples from foxes were kindly provided by Dr. Anette Schliephake from the State Office of Consumer Protection in Saxony-Anhalt.

APPENDIX A. SUPPLEMENTARY DATA

REFERENCES

1. Magnarelli, L., Levy, S., and Koski, R. (2007) Detection of antibodies to *Francisella tularensis* in cats. Research in vetenerary science 82:22-26.
2. Kleo, K., Schafer, D., Klar, S., Jacob, D., Grunow, R., and Lisdat, F. (2012) Immunodetection of inactivated *Francisella tularensis* bacteria by using a quartz crystal microbalance with dissipation monitoring. Analytical Bioanalytical Chemistry 404:843-851.
3. Sharma, N., Hotta, A., Yamamoto, Y., Fujita, O., Uda, A., Morikawa, S., Yamada, A., and Tanabayashi, K. (2013) Detection of *Francisella tularensis*-specific antibodies in patients with tularemia by a novel competitive enzyme-linked immunosorbent assay. Clinical and vaccine immunology 20(1):9-16.
4. Su, J., Yang, J., Zhao, D., Kawula, T. H., Banas, J. A., and Zhang, JR. (2007) Genome-wide identification of *Francisella tularensis* virulence determinants. Infection and immunity 75(6):3089-3101.
5. Johansson, A., Ibrahim, A., Göransson, I., Eriksson, U., Gurycova, D., Clarridge, J. E, and Sjöstedt, A. (2000) Evaluation of PCR-based methods for discrimination of Francisella species

and subspecies and development of a specific PCR that distinguishes the two major subspecies of *Francisella tularensis*. Journal of clinical microbiology 38(11):4180-4185.

6. Bystrom, M., Bocher, S., Magnusson, A., Prag, J., Johansson, A. (2005) Tularemia in Denmark: identification of a *Francisella tularensis* subsp. holarctica strain by real-time PCR and high-resolution typing by multiple-locus variable-number tandem repeat analysis. Journal of clinical microbiology 43(10):5355–5358.
7. Simşek, H., Taner, M., Karadenizli, A., Ertek, M., and Vahaboğlu, H. (2012) Identification of *Francisella tularensis* by both culture and real-time TaqMan PCR methods from environmental water specimens in outbreak areas where tularemia cases were not previously reported. European journal of clinical microbiology and infectious diseases 31(9):2353-2357.
8. Versage JL, S.D., Chu M. C. and Petersen J. M. (2003) Development of a multitarget real-time TaqMan PCR assay for enhanced detection of *Francisella tularensis* in complex specimens. Journal of clinical microbiology 41:5492–5499.
9. Porsch-Ozcürümez, M., Kischel, N., Priebe, H., Splettstösser, W., Finke, E. J. and Grunow, R. (2004) Comparison of enzyme-linked immunosorbent assay, Western blotting, microagglutination, indirect immunofluorescence assay, and flow cytometry for serological diagnosis of tularemia. Clinical and diagnostic laboratory immunology 11(6):1008-1015.
10. Otto P., Valerie, C., Klimpel D., Diller R., Melzer F., Müller W. and Tomaso H. (2014) Serological investigation of wild boars *(Sus scrofa)* and red foxes *(Vulpes vulpes)* as indicator animals for circulation of *Francisella tularensis* in Germany. Vector borne and zoonotic diseases 14(1):46-51.
11. Splettstoesser, W., Guglielmo-Viret, V., Seibold, E. and Thullier, P. (2010) Evaluation of an immunochromatographic test for rapid and reliable serodiagnosis of human tularemia and detection of *Francisella tularensis*-specific antibodies in sera from different mammalian species. Journal of clinical microbiology 48(5):1629–1634.
12. Pohanka, M., and Skládal, P. (2008) Electrochemical biosensors – principles and applications. Journal of applied biomedicine 6:57-64.
13. Dahouk, S.A., Nockler, K. N., Tomaso, H., Splettstoesser, W. D., Jungersen, G., Riber, U., Petry, T., Hoffmann, D., Scholz, H. C., Hensel, A., and Neubauer, H. (2005) Seroprevalence of brucellosis, tularemia, and yersiniosis in wild boars (*Sus scrofa*) from north-eastern Germany. Journal of veterinary medicine B. Infectious diseases and veterinary public health 52(10):444-455.
14. Lazcka, O., Javier Del Campo, F., Xavier Munoz, F. (2007) Pathogen detection: A perspective of traditional methods and biosensors. Biosensors and Bioelectronics 22:1205-1217.
15. Pividori, M.I., Lermo, A., Bonanni, A., Alegret, S., del Valle, M. (2009) Electrochemical immunosensor for the diagnosis of celiac disease. Analytical Biochemistry 388:229 - 234.
16. Warsinke, A., Benkert, A., Scheller, F. W. (2000) Electrochemical immunoassays. Fresenius Journal o fAnalytical Chemistry 366(6-7):622-634.
17. Pohanka, M., Skládal, P., and Kroèa, M. (2007) Biosensors for Biological Warfare Agent Detection. Defence Science Journal 57(3):185-193.
18. Fragoso, A., Latta, D., Laboria, N., von Germar, F., Hansen-Hagge, T. E, Kemmner, W, Gartner, C., Klemm, R., Dreseb, K. S., and O'Sullivan, C. K. (2011)Integrated microfluidic platform for the electrochemical detection of breast cancer markers in patient serum samples. Lab on a Chip 11:625-631.

Chapter 3: Supplementary information

Development of an immunosensor for the detection of *Francisella tularensis* antibodies

Samuel B. Dulay*, Sandra Julich, Herbert Tomaso, and Ciara K. O'Sullivan*

This supporting information material includes figures:

FIGURES

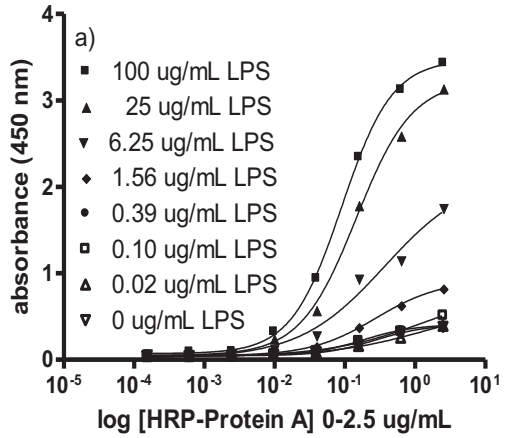

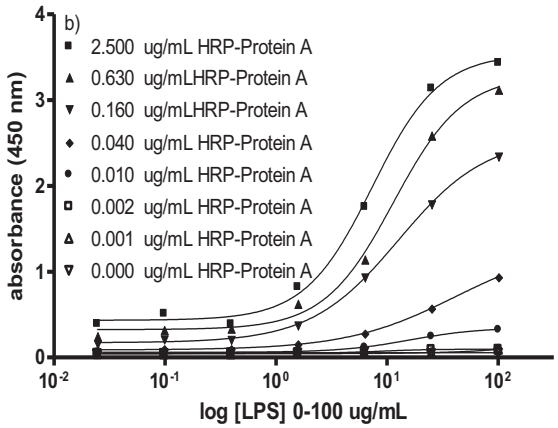

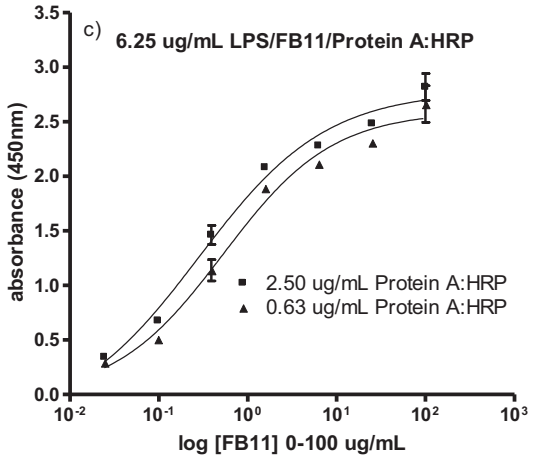

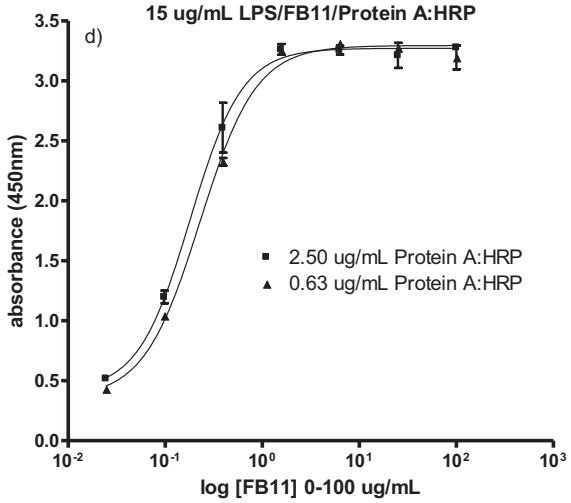

[Coating LPS], µg/mL	15		6.25	
[HRP-Protein A:HRP], µg/mL	2.5	0.63	2.5	0.63
L.O.D µg/mL	0.06	0.05	0.20	0.17

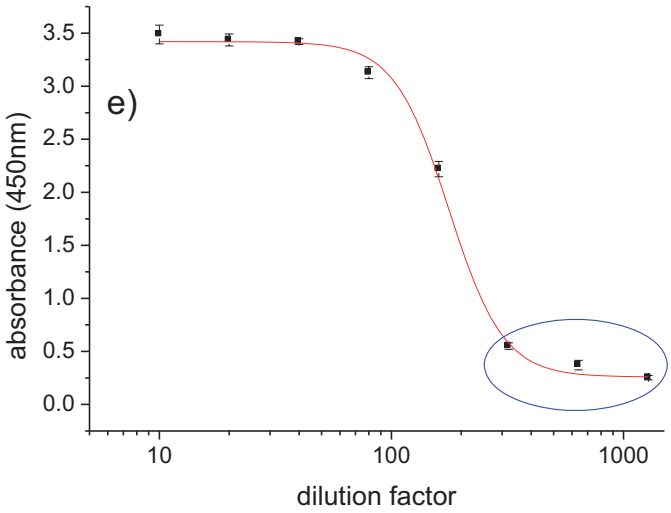

Figure 3.S1: ELISA evaluation of the immunoassay format for the optimum concentration of a) coating label (LPS) at 150 μg/mL of FB11 antibody, b) HRP-Protein A reporter probes at 150 μg/mL of FB11 antibody, c) 6.25 μg/mL of LPS as coating and 2.5 and 0.63 μg/mL of HRP-Protein A reporter probes, d) 15 μg/mL of LPS as coating and 2.5 and 0.63 μg/mL of HRP-Protein A reporter probes and e) typical quantification of concentration of serum sample from red fox (*Vulpes vulpes)* at different dilution factor at 15 μg/mL of LPS as capture antigen and 0.63 μg/mL of HRP-labelled protein A reporter probe.

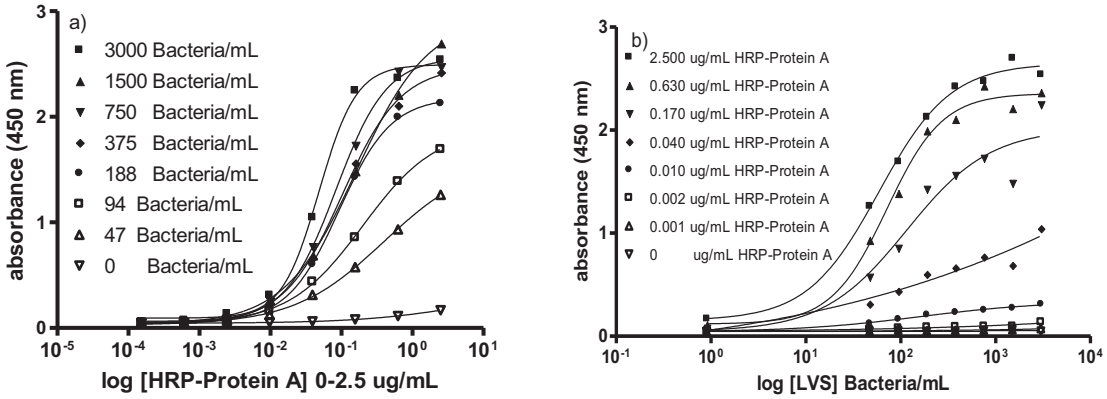

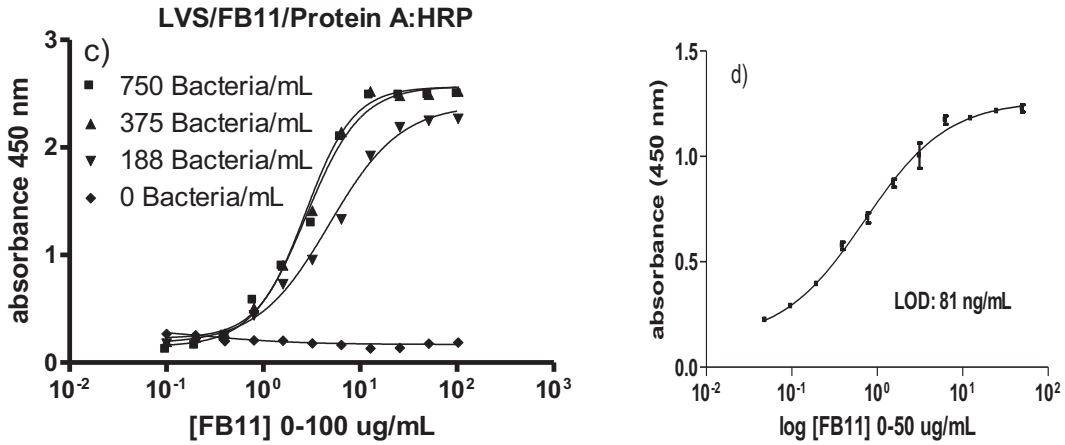

[Coating] Bacteria/mL	LOD (ng/mL)
750	651
375	587
188	636

Figure 3.S2: ELISA evaluation of the immunoassay format for the optimum concentration of a) coating label (LVS) at 0.63 μg/mL of HRP-Protein A, b) HRP-Protein A reporter probes at 0.63 μg/mL of HRP-Protein A, and c) re-evaluation of the optimum LVS coating concentrations of 188, 375, and 750 Bacteria/mL and d) 280 Bacteria/mL of LVS as coating concentration at 0.63 μg/mL of HRP-Protein A.

Table 3.S1. Comparison with other techniques showing the analytical performance obtained on the methods used

Techniques/Methods	Total assay time, min	Detection limit characteristics	References
Microtiter plate-based immunofluorescence assays	75	10 ng/mL	[1]
Piezoelectric and Amperometric immunosensor	15	Qualitative (real time observation after immunisation)	[2]
ELISA	135	Qualitative 4.2% (33/774)	[3]

Western blotting	90	3.1% (24/774)	
Indirect Fluorescent antibody (IFA)	60	Qualitative 24% (22/91)	[4]
Microagglutination	120	12% (11/91)	
Immunochromatographic test	120	100% (22/22)	[5]

References:

1. Thirumalapura, N.R., Morton, R. J., Ramachandran, A. and Malayera, J. R. (2005) Lipopolysaccharide microarrays for the detection of antibodies. Journal of immunological methods **298**(1-2):73 – 81.
2. Skládal, P., Pohanka, M., Kupská, E., and Šafář, B. (2010) Biosensors for Detection of Francisella tularensis and Diagnosis of Tularemia. In: Biosensors, INTECH, Vienna 115-126.
3. Dahouk, S.A., Nockler, K. N., Tomaso, H., Splettstoesser, W. D., Jungersen, G., Riber, U., Petry, T., Hoffmann, D., Scholz, H. C., Hensel, A., and Neubauer, H. (2005) Seroprevalence of brucellosis, tularemia, and yersiniosis in wild boars (*Sus scrofa*) from north-eastern Germany. Journal of veterinary medicine B. Infectious diseases and veterinary public health **52**(10):444-455.
4. Magnarelli, L., Levy, S., and Koski, R. (2007) Detection of antibodies to *Francisella tularensis* in cats. Research in vetenerary science **82**:22-26.
5. Splettstoesser, W., Guglielmo-Viret, V., Seibold, E. and Thullier, P. (2010) Evaluation of an immunochromatographic test for rapid and reliable serodiagnosis of human tularemia and detection of *Francisella tularensis*-specific antibodies in sera from different mammalian species. Journal of clinical microbiology **48**(5):1629–1634.

Chapter 4

Integrated microsystem for multiplexed genosensor detection of biowarfare agents

For submission

Integrated microsystem for multiplexed genosensor detection of biowarfare agents

Samuel B. Dulay[1], Rainer Gransee[2], Sandra Julich[3], Herbert Tomaso[3], and Ciara K. O'Sullivan[1,4*]

[1]Departament d'Enginyeria Quimica, Universitat Rovira i Virgili, Avinguda Països Catalans 26, 43007 Tarragona, Spain

[2]Fraunhofer ICT-IMM, Carl-Zeiss-Strasse 18-20, 55129, Mainz, Germany

[3]Institute of Bacterial infections and Zoonoses, Friedrich-Loeffer-Institut, Naumburger Str. 96A, Jena, D-07743, Germany

[4]Institució Catalana de Recerca i Estudis Avancats,Passeig Lluís Companys, 23, 08010 Barcelona, Spain

*To whom correspondence should be addressed. Tel: +34 977 55 8721; Fax: +34 977 55 8205; Email: ciara.osullivan@urv.cat (C.K.O'Sullivan).

Abstract

An early, rapid and definite detection for the presence of biowarfare agents, pathogens, viruses and toxins is required in different situations which include civil rescue and security units, homeland security, military operations, public transportation securities such as airports, metro and railway stations due to its harmful effect to human population. In this work, an electrochemical genosensor array that allows simultaneous detection of different biowarfare agents with integrated microsystem that provides an easy handling of the technology which combines with microtube

fluidics setup has been developed and optimised for the following specific genoassay: *Bacillus anthracis, Brucella melitensis, Bacteriophage lambda, Francisella tularensis, Burkholderia mallei, Coxiella burnetii, Yersinia pestis,* and *Bacillus thuringiensis var. kurstaki*. The chip electrodes arrays were modified via co-immobilisation of a 1:100 (mol/mol) mixture of a thiolated probe and a polyethyleneglycol-terminated bipodal thiol. PCR products from these relevant biowarfare agents were detected reproducibly through a sandwich assay format with the target hybridised between a surface immobilised probe into the electrode and a horseradish peroxidase-labelled secondary reporter probe, which provided an enzyme based electrochemical signal. The potential of the designed microsystem for multiplexed genosensor detection and cross-reactivity studies over potential interfering DNA sequences has demonstrated high selectivity using the developed platform producing high-throughput.

Keywrods: Electrochemical DNA biosensor, Biowarfare agent, Multiplex detection, Self-assembled monolayer (SAM)

4.1. Introduction

Considering the general availability of know-how to culture microorganisms in large quantities, there is now a global argument about the possibility of using different pathogens with high risk not only limited to public health safety but also in plants and animals for bioterroristic attacks. The threat on bioterrorism attacks has attracted attention due to the recent event that has struck Syria [1] which killed hundreds men, women, and children aside from the anthrax spore-containing letter attack [2] that happened in United States which threatened the whole world. There are numerous pathogens which include bacteria, viruses, fungi, toxins and among others, are listed by various agencies that are potentially dangerous agents[3]. Thus, immediate detection of these potential biowarfare agents is required in different situations which include civil rescue and security

units, homeland security, military operations, public transportation securities such as airports, metro and railway stations due to its harmful effect on the human population [4] as well as to environment. Therefore, there is a need to develop analytical screening tools which could be portable, rapid, cost-effective and simple detection for the responders as well as specialised laboratories.

To date, plenty of techniques to detect and identify biowarfare agents like cell culture [6], molecular techniques including polymerase chain reaction (PCR) [7] as well as recombinase polymerase amplification, real time PCR [6, 8, 9], or, alternatively using enzyme-linked immunosorbent assay (ELISA) [10] have been developed. Nucleic acid-based detection systems have been widely explored and it is more sensitive than antibody-based detection systems[3]. Recent advances have taken place for multiple analyte detection using microarrays for pathogenic species detection that involves nucleic acid-based detection system [11-13]. Although these standard techniques are sensitive, the use of microarrays involves many manual handling steps that rather time consuming due to long hybridisation times, requires intensive handling of the infectious agent and has no direct combination with an automated biosensor system.

Multiplexed assays can screen multiple analytes in a single assay which is significantly simpler, more rapid and requires less sample and reagent consumption in comparison to multiple single target. Several studies have been explored for the multiplex detection of target analytes through electrochemical measurement system [14-17]. Electrochemical biosensors are popular for their excellent sensitivity, selectivity, versatility, simplicity [18, 19] and are capable of detecting low concentrations of target agents without interference from background materials[20]. The development of these technologies has garnered a continual interest for application in clinical diagnostics[14], food quality control[21] and environmental monitoring [22], as promising alternatives to traditional methods in detecting pathogens.

Overall, biowarfare agents' threat has created a rapidly rising demand for new emerging sensor technologies to speed up testing. Here we describe an electrochemical sensor array for the simultaneous recognition of PCR amplified gene segments of *Bacillus anthracis, Brucella melitensis, Bacteriophage lambda, Francisella tularensis, Burkholderia mallei, Coxiella burnetii, Yersinia pestis, and Bacillus thuringiensis var. kurstaki*. These eight pathogens are among the biowarfare agents of the highest threat potential listed[23, 24]. The biosensor array was housed within a microfluidic set-up and the assay was automated via the use of a peristaltic pump, with the only required end-user intervention being sample addition. Parameters such as incubation time and temperature were optimised and applied to the detection of complementary target for each biothreats agents.

4.2. Experimental Details

4.2.1 Materials

All the starting materials were obtained from commercial suppliers and used without further purification. Eight thiolated ssDNA probes designed specifically for eight specific synthetic ssDNA complementary target and eight ssDNA as secondary reporter probes were purchased from biomers, Germany, (see Supplementary Information Table 4.S1). Biotynilated PCR products of *Bacillus anthracis, Brucella melitensis, Bacteriophage lambda, Francisella tularensis, Burkholderia mallei, Coxiella burnetii, Yersinia pestis, and Bacillus thuringiensis var. kurstaki* were kindly provided by the Friedrich-Loeffler-Institut, Institut für bakterielle Infektionen und Zoonosen, Germany. Dithiol 16-(3,5-bis((6-mercaptohexyl)oxy)phenyl)-3,6,9,12,15-pentaoxahexa-decane) (DT1) was purchased from SensoPath Technologies (USA), sulfuric acid, potassium dihydrogen phosphate, phosphate-buffered saline (PBS) (dry powder), PBS-Tween-20, hydrogen peroxide 30%, acetone and ethanol (synthetic grade), 0.1 M hydrochloric acid, and acetic acid were purchased from Scharlau (Spain); Tris(hydroxymethyl)aminomethane, Sodium Hydroxide, Sodium Chloride and 3,3,5,5-

Tetramethylbenzidine (TMB) Liquid Substrate System for ELISA was obtained from Sigma. Aqueous solutions were prepared with Milli-Q water Millipore (18mΩ.cm) and all reagents were used as received.

4.2.2 Instrumentation

Electrochemical studies were carried out using an Autolab PGSTAT 10 potentiostat with measurements performed using an array of 24 gold electrodes (1 mm-diameter) with internal reference and counter electrodes. The final format of the biosensor assay has been integrated within the microfluidic set-up. The lithographically produced gold electrodes were provided by Fraunhofer ICT-IMM (IMM), Germany, and were produced as previously reported [25]. All sonication procedures were conducted with an ultrasonic bath (Branson ultrasonic corporation, model 2510E-MT, USA). Enzyme-linked oligonucleotide assay (ELONA) studies were performed using bioNOVA cientifica, S.L. (Madrid, Spain) and HydroFlex 3-in-1 well washer, TECAN (Spain).

The microfluidic set-up for incubation of analytes and flushing/washing with built in peristaltic pump was provided by IMM, Germany and the polymeric microfluidics were supplied by microfluidic ChipShop GmbH, Germany.

4.2.3 Cultivation and inactivation of raw bacterial cells for DNA preparation

Bacterial cells were cultivated on cysteine heart agar (Becton Dickinson GmbH, Heidelberg, Germany) supplemented with 10 % chocolatized sheep blood. Incubation was carried out for 3 days at 37 °C in an atmosphere with 5 % CO2. Heat assisted inactivation was carried out for 10 min at 95 °C (Thermomixer Compact, Eppendorf AG, Hamburg, Germany).

To check sterility, the suspension was plated on agar plates and incubated for 7 days and no growth was observed.

Preparation of DNA from bacteria suspension

2 mL of each bacteria suspension were centrifuged for 10 min at 13400 rpm (MiniSpin, Eppendorf Ag, Hamburg, Germany). The supernatant was removed and the pellet was washed with 1x PBS (Carl Roth GmbH, Karlsruhe, Germany) and 1x TE (Carl Roth GmbH, Karlsruhe, Germany) using centrifugation steps with 11400 rpm and removing the supernatant again. For lysis, the pellet was mixed with 10 µl 1x TE 1 ml 1 % SDS (Carl Roth GmbH, Karlsruhe, Germany) and 12,5 µl RNAse A and incubated in a thermoblock (TMix, Analytik Jena AG, Jena, Germany) for 30 min at 37 °C followed by addition of 12,5 µl Proteinase K and an additional incubation step for 10 min at 72 °C. 100 µl 5 M potassium acetate were added, the solution was mixed and incubated on ice for 30 min. Centrifugation was again carried out for 10 min at 114000 rpm and the supernatant was transferred into a clean reaction vessel. One volume of phenol was added, and centrifugation was repeated for 5 min. Again, the upper phase was transferred into a clean reaction vessel and one volume of chloroform/isoamylalcohol (24:1) was added, mixed and centrifuged for 5 min. Upper phase was separated again and mixed with two volumes of ethanol. Nucleic acid precipitation was carried out for 20 min at -20 °C. Final centrifugation was carried out for 10 min and the supernatant was removed. Remaining DNA was dried, finally diluted in aqua bidest and stored at -20 °C.

4.2.4 Preparation and characterisation of complementary PCR products

PCR protocol

PCR was performed using 1 x MasterMix (Jena Bioscience, Jena, Germany), 1 µM primers (TIB MOLBIOL Syntheselabor GmbH, Berlin, Germany), 0.2 % BSA (Hersteller, Ort, Land), 10 µl DNA were added including 450 GE/µl. Reverse primers were applied with 5´-biotin-labelling including a 15 atomar spacer TEG. An overview about the applied templates and primer sequences is given in Supplementary Information Table 4.S2. Previously to amplification, an initial

denaturation step with 95 °C for 10 min was carried out. PCR was performed with 41 cycles of 15 s at 95 °C and 60 s 60 °C for most of the targets using a Mastercycler nexus thermocycler (Eppendorf AG, Hamburg, Germany). For amplification of the bcsp31 target from *Brucella melitensis* the temperature for annealing and elongation was set to 57 °C and for amplification of the fliC target from *Burkholderia mallei* a three step protocol was applied consisting of 15 s 95 °C, 30 s 50 °C and 15 s 72 °C. Amplicons were verified via electrophoresis using 2 % agarose Gel in 1x TBE for 60 min at 200 V.

Preparation of ssDNA PCR product

Capture of the biotinylated PCR product (biotinylated forward primer) using the SiMAGstreptavidin-coated magnetic beads by chemicell™ was carried out according to the manufacturer's instructions. Firstly, 150 µL of magnetic beads was washed to remove any preservatives by 3 consecutive washings with 1X B&W buffer (5 mM Tris-HCl pH 7.5, 0.5 mM EDTA and 2 M NaCl). Between each washing step, Eppendorf tubes containing the solution with the magnetic beads were placed in contact with a magnet for 2 min and the supernatant was removed by aspiration with a micro-pipette. The isolated magnetic beads were subsequently re-suspended with 100 µl of biotinylated PCR product and the same volume of 2X B&W buffer and incubated for 30 min at room temperature with gentle rotation. Following immobilisation of the biotinylated PCR product on the streptavidin magnetic beads, the Eppendorf tubes were again placed in contact with a magnet for 3 mins in order to discard the supernatant and the isolated beads were washed three times with 1X B&W buffer. Separation of ssDNA was performed by alkaline denaturation[26]. This procedure has been done to eight biotinylated PCR products separately. The single-stranded DNA amplicons generated were characterised using gel electrophoresis.

Preparation of ssDNA labelled with horseradish peroxidase as reporter probe

Eight different designed thiolated reporter probes were purified prior to conjugation experiment to eliminate any preservatives present that would affect the efficiency of conjugation. The purified thiolated reporter probes were added separately to Maleimide activated horseradish peroxidase (Maleimide HRP) to form a final concentration of 24:1 (Maleimide HRP:DNA ratio) and incubated for 90 min at 37 °C, after which 2-mercapto ethanol was added to a final concentration of 0.0015 M to stop the reaction. The final products were purified using a YM10 KDa cut-off microcon and were washed with buffer and were stored at -20°C at 50% glycerol.

Enzyme linked oligonucleotide assay (ELONA) evaluation on cross-reactivity and specificity of designed probes

Eight (8) different designed thiolated capture probes (1 μM in carbonate buffer) were prepared separately and were added to each well of a NUNC maleimide plate and incubated for 30 min at 37 °C. Following thorough washing with PBS-Tween 20 (pH 7.4, 0.01 M), the plate was then blocked by addition of 200 μL of 1mM mercaptohexanol (MCH) in PBS-Tween 20 (pH 7.4, 0.01 M) and incubated for 1 h at 37 °C, followed by thorough washing of the plate. Genorecognition step was carried in three ways: 1) individual assay detection, 2) mixed complementary target where 50 μL each at 5nM of each synthetic complementary target and 3) mixed HRP-labelled ssDNA reporter probe that has been prepared in PBS-Tween 20 (pH 7.4, 0.01 M) were added to each well coated with capture probes. The plate was again incubated, under shaking conditions for 30 min at 37 °C, and subsequently thoroughly washed with PBS-Tween 20, prior to exposure to 50 nM of DNA-HRP conjugates as a secondary labelled ssDNA in individual assay detection and mixed reporter probes and again left to incubate under shaking conditions for 30 min at 37 °C. After a final wash, 50 μL of TMB for ELISA substrate was added to each well and product formation were allowed to

proceed for at least 15 min at room temperature. The reaction was finally stopped by addition of 1 M H_2SO_4, and the absorbance read at 450 nm. Analysis was carried out in triplicate.

4.2. 5 Probe immobilisation on electrode array

Prior to modification of the electrode arrays, a two-step cleaning protocol was applied. Initially in order to remove the protective resist used during storage, the arrays were sonicated for 5 min in acetone, 5 min in iso-propanol (3 times) and rinsed with water. In a second step, electrochemical cleaning was performed in 0.5 M H_2SO_4 by application of a constant potential of 1.6 V for 10 s followed by 40 voltammetric cycles in the potential range −0.2 to 1.6 V at a scan rate of 0.3 $V.s^{-1}$. Finally, the electrodes were rinsed with Milli-Q water and dried with nitrogen. Modification of the cleaned electrode arrays was carried out via co-immobilization of the specific thiolated probe (1 μM) and DT1 (100 μM) in 1 M KH_2PO_4 aqueous solution (pH 3.5) by deposition of 1 μL of the mixture over the working electrodes for 3 h at room temperature in a humid (>90%) environment. Dithiol DT1 was co-immobilized with the thiolated probe in order to eliminate non-specific binding of the labelled reporter probe, whilst also spacing out and orientating the probe to facilitate efficient hybridization of the target. In order to remove the non-attached molecules, the electrode arrays were washed in a stirring solution of 0.1 M PBS–Tween for 20 min, rinsed with water and dried with nitrogen.

4.2.6 Electrochemical DNA detection

DNA detection of both synthetic oligonucleotides and PCR product from bacterial cell samples were performed in a sandwich hybridization format. In the developmental work, construction of a typical calibration curve of the genosensor as a model system has been done using the synthetic complementary target. A typical target of various concentrations of *F. tularensis* ranging

from 0 to 10 nM (in triplicate) in 0.1 M hybridisation buffer (0.1 M Trizma buffer in 0.15 M NaCl, pH 7.4) were deposited on the oligonucleotide modified gold electrodes and incubated for 20 min at room temperature. The sensors were subsequently washed for 15 min, under stirring conditions, in 0.1 M PBS–Tween and then dried with nitrogen. A second hybridisation was performed by spotting 0.5 μL of 10 nM labelled reporter in hybridisation buffer and incubating for another 20 min at room temperature with both hybridisations carried out in a humid environment. The hybridized microarray was subsequently washed with 0.1 M PBS–Tween for 15 min and dried in nitrogen. For real sample analysis, the modified electrodes were then exposed to known concentration of the ssDNA generated from PCR product quantified using Nanodrop™, in hybridisation buffer, and incubated for (2-20 min) and then incubated for a defined period of time (2-20 min) with the corresponding horseradish peroxidase labelled secondary ssDNA.

The detection process was carried out in the microfluidic channels in the presence of TMB substrate where the HRP-catalysed reduction of TMB [27, 28] and was detected by steps and sweeps technique by applying two consecutive potential steps of 0 V for 1 ms and −0.2 V for 0.5 s. All the electrochemical measurements were performed at room temperature. The overall immobilization process and detection mechanism can be seen in figure 4.1.

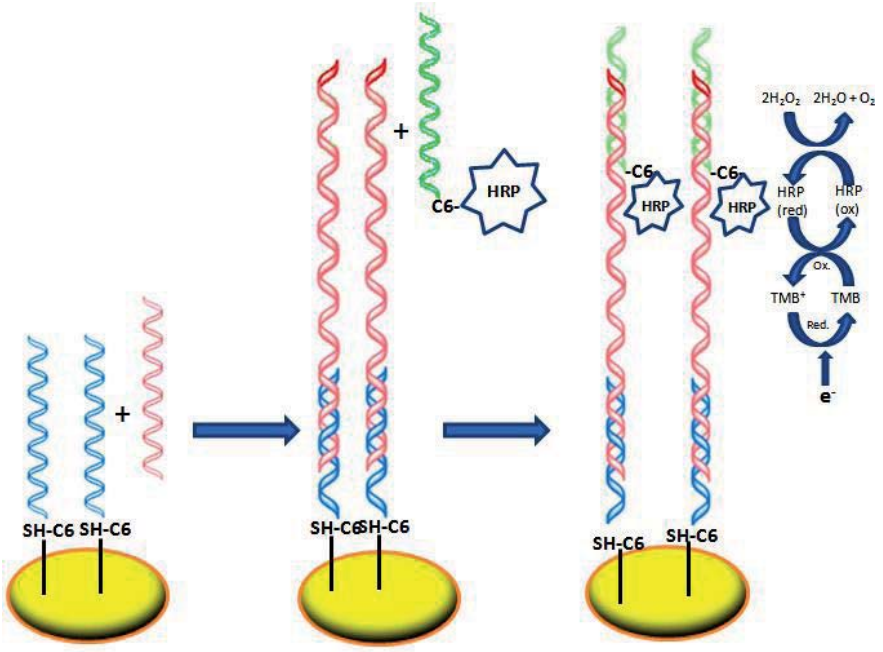

Figure 4.1 Schematic representation on the immobilization of thiolated ssDNA and its hybridization process to complete the sandwich assay format illustrating how the electroactive species detected into electrode surface.

4.3. Results and Discussion

4.3.1 Characterisation of complementary PCR products

The extracted DNA's from bacterial cells were amplified by Friedrich-Loeffler-Institut, Institut für bakterielle Infektionen und Zoonosen, Germany. The generated dsDNA PCR products of the eight species were characterised through gel electrophoresis as shown in figure 4.2 confirming the number of bases in each amplicons (see Supplementary Information Table 4.S2) and the separation of ssDNA by alkaline denaturation. The obtained ssDNA were quantified using Nanodrop™ instrument.

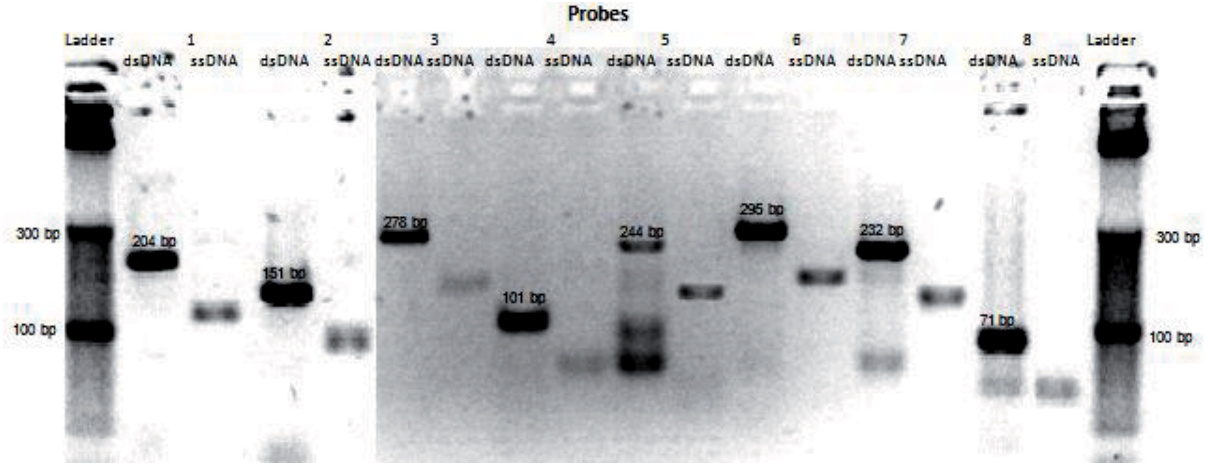

Figure 4.2. Gel characterisation of dsDNA and ssDNA PCR products produced. 1. *Bacillus anthracis* (BA), 2. *Brucella melitensis* (Bram), 3. *Bacteriophage lambda* (BL), 4. *Francisella tularensis* (FrT), 5. *Burkholderia mallei* (Brum), 6. *Coxiella burnetii* (CB), 7. *Yersinia pestis*(YeP) and 8. *Bacillus thuringiensis var. kurstaki*(BaT).

4.3.2 Evaluation of in-house prepared ssDNA labelled with horseradish peroxidase (HRP) as reporter probe and surface chemistry optimisation

The conjugation of Maleimide HRP to the thiolated reporter probe has been thoroughly optimised in terms of incubation time for conjugation and the ratio concentration of each molecule to achieve an optimum ratio in order to obtain a good signal response when used for sandwich assay analysis. The concentration of the conjugates were determined by using Quant-iT™ OliGreen® ssDNA reagent which has an ultra-sensitive fluorescent nucleic acid stain for quantitating oligonucleotides and single-stranded DNA (ssDNA) in solution and through the standard calibration curve for each reporter probe obtained in UV-VIS spectrofluorometer. It has been observed that 3 hr incubation and a ratio of 24:1 (DNA:HRP) gave the best condition for the conjugation (see Supplementary Information Figure 4.S1-4.S2). It can also be clearly observed that the prepared conjugates gave similar performance when used in electrochemical measurement as shown in figure 4.3. Furthermore, the use of bipodal dithiol (DT1) as a backfiller has proven to be

effective in eliminating non-specific adsorption due to the presence of the polyethylene glycol moiety, which effectively eliminates non-specific binding of any sample matrix components, whilst its' bipodal structure facilitated optimal spacing on the electrode surface and consequently, good electron transfer when compared to conventional sequential backfilling with short single alkyl thiol (MCH).

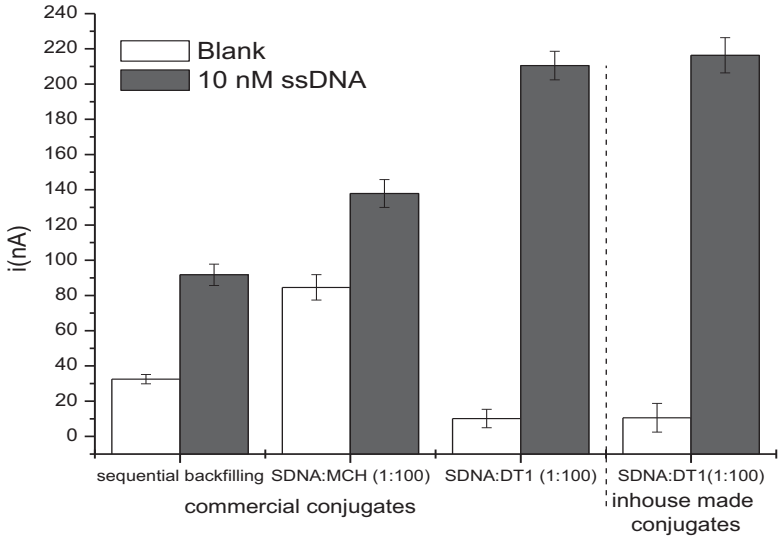

Figure 4.3. Optimum condition for assay development using commercial conjugates and the prepared in-house made conjugates. Each data point represents the average of three measurements on three separate electrode sensors.

4.3.3 Enzyme linked oligonucleotide assay (ELONA) evaluation on cross-reactivity and specificity of designed probes

The designed probes for the detection of eight different species were evaluated through ELONA techniques to ensure the specificity of each probe towards their respective complementary target. Figure 4 clearly shows that there is no apparent cross-reactivity reaction between designed

probes when mixtures of complementary target and reporter probes were introduced to microarrays as compared to its baseline individual assay measurement.

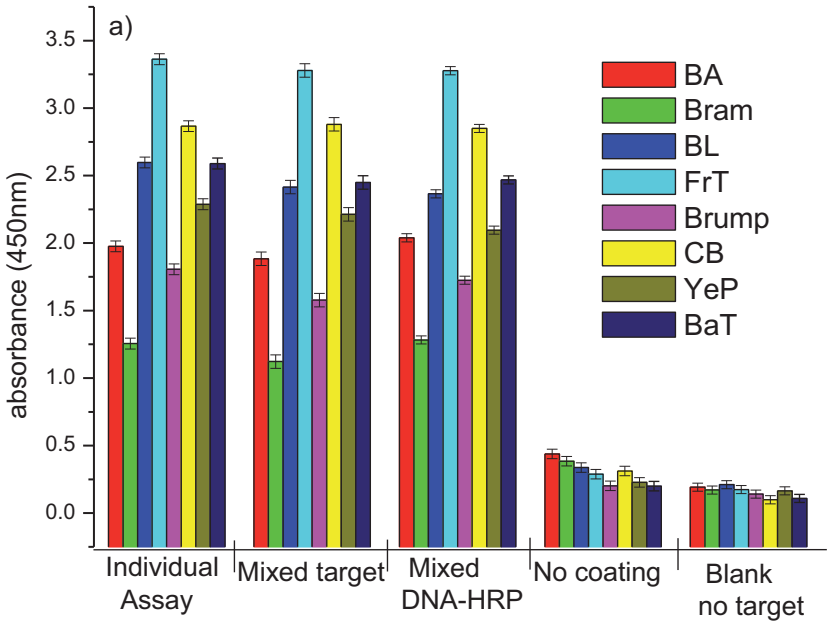

Figure 4.4. ELONA cross-reactivity and specificity characterisation of designed capture thiolated DNA probes and DNA-HRP labelled reporter probes hybridised with produced PCR products from bacterial cells. Concentrations: capture probe-200nM, target-10nM synthetic target, reporter probe-20nM.

4.3.4 Fluidics and set-up

After ELONA characterisation of the designed probe, electrochemical detection of PCR products from real samples were done using an electrode array that has been functionalised with thiolated capture probes and housed within a microfluidic set-up developed together with IMM (Figure 4.5). The device consists of several reservoirs for analytes and buffers, silicone tubes, waste tanks, fluidics, and script-based assay programmer. The whole set-up enabled complete automation

of the immunosensor as well as allowing for the use of smaller quantities of reagents. Electrode functionalisation with the optimum surface platform, i.e. co-immobilised thiolated ssDNA and bipodal dithiol (DT1), was carried out outside the microfluidics set-up (figure 4.3).

Following the modification process, the electrode array was housed in the microfluidic set-up (Figure 4.5c) using an adhesive gasket which acts as spacer between the polycarbonate microfluidic chip and the glass electrode. This generates an actual flow cell above the electrode area with a width of 4.5 mm, a height of 0.1 mm and a total length of 24 mm, housing 24 individual working electrodes (which could be separately functionalized, allowing multiplex detection or the incorporation of controls). The flow cell has an inlet resp. outlet with a diameter of 1 mm that is connected with a feeding channel with a width of 0.8 mm and a height of 0.3 mm leading to tube inlets resp. a waste outlet. The silicone tubes connected to the reservoirs containing all reagents required were connected to the tube inlets of the microfluidic set-up via Mini-Luer adapters (supplied by microfluidic ChipShop GmbH), allowing flowing of different liquid samples as required throughout the assay. The four reservoirs available were used to store mixed/unmixed complementary PCR products target in hybridisation buffer solution, mixed/unmixed labelled reporter probes in hybridisation solution, TMB substrate, and PBS (pH 7.4) solution for washing. The flowing of liquids over the electrode was carried out automatically using an assay programmer directly, which was also used to process the data obtained (see Supplementary Information Table 4.S3 for a detailed protocol for assay measurement within microfluidics).

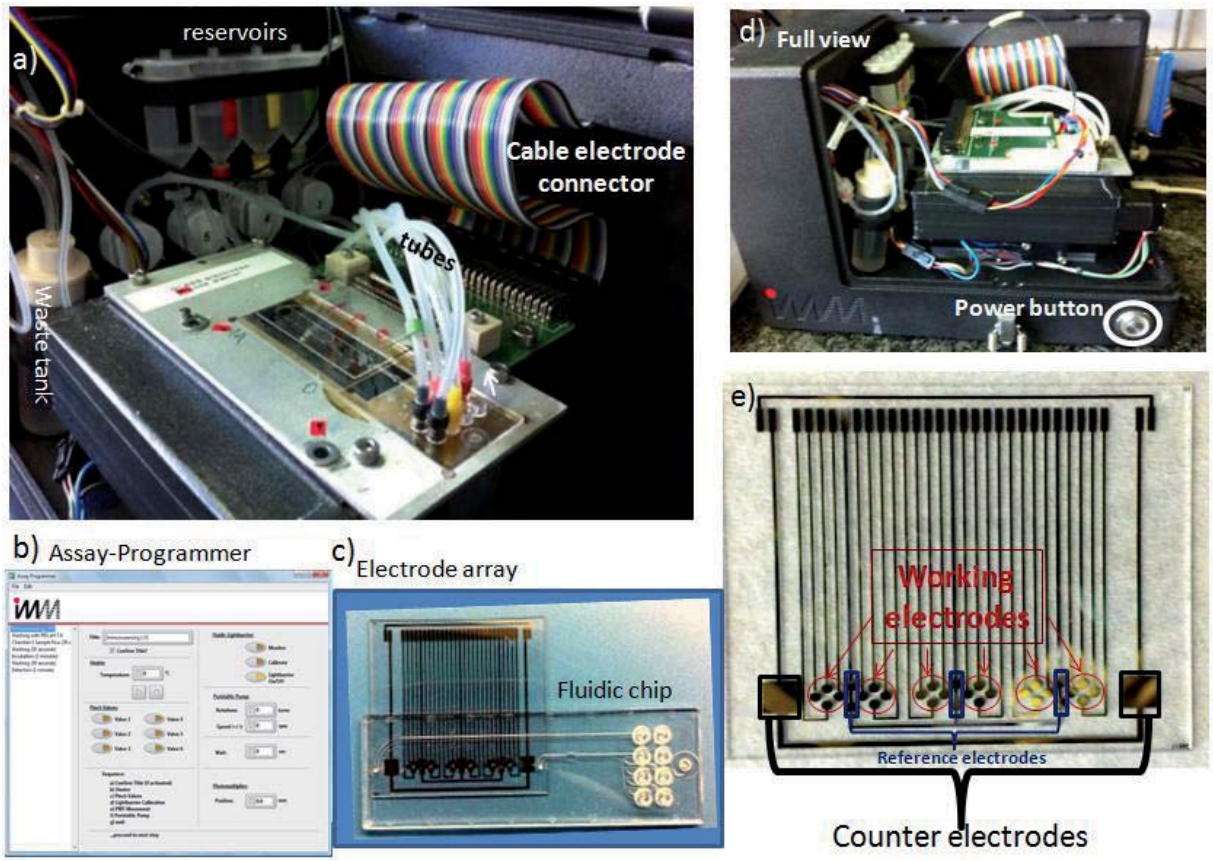

Figure 4.5. The amperometric immunosensor detection set-up. The set-up contains a peristaltic pump positioned behind the reservoirs to flow the solutions into electrode array mounted within the microfluidics. (a) the electrode array with microfluidics placed in the platform and connected to the potentiostat for amperometric measurement; (b) a sample script-based assay program; (c) the electrode array integrated with microfluidics; (d) a full front view of the tester set-up device; (e) lithographically produced gold electrode array with internal reference electrode and counter electrode.

Construction of a typical linear calibration curve for the DNA biosensor and optimisation of the incubation temperature inside the microfluidics set-up was carried out as shown in figure 4.6. The typical limit of detection of the DNA biosensor was 0.35 nM and an increased signal

measurement was better when hybridisation for both complementary target and reporter probes is done at 37 °C. Moreover, stability of the modified electrodes was done. The prepared electrodes were assessed after a month and no significant decrease in amperometric response (<7%) observed. This further indicates that the immobilised probes do not lose their recognition ability upon storage in PBS, pH 7.4, at 4 °C.

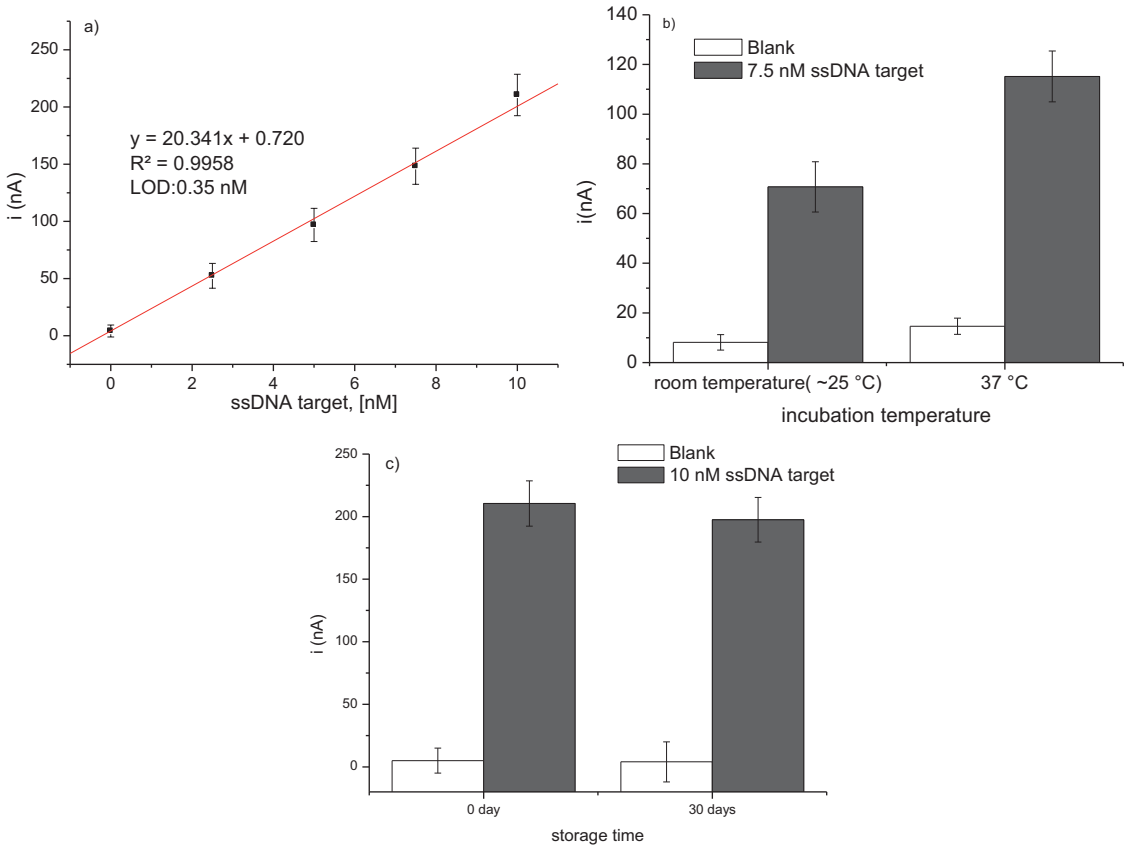

Figure 4.6. a) Typical dynamic linear range in the calibration curve obtained for the developed genosensor, b) optimum incubation time of the developed DNA biosensor. Each data point represents the average of three measurements on three separate electrode sensors and c) stability of the immobilised probes into the electrodes.

Finally, using the optimised surface chemistry condition and incubation time, detection of known concentration of PCR products from different pathogenic species were done. The individual complementary target detection has been done first with respect to their corresponding reporter probes (Figure 4.7a). To demonstrate the specificity of DNA biosensor with respect to the designed probes, i.e. capture probes and reporter probes, the electrode array modified with eight different capture probes was exposed with a single PCR product (ssDNA). It was observed that the ssDNA PCR product reacts only to the electrode modified with its specific capture probe and did not give any sensor response to the rest of electrodes modified with other seven thiolated probes as shown in figure 4.7b, highlighting the specificity of each designed probes. Multiplex detection of eight PCR products were done by simply mixing the ssDNA PCR products and introducing them to the modified electrode array and incubated for 30 min at 37 °C and subsequent addition of mixtures of reporter probes (20 nM each) were done following with in between washing steps. Interestingly, the results obtained for the multiplex detection were of similar range of sensor response as obtained in figure 4.7a showing reproducible responses.

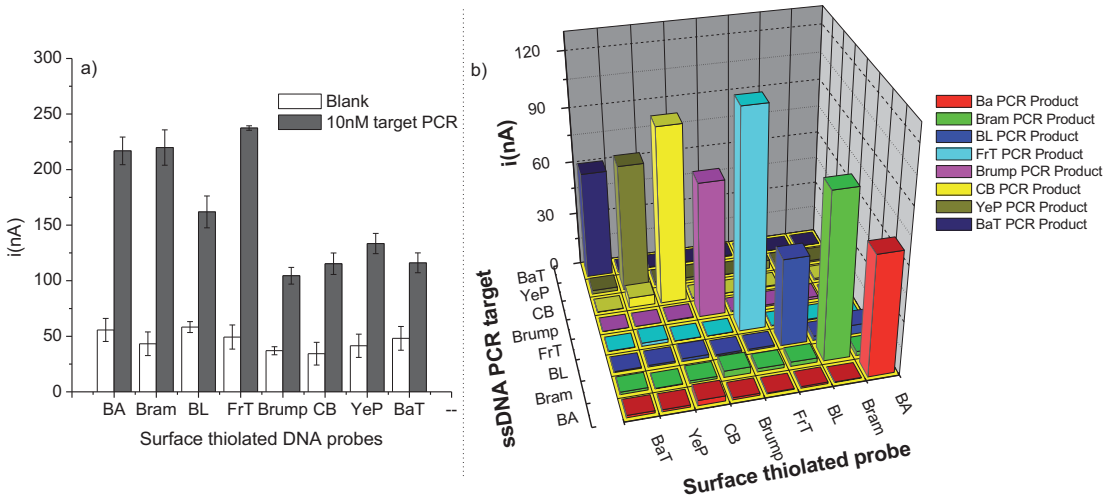

Figure 4.7. Electrochemical based measurement of a) typical single probe co-immobilised with DT1 1:100 (mol/mol) individual assay detection of ssDNA PCR product and b) typical single probe co-immobilised with DT1 1:100 (mol/mol) with only one fixed concentration (5 nM) of complementary target PCR product from real sample specific to one surface thiolated DNA capture probe and label probe. Each data point represents the average of three measurements on three separate electrode array sensors.

4.4 CONCLUSIONS

This report details the development of DNA biosensor for the automated simultaneous detection of a range of biowarfare agents (*Bacillus anthracis, Brucella melitensis, Francisella tularensis, Bacteriophage lambda, Burkholderia mallei, Coxiella burnetii, Yersinia pestis* and *Bacillus thuringiensis var. kurstaki*). Oligonucleotide-enzyme conjugates were prepared in-house using thiolated ssDNA and

covalently linked to Maleimide activated HRP and similar results were obtained when compared to commercially obtained conjugates. PCR product samples did not affect the performance of the electrodes due to the presence of the co-immobilised DT1 backfiller which contains polyethylene glycol moiety and due to its hydrophilicity effectively eliminates non-specific binding of any sample matrix components, whilst its structure facilitated good electron transfer giving a good level of sensitivity and detection limit. The developed electrochemical multiplex DNA biosensor was then transferred to an automated microfluidic set-up housed within a tester set-up and the assay parameters were optimised. The specificity of the genosensor has been clearly determined and no cross-reactivity has been found.

This is the first stage of further development of a platform for the multiplexed detection of a more range of bioterrorism agents. The applicability of the developed system to real situations such as an early detection of bioterrorism events is very promising as the obtained LOD was very low and the assay time quite short when compared to conventional system ELONA. This facilitates a rapid alarm based detection of different biowarfare agents when linked e.g. to an air-sampling system. Ongoing and future work will focus on attempting the use of a common reporter probes that would not only decrease the cost for the use of different designed reporter probes but this would also eliminates the complex procedure of mixing all together the reporter probes for labelling the complementary targets, further reduce the incubation and sampling time, to increase the stability of the thiolated ssDNA functionalised sensors using stabilising agents.

ACKNOWLEDGMENTS

The authors thank microfluidic ChipShop (http://www.microfluidic-chipshop.com/) for provision of the microfluidics.

FUNDING

The research leading to these results has received funding from the European Community's Seventh Framework Programme "The lab-free CBRN detection device for the identification of biological pathogens on nucleic acid and immunological level as lab-on-a-chip system applying multisensor technologies", MultisenseChip [FP7/2007-2013].

APPENDIX A. SUPPLEMENTARY DATA

REFERENCES

1. Enserink, M., and Kaiser, J., *U.N. Taps special labs to investigate syrian attack*. Science, 2013. **341**(6150): p. 1050-1051.
2. Bush, L.M., andPerez, M. T., *The Anthrax Attacks 10 Years Later*. Annals of internal medicine, 2012. **156**(1): p. 41-44.
3. Lim, D.V., Simpson, J. M., Kearns, E. A., Kramer, M. F., *Current and developing technologies for monitoring agents of bioterrorism and biowarfare*. Clinical Microbiology Reviews, 2005. **18**: p. 583-607.
4. Skládal, P., Pohanka, M., Kupská, E., and Šafář, B., *Biosensors for Detection of Francisella tularensis and Diagnosis of Tularemia*. In: Biosensors, INTECH, Vienna, 2010: p. 115-126.
5. Walczak, M.M., Popenoe, D. D., Deinhammer, R. S., Lamp, B. D., Chung, C., and Porter, M. D., *Reductive desorption of alkanethiolate monolayers at gold: A measure of surface coverage*. Langmuir, 1991. **7**: p. 2687 - 2693.
6. Simşek, H., Taner, M., Karadenizli, A., Ertek, M., and Vahaboğlu, H., *Identification of Francisella tularensis by both culture and real-time TaqMan PCR methods from environmental water specimens in outbreak areas where tularemia cases were not previously reported*. Eur J Clin Microbiol Infect Dis., 2012 **31**(9): p. 2353-2357.
7. Johansson, A., Ibrahim, A., Göransson, I., Eriksson, U., Gurycova, D., Clarridge, J. E, and Sjöstedt, A., *Evaluation of PCR-Based Methods for Discrimination ofFrancisella Species and Subspecies and Development of a Specific PCR That Distinguishes the Two Major Subspecies of Francisella tularensis*. Journal of clinical microbiology, 2000. **38**(11): p. 4180-4185.
8. Bystrom, M., Bocher, S., Magnusson, A., Prag, J., Johansson, A., *Tularemia in Denmark: identification of a Francisella tularensis subsp. holarctica strain by real-time PCR and high-resolution typing by multiple-locus variable-number tandem repeat analysis*. Journal of clinical microbiology 2005. **43**(10): p. 5355–5358.
9. Versage, J.L., Severin, D. D., Chu, M.C. and Petersen, J. M., *Development of a multitarget real-time TaqMan PCR assay for enhanced detection of Francisella tularensis in complex specimens*. Journal of clinical microbiology, 2003. **41**: p. 5492–5499.
10. Pohanka, M., Pavlis, O., Kroca, M., *ELISA detection of Francisella tularensis using polyclonal and monoclonal antibodies*. DEFENCE SCIENCE JOURNAL, 2008. **58** (5): p. 698-702

11. Mollasalehi, H.a.Y., R., *Development and evaluation of a novel nucleic acid sequence-based amplification method using one specific primer and one degenerate primer for simultaneous detection of Salmonella enteritidis and Salmonella typhimurium.* Analytica Chimica Acta, 2013. **770**: p. 169-174.
12. Vanlalhmuaka, T., K., Tuteja, U.,Sarika, K., Nagendra, S. and Kumar, S., *Reverse Line Blot Macroarray for Simultaneous Detection and Characterization of Four Biological Warfare Agents.* Indian Journal of Microbiology, 2013. **53**(1): p. 41-47.
13. Mohtashemi, M., Walburger, D. K., Peterson, M. W., Sutton, F. N., Skaer, H. B. and Diggans, J. C., *Open-target sparse sensing of biological agents using DNA microarray.* BMC Bioinformatics, 2011. **12**: p. 314.
14. Civit, L., Fragoso, A., Hölters, S., Dürst, M., and O'Sullivan, C. K., *Electrochemical genosensor array for the simultaneous detection of multiple high-risk human papillomavirus sequences in clinical samples.* Analytica Chimica Acta, 2012. **715**: p. 93-98.
15. Du, Y., Chen, C., Zhou, M., Dong, S. and Wang, E., *Microfluidic Electrochemical Aptameric Assay Integrated On-Chip: A Potentially Convenient Sensing Platform for the Amplified and Multiplex Analysis of Small Molecules.* Analytical Chemistry, 2011. **83**(5): p. 1523-1529
16. Zhang, M., Yin, B. C., Tan, W. and Ye, B. C., *A versatile graphene-based fluorescence "on/off" switch for multiplex detection of various targets.* Biosensors and Bioelectronics, 2011. **26**(7): p. 3260-3265.
17. Elsholz, B., Nitsche, A., Achenbach, J., Ellerbrok, H., Blohm, L., Albers, J., Pauli, G., Hintsche, R. and Wörl, R., *Electrical microarrays for highly sensitive detection of multiplex PCR products from biological agents.* Biosensors and Bioelectronics, 2009. **24**(6): p. 1737-1743.
18. Lazcka, O., Javier Del Campo, F., Xavier Munoz, F., *Pathogen detection: A perspective of traditional methods and biosensors.* Biosensors and Bioelectronics, 2007. **22** p. 1205-1217.
19. Pividori, M.I., Lermo, A., Bonanni, A., Alegret, S., del Valle, M., *Electrochemical immunosensor for the diagnosis of celiac disease.* Analytical Biochemistry, 2009. **388**: p. 229 - 234.
20. Ivnitski, D., O'Neil, D. J., Gattuso, A., Schlicht, R., Calidonna, M., and Fisher, R., *Nucleic acid approaches for detection and identification of biological warfare and infectious disease agents.* BioTechniques, 2003. **35**(4): p. 862-869.
21. Arora, P., Sindhu, A., Dilbaghi, N. and Chaudhury, A., *Biosensors as innovative tools for the detection of food borne pathogens.* Biosensors and Bioelectronics, 2011. **28**(1): p. 1-12.
22. Warsinke, A., Benkert, A., Scheller, F. W., *Electrochemical immunoassays.* Fresenius Journal o fAnalytical Chemistry, 2000. **366**(6-7): p. 622-634.
23. Klietmann, W.F., and Ruouff, K. L., *Bioterrorism: Implications for the Clinical Microbiologist.* Clinical Microbiology Reviews, 2001. **14**(2): p. 364–381.
24. Frischknecht, F., *The history of biological warfare.* EUROPEAN MOLECULAR BIOLOGY ORGANIZATION, 2003. **4**(Special issue): p. S47-S52.
25. Fragoso, A., Latta, D., Laboria, N., von Germar, F., Hansen-Hagge, T. E, Kemmner, W, Gartner, C., Klemm, R., Dreseb, K. S., and O'Sullivan, C. K, *Integrated microfluidic platform for the electrochemical detection of breast cancer markers in patient serum samples.* Lab on a Chip, 2011. **11**: p. 625-631.
26. Civit L., F.A., and O'Sullivan C. K., *Evaluation of techniques for generation of single-stranded DNA for quantitative detection.* Analytical Biochemistry, 2012. **431**(2): p. 132-138.
27. Wang, J., Cao, Y., Li, Y., Liang, Z., and Li, G., *Electrochemical strategy for detection of phosphorylation based on enzyme-linked electrocatalysis.* Journal of Electroanalytical Chemistry, 2011. **656**(1-2): p. 274-278.
28. Wang, Z., Liu, L., Xu, Y., Sun, L. and Li. G., *Simulation and assay of protein biotinylation with electrochemical technique.* Biosensors and Bioelectronics, 2011. **26**(11): p. 4610-4613.

Chapter 4: Supplementary Information

Integrated microsystem for multiplexed genosensor detection of biowarfare agents

Samuel B. Dulay[1], Rainer Gransee[2], Sandra Julich[3], Herbert Tomaso[3], and Ciara K. O'Sullivan[1,4*]

This supplementary online material includes:

Materials and methods
Figures
References

MATERIALS AND METHODS

DNA Sequences

Table 4.S1: ssDNA sequences

Specie	Capture probe, (5'-3')	Complementary target, (5'-3')	Reporter probe, (5'-3')
Francisella tulrensis spp. Holarctica	**CTTAGTAATTGGGAAGCTTGTATCATGGCACTTAGAA**	AAGGAAGTGTAAG*ATTACAATGGCAGGCTCCAGA*AGG**TTCTAAGTGCCATGATACAAGCTTCCCAATTACTAAG**TATGCTGAGAAGAACGATAAAACTTGGGCAACTGTAACAGTT	*TCTGGAGCCTGCCATTGTAAT*
Bacillus thuringiensis berliner var. Kurstaki	**AGCGGAAACGTGAATTCTGG**	AGGGCATCAAATA*ATGGCTTCTCCTGTCGGTTTTTC*GGGG**CCAGAATTCACGTTTCCGCT**ATATGGAACCATGGGAAATGCAGCTCCACAACAACGTATTGTTGCTCAACTAGGTC	*GAAAAACCGACAGGAGAAGCCAT*
Yersinia pestis	**ACTGGCCTGCAAGTCCAATATATGGCAT**	CCCGAAAGGAGTGCGG*GTAATAGGTTATAACCAGCGCTT*TTCT**ATGCCATATATTGGACTTGCAGGCCAGT**ATCGCATTAATGATTTTGAGTTAAATGCATTATTTAAATTCAGCGACTGGGTTCGGGCACATGATAATGATGAGCACTATATGAGAGATCTTACTTTCCGTGAGAAGACATCCGGCTCACGTTATTATGGTACCGTAATTAACGCTGGATATTATGTCACACCTAATGCCAAAGTCTTTGCGGAATTTACATACAGTAAATATGATGAGGGCAAAGGAGGTACTC	*AAGCGCTGGTTATAACCTATTAC*
Bacteriophage Lambda	**TTATAAATCTGCTCTTTCGCGGT**	CCCCATTAAAGGGGCATCCGTCTACGGAAAGCCGGTGGCCAGC*ATGCCACGTAAGCGAAACA*AAAACGGGGTTTACCTTACCGAAATCGGTACGGAT**ACCGCGAAAGAGCAGATTTATAA**CCGCTTCACACTGACGCCGGAAGGGGATGAACCGCTTCCCGGTGCCGTTCACTTCCCGAATAACCCGGATATTTTTGATCTGACCGAAGCGCAGCAGCTGACTGCTGAAGAGCAGGTCGAAAAATGGGTGGATGGCAGGAAAAAATACTGTGGGACAGCAAAAAGCGACGCAATGAGGCACTCGACTGCTTCGTTTATGCG	*TGTTTCGCTTACGTGGCAT*

		CTGGCGGCGCTGCGCATCAGTATTTCCCGCTG GC	
Coxiella burnetii	**AACGTCCGATACC AATGGTTCGCT**	GCTCAGTATGTATCCACCGTAGCCA*GTCTTAAG GTGGGCTGCGTG*GTGATGGAAGCGTGTGGAGG **AGCGAACCATTGGTATCGGACGTT**TATGGGGA TGGGTATCCCAACGCAGTTGATCAGTCCGCAG CACGTCAAACCGTATGTCAAAAGTAACAAGAAT GATCGTAACGATGCGCAGGCGATAGCTGAAGC GGCTTCCCGCGCCTCGATGCGGTTTGTGCAGG GTAAAACGGTGGAACAACAAGACGTTCAAGCG CTGTTAAAGATACGCGATCGTTTAGTCAAAAGC CGCACGGCGCTGATCAATGAGATTCGGGGGTT GTTGCAAGAATACGGACTCACGATGGCGCGTG G	*CACGCAGCCCACCTT AAGAC*
Bacillus anthracis	**ATTTGCGGTAACA CTTCACTCCAGTT CGAG**	CAATTAAGATTAGATA*CGGATCAAGTATATGG GAATATAGCAA*CATACAATTTTGAAAATGGAA GAGTGAGGGTGGATACAGG**CTCGAACTGGAG TGAAGTGTTACCGCAAAT**TCAAGAAACAACTG CACGTATCATTTTTAATGGAAAAGATTTAAATC TGGTAGAAAGGCGGATAGCGGCGGTTAATCCT AGTGATCCATTAGAAACGACTAAACCGGATAT GACATTAAAAGA	*TTGCTATATTCCCATA TACTTGATCCG*
Burkholderia mallei	**GCCGTCGACGACA GCGCCTGGTT**	TGTCGGACGGC*AAGGGCGGCTTCACGTTCA*CC GATCAGAAC**AACCAGGCGCTGTCGTCGACGGC** CGTGACCGCCGTGTTCGGCTCGTCGACCGCCG GCACGGGCACGGCGGCCTCGCCGTCGTTCCAG ACGCTGGCGCTGTCGACTTCGGCAACCAGCGC GCTGTCCGCGACGGACCAGGCGAACGCCACGG CGATGGTTGCGCAGATCAACGCGGTCAACAAG CCGCAAACGGTCTCGAACCTCGACATCAGCACG CAGACGGGCGCGTACCAGGCGATGGTATCGAT CGACAAC	*TGAACGTGAAGCCGC CCTT*
Brucella melitensis	**AAATCTTCCACCT TGCCCTTGCCATC A**	GTCTCGTCGCGACGGCCGTTTCGTCGAATG*GCT CGGTTGCCAATATCAATGC*GATCAAGTCGGGC GCTCTGGAGTCCGGCTTTACGCAGTCAGACGT TGCCTATTGGGCCTATAACGGCACCGGCCTTTA **TGATGGCAAGGGCAAGGTGGAAGATTT**GCGCC TTCTGGCGACGCTTTACCCGGAAACGATCCATA TCGTTGCGCGTAAGGATGCAAACATCAAATCG GTCGCAGAC	*GCATTGATATTGGCA ACCGAGC*

Table 4.S2: Overview about applied bacteria strains and PCR assays

Specie	Target	Primers (5´-3´) forward, reverse	Amplicon size	Reference
Francisella tulrensis spp. Holarctica	Tul4	ATTACAATGGCAGGCTCCAGA TGCCCAAGTTTTATCGTTCTTCT	101 bp	Versage et al 2003[1]
Bacillus thuringiensis berliner var. Kurstaki	cryT	ATGGCTTCTCCTGTAGGGTTTTC GCTGCATTTCCCATGGTTCCA	71 bp	Matero et al. 2011[2]
Yersinia pestis	pla	GTAATAGGTTATAACCAGCGCTT AGACTTTGGCATTAGGTGTG	232 bp	Riehm et al. 2011[3]
Bacteriophage Lambda	gp17	ATGCCACGTAAGCGAAACA GCATAAACGAAGCAGTCGAGT	278 bp	Riehm et al. 2011[3]

Coxiella burnetii	IS1111	GTCTTAAGGTGGGCTGCGTG CCCCGAATCTCATTGATCAGC	295 bp	Klee et al. 2006[4]
Bacillus anthracis	pag	CGGATCAAGTATATGGGAATATAGCAA CCGGTTTAGTCGTTTCTAATGGAT	204 bp	Ellerbrok et al. 2002[5]
Burkholderia mallei	fliC	AAGGGCGGCTTCACGTTCA GTGCTGATGTCGAGGTTCGAGA	141 bp	Tomaso et al. 2004[6]
Brucella melitensis	bcsp31	GCTCGGTTGCCAATATCAATGC GGGTAAAGCGTCGCCAGAAG	151 bp	Probert et al. 2004[7]

FIGURES

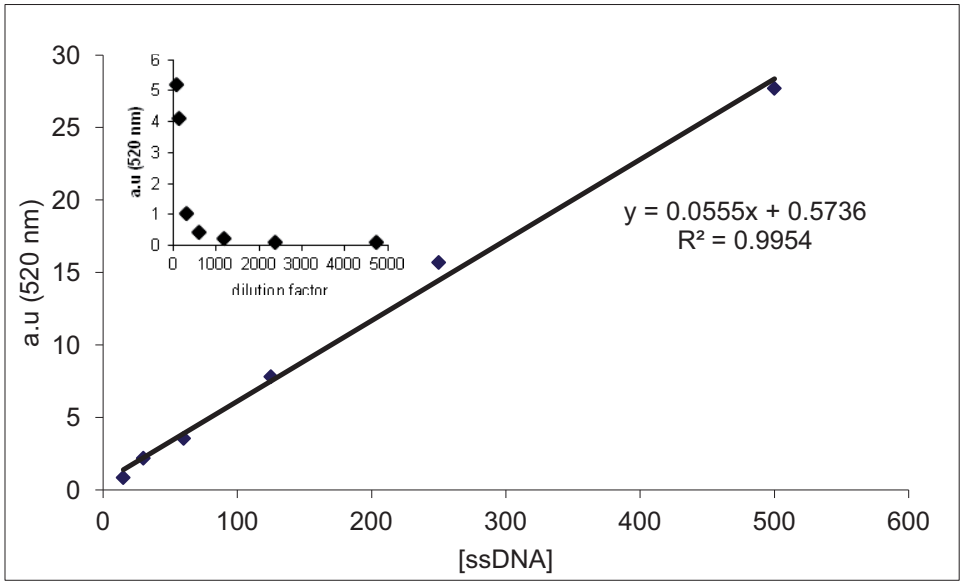

Figure 4.S1 Calibration curve of known concentration of the thiolated ssDNA used for conjugation. Inset graph is a typical absorbance of unknown concentration of inhouse conjugated ssDNA with HRP at different dilution factor

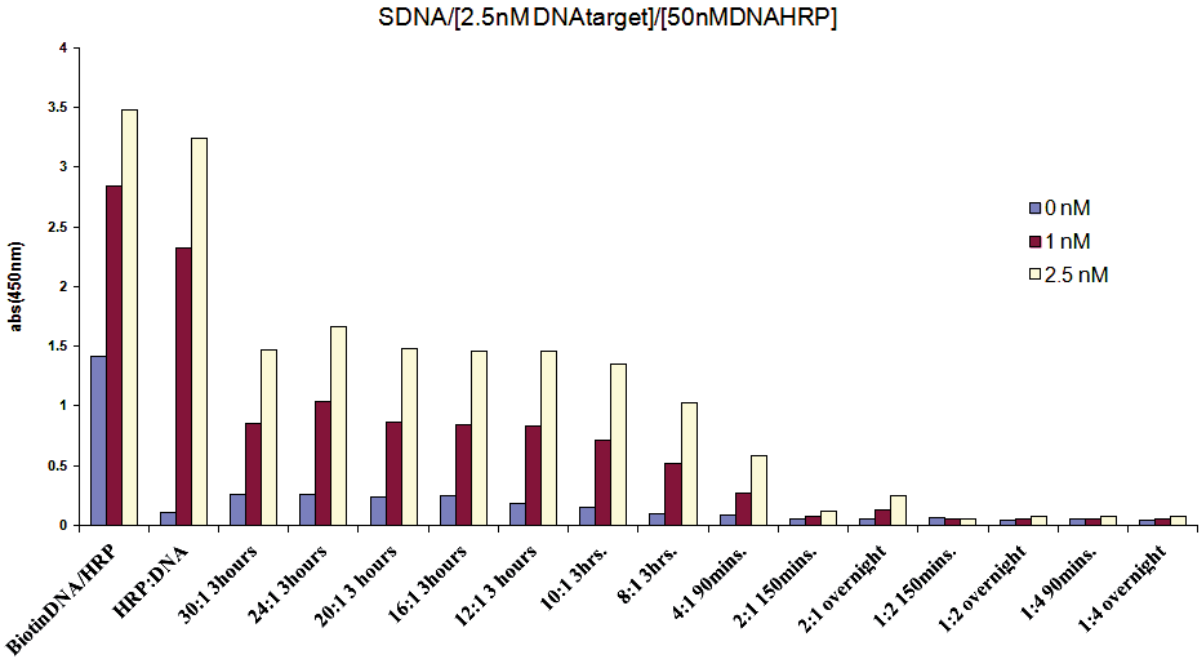

Figure 4.S2 Comparison of DNA-biotin/strep-HRP, commercial DNA-HRP conjugate, and inhouse made DNA-HRP conjugate as a label

Size of thiolated DNA: ~6KDa
Size of StrepHRP: ~40KDa
Total size of the DNA-HRP conjugates: ~46KDA

Thiolated ssDNA probe (200 nM in PBS, pH 7.4) were prepared and added to each well of a maleimide plate and incubated for 120 min. at 37 °C. Following thorough washing with PBS-Tween 20 (pH 7.4, 0.01M), the plate was then blocked by addition of 200 µL of aqueous 100 µM mercaptohexanol (MCH) incubated for 1 h at 37 °C, followed by thorough washing of the plate. In the complementary target recognition step, 50 µL of 2.5 nM ssDNA in PBS (pH 7.4, 0.01 M) was added in each well coated with thiolated ssDNA. The plate was again incubated, under shaking conditions for 30 min at 37 °C, and subsequently thoroughly washed with PBS-Tween 20, prior to exposure to 50 nM reporter probe (in-house conjugates and commercially obtained), and again left to incubate under shaking conditions for 30 min at 37 °C. After a final wash, 50 µL of TMB for ELISA substrate was added to each well and product formation was allowed to proceed for at least 15 min at room temperature. The reaction was finally stopped by addition of 1 M H_2SO_4, and the absorbance read at 450 nm. Analysis was carried out in triplicate.

Protocol for assay measurement within microfluidics:

To avoid build up of bubbles within the microfluidics, the speed of the liquid flow was optimised and a 70 rotation per minute (rpm) was found to be the optimum speed to avoid bubble formation. Turning valves with minileur connections to 4 inlet ports were used with one outlet and one venting port, where simple rotational turning of the valve aligns specific inlet-outlet channels

that connect individual reservoirs with microchannels for introduction of each of the reagents to the microsystem and the electrode array. A syringe pump was used to drive the fluids, and the rotation and syringe pump speed, as well as the incubation times are given in Table 4.S2.

Table 4.S2. Assay procedure protocol used in the microfluidic set-up for amperometric measurements.

Protocol	**Rotation (turn)**	**Speed (rpm)**	**Waiting (s)**
1. Incubation of mixed/unmixed ssDNA PCR target	70	70	1800
2. Venting (vacuum sucking)	150	1000	5
3. Washing with PBS, pH 7.4	200	100	10
4. Incubation of mixed/unmixed reporter probe	70	70	1800
5. Venting (vacuum sucking)	150	1000	5
6. Washing with PBS, pH 7.4	200	100	10
7. Amperometric measurement, TMB substrate	50	20	160
Total assay time			3780

REFERENCES

1. Versage, J.L., Severin, D. D., Chu, M.C. and Petersen, J. M., *Development of a multitarget real-time TaqMan PCR assay for enhanced detection of Francisella tularensis in complex specimens.* Journal of clinical microbiology, 2003. **41**: p. 5492–5499.
2. Matero, P., Hemmila, H., Tomaso, H. et al., *Rapid field detection assays for Bacillus anthracis, Brucella spp., Francisella tularensis and Yersinia pestis.* Clinical Microbiology and Infection, 2011. **17**(1): p. 34-43.
3. Riehm, J.M., Rahalison, L., Scholz, H. C et al., *Detection of Yersinia pestis using real-time PCR in patients with suspected bubonic plague.* Molecular and Cellular Probes, 2011. **25**(1): p. 8-12.
4. Klee, S., Tyczka, J., Ellerbrok, H. et al., *Highly sensitive real-time PCR for specific detection and quantification of Coxiella burnetii.* Bmc Microbiology, 2006. **6**.
5. Ellerbrok, H., Nattermann, H., Ozel, M., Beutin, L., Appel, B. and Pauli, G., *Rapid and sensitive identifcation of pathogenic and apathogenic Bacillus anthracis by real-time PCR.* FEMS Microbiology Letters 2002. **214** (1): p. 51-59.
6. Tomaso, H., Pitt, T. L., Landt, F. et al., *Rapid presumptive identification of Burkholderia pseudomallei with real-time PCR assays using fluorescent hybridization probes.* Molecular and Cellular Probes, 2005. **19**(1): p. 9-20.
7. Probert, W.S., Schrader, M. N., Khuong, N. Y. et al., *Real-time multiplex PCR assay for detection of Brucella spp., B-abortus, and B-melitensis.* Journal of clinical microbiology, 2004. **42**(3): p. 1290-1293.

Chapter 5

Lyotropic liquid crystals as a template for DNA self-assembled monolayers

For submission

Lyotropic liquid crystals as a template for DNA self-assembled monolayers

Samuel B. Dulay[†], Pablo Lozano-Sanchez[†], Iris S. Nandhakumar[‡], George S. Attard[*,‡], and Ciara K. O'Sullivan[*,†,§]

[†]Nanobiotechnology and Bioanalysis Group, Department of Chemical Engineering, Universitat Rovira I Virgili, Avinguda Paisos Catalans, 26, 43007, Tarragona, Spain,

[‡]School of Chemistry, University of Southampton, Southampton SO17 1BJ, UK

[§]Institucio Catalana de Recerca i Estudis Avancats, Passeig Lluis Companys 23, 08010 Barcelona, Spain

Abstract

Ensuring good coverage of DNA probes on the transducer's surface maintaining an appropriate spacing and ordering among them to avoid probe cluttering and excessive fouling of the electrode surface to achieve maximal target binding efficiency and detection is a very important factor for DNA sensor. Herein we report the use of lyotropic liquid crystalline (LLC) phases as a templating strategy to immobilize thiolated DNA molecule in a gold electrode surface. Thiolated single strand DNA (ssDNA) is mixed with the liquid crystal template before immobilization. The mixture has then been washed off and subsequent alkanethiol backfilling is applied before simple complementary target and labeled DNA sequences have been incubated in a classical sandwich format to record the amperometric detection. The result for the templated immobilization of

thiolated DNA molecules gave better performance characteristics compared to non-templated system; obtaining a 0.10 nM limit of detection with very low non-specific adsorption signals.

Keywords: Lyotropic liquid crystals, DNA biosensors, Self-assembled monolayers (SAM)

5.1. Introduction

In recent years, there has been an intensive research effort in the field of DNA electrochemical biosensors seeking designs to provide better analytical characteristics in terms of sensitivity, selectivity, reliability, ease of fabrication and use, and lower limits of detection[1]. The performance of a DNA biosensor is dependent on the overall efficiency of hybridization between surface immobilized nucleic acids and target complementary sequences and it is well established that the surface chemistry is a critical factor. Formation of self assembled monolayers (SAM) of short DNA probes modified with a thiol moiety on surfaces of electrodes is one of the most straightforward approaches to immobilize a DNA molecule on a metal surface but the main fallback is the formation of highly packed DNA SAMs that affect the overall efficiency of the biosensor due to high DNA probe density. One issue on the highly packed system is the steric or electrostatic interactions between probe molecules that prevent target binding.

Immobilized probe interactions can be reduced by lowering the overall probe density of molecule in the surface. On the other hand, lowering the density of probe molecules may inhibit detection of target molecules especially for detecting low concentrations. Therefore, it is important to consider optimizing the density of probe molecules immobilized on the surface.

To date, several strategies have been reported to have controlled surface probe density, including space controlled SAM using dendrons[2, 3], co-immobilization of DNA probes and thiolated backfiller[4], sequential backfilling[5] and nanopatterning strategies to ensure a good

coverage of DNA whilst maintaining appropriate spacing[6] and order to avoid probe cluttering and excessive fouling[7] of the electrode surface to achieve maximal target binding and detection. However, mixed monolayers has found to be likely forming island-like features when immobilized in the surface[8]. Hence, lowering the density of probe molecules for SAM does not plainly guarantee to generate optimal surface for probe binding. An effective method in forming SAM surface of probe molecules allows organizing spaces between immobilized molecules. This would not only reduce immobilized probe interactions but also facilitates optimal target binding and detection, attributes that are useful for applications that demands higher sensitivity for biosensing especially for arrayed interfaces.

A rich polymorphism of nanostructures can be achieved using lyotropic liquid crystals (LLC) where different crystalline phases of amphiphiles are formed dependant on the ratio of surfactant to solvent[9-11]. LLC's have long range periodicities and orientational order characteristic repeat distances range from 2 to 15 nanometers[9, 12] and have been used as a template to produce mesoporous materials such as films of metals[9, 13-17], non-metals [18], and polymers [19, 20].

In this paper, we exploit the use of LLC's to act as a template to produce spaces between immobilized DNA probes whilst rendering more of the electrode surface available for electron transfer as depicted in figure 5.1. A thiolated ssDNA molecule is mixed in different phases of surfactant octaethylene glycol monohexadecyl ether ($C_{16}EO_8$) and the hydrophobic and hydrophilic domains imposed on the surface of the electrode by the amphiphilic nature of the surfactant molecules act as the driving force to achieve a homogenous, and even ordered distribution of probes on the surface.

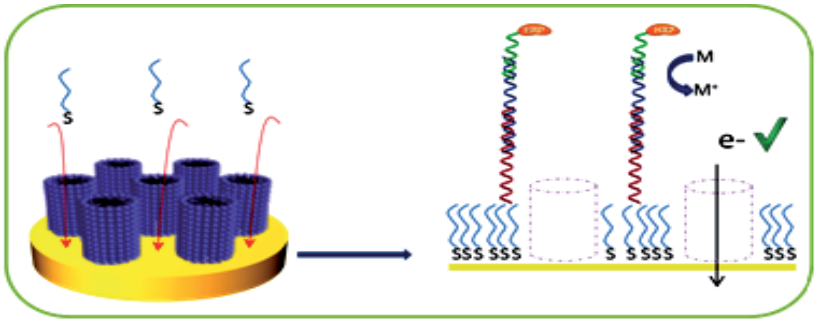

Figure 5.1 Schematic representation on the immobilization of thiolated ssDNA in hexagonal phase (H_1) of $C_{16}EO_8$ and its hybridization process to complete the sandwich assay format illustrating how the electroactive species diffuses to be detected into electrode surface.

5.2. Experimental Details

5.2.1 Materials

All the starting materials were obtained from commercial suppliers and used without further purification. Sulfuric acid, potassium dihydrogen phosphate, phosphate-buffered saline (PBS) (dry powder), PBS-Tween-20, hydrogen peroxide 30%, acetone and ethanol (synthetic grade), 0.1 M hydrochloric acid, and acetic acid were purchased from Scharlau (Spain); Octaethylene glycol monohexadecyl ether, Ferrocyanide, Ferricyanide, Strontium nitrate, Hexane, Tris(hydroxymethyl)aminomethane, Sodium Hydroxide, Sodium Chloride, 6-mercaptohexanol (MCH) and 3,3,5,5-Tetramethylbenzidine (TMB) Liquid Substrate System for ELISA was obtained from Sigma. Aqueous solutions were prepared with Milli-Q water Millipore (18mΩ.cm) and all reagents were used as received.

The following oligonucleotides sequences were purchased from ATDbio, England, U.K:

Capture probe thiolated ssDNA: 5' modified with C3thiol

5'-CTTAGTAATTGGGAAGCTTGTATCATGGCACTTAGAA-3'

Complementary target ssDNA: 5' either modified with or without Cy3 fluorophore

5'-ATTACAATGGCAGGCTCCAGAAGGTTCTAAGTGCCATGATACAAGCTT

CCCAATTACTAAGTATGCTGAGAAGAACGATAAAACTTGGGC A-3'

Reporter probe labeled with horseradish peroxidase (HRP) was purchased from Biomers, Germany:

5' modified with HRP

5'-TCT GGA GCC TGC CAT TGT AAT-3'

5.2.2 Instrumentation

Electrochemical studies were carried out using an Autolab PGSTAT 10 potentiostat and measurements were performed using a conventional three-electrode cell. 3 mm-diameter lithographically produced gold electrodes were used as working electrode, a standard silver/sliver chloride (sat. KCl) as a reference electrode (CHI 111 CH Instruments) and a platinum gauze as the counter electrode. The lithographically produced gold electrodes were provided by Fraunhofer ICT-IMM (IMM), Germany, and were produced as previously reported[21]. All sonication procedures were conducted with an ultrasonic bath (Branson ultrasonic corporation, model 2510E-MT, USA). Atomic force microscopy imaging was done using Nanoscope IIIA. Fluorescence microscopy imaging was done using Nikon Instruments Inc. Optical polarizing microscope imaging were done using an inverted microscope, Brand-Hund, Germany.

5.2.3 Preparation of lyotropic liquid crystals (LLCs)

5.2.3.1 Mixture of 5mM of $[Fe^{II}(CN)_6]^{4-}$/$[Fe^{III}(CN)_6]^{3-}$ couple with 0.1 M $Sr(NO_3)_2$ solution in LLCs

To obtain different phases of the lyotropic liquid crystals, 5mM of $[Fe^{II}(CN)_6]^{4-}$ /$[Fe^{III}(CN)_6]^{3-}$ couple with 0.1 M $Sr(NO_3)_2$ solution has been added to the surfactant at certain ratio by weight, i.e. L_1 (80:20), H_1 (60:40), and L_α (30:70) of Solvent:$C_{16}EO_8$ % by weight. Mixing time of

about 5 minutes was required to obtain a homogenous mixture for each phase using a small glass rod in an eppendorf vial.

5.2.3.2 Addition of hexane to H_1 template

Different mole fraction of hexane, i.e. 0.15, 0.25 and 0.34, has been added to H_1 containing *5mM of $[Fe^{II}(CN)_6]^{4-}/[Fe^{III}(CN)_6]^{3-}$ couple with 0.1 M $Sr(NO_3)_2$ solution*. In the preparation of the mixtures, different mole fractions of hexane were prepared separately in an eppendorf vial and mixed manually to H_1 containing the redox couple using a glass rod. Mixing time of about 5 minutes was required to obtain a homogenous mixture for each phase. The prepared mixtures were immediately used for electrochemical analysis.

5.2.4 Electrode modification and electrochemical detection

Prior to modification of the lithographic gold electrodes, a three-step cleaning protocol was applied. Initially, in order to remove the protective resist used during storage, the electrodes were sonicated for 5 min in acetone (2 times), 5 min in isopropanol (3 times) and rinsed with water and dried with compressed air. In a second step, the electrodes were then further treated with cold Piranha's solution (*Warning: Piranha's solution is highly corrosive and violently reacts with organic materials; this solution is potentially explosive and must be used with extreme caution*) for 30s and subsequently washed with Milli-Q water before use. In the last step, electrochemical cleaning was performed in 0.5 M H_2SO_4 by application of a constant potential of 1.6 V for 10s followed by 10 voltammetric cycles in the potential range −0.2 to 1.6 V at a scan rate of 0.3 V/s. Finally, the electrodes were rinsed with Milli-Q water and dried with nitrogen.

5.2.4.1 Non templated immobilization

Immobilization of thiolated ssDNA without the presence of a template was done in three ways: (i) non-backfilled immobilized thiolated ssDNA, (ii) sequential backfilling after thiolated ssDNA immobilization and (iii) co-immobilization of thiolated ssDNA and backfiller. In the immobilization of thiolated ssDNA without backfiller, electrodes were exposed to 1 μM of thiolated ssDNA in 0.4 M KH_2PO_4 (pH 3.5) overnight then the modified electrode was washed with MilliQ water for 15 minutes under gentle stirring and dried with Nitrogen gas. The electrodes were then immersed in 1mM aqueous solution of MCH for 60 minutes as a backfiller to prevent further non-specific adsorption and to help the immobilized thiolated ssDNA probes to stand still[22] then rinsed with Milli-Q water. In the case of co-immobilization method, a ratio of 1:100 thiolated ssDNA and MCH respectively in 0.4 M KH_2PO_4 (pH 3.5) has been prepared and were exposed to electrodes for an overnight incubation. The electrode were then washed with MilliQ water under gentle stirring condition and dried with Nitrogen gas. All incubation was done in a humidity chamber to avoid evaporation of the solution.

5.2.4.2 Templated immobilization

1 μM of thiolated ssDNA in 0.4 M KH_2PO_4 (pH 3.5) was mixed to the surfactant at certain ratio by weight to form different phases, i.e. L_1 (80:20), H_1 (60:40), and L_α (30:70) of Aqueous ssDNA:$C_{16}EO_8$ % by weight. In the preparation of the mixtures, each phase of surfactants used was prepared separately in an eppendorf vial and mixed manually using a glass rod upon addition of the aqueous thiolated DNA probe to the weighed amount of $C_{16}EO_8$. Mixing time of about 5 minutes was required to obtain a homogenous mixture for each phase. The prepared mixtures were deposited on gold electrode and were incubated overnight. The electrodes were then washed in a stirring solution of Milli-Q water for 15 minutes until no more traces of surfactant pastes can be observed on the surfaces of the electrodes and then dried with nitrogen. The electrodes were then

immersed in 1mM aqueous solution of MCH for 60 minutes as a backfiller then rinsed with Milli-Q water.

5.2.4.3 Electrochemical DNA detection

The modified electrodes, i.e. Non templated and templated immobilization, were then incubated for 15 min in different concentrations of ssDNA target and then for another 15 min with the corresponding horseradish peroxidase labeled ssDNA both prepared in hybridization buffer (pH adjusted to 7.4) at 37 °C. Amperometric measurement was carried out at 0.15 V vs. Ag/AgCl. All electrochemical measurements were performed at room temperature.

5.3. Results and Discussion

5.3.1 Electrochemical surface characterization

Prior to the immobilization of thiolated ssDNA mixed with the template to the electrode surface, evaluation of the mixtures has been done to ensure the type of phase being used. At room temperature, the mixtures have a characteristic optical texture of liquid crystalline phase when viewed under a polarizing light microscope. In the case of micellar phase, it is isotropic and does not have any characteristics under the polarizing microscope (see Supplementary Information Figure 5.S1).

5.3.1.1 Calculating available active areas and the number of immobilized thiol molecules

Firstly, the transport of electroactive species through the hydrophilic domains of the various liquid crystal phases, revealing the available active area of the electrode was investigated. The different phases investigated were micellar (L_1), hexagonal (H_I), and lamellar (L_α) which were formed with 20, 40, and 70% $C_{16}EO_8$ respectively in aqueous 5 mM of $[Fe^{II}(CN)_6]^{4-}/[Fe^{III}(CN)_6]^{3-}$ couple

with 0.1 M $Sr(NO_3)_2$ solution. Each of the prepared electrodes was immersed in different phases prepared and aqueous solution (A, no surfactant added). Cyclic voltammetry was carried out at different sweep rates from 0.150 to 0.01 V/s in the potential range of -0.2 to 0.7V. As expected, a diffusion controlled mechanism was observed with increasing surfactant concentrations changing the lyotropic crystalline phases from $L_1 \rightarrow H_1 \rightarrow L_\alpha$ and resulting in decreasing available electrochemically active area as the surfactant acts an effective insulator (Figure 5.2a).

After accounting the available active area where thiolated molecules could be immobilized for each templates, thiolated ssDNA (1μM) was mixed with each of the crystalline phases and added to gold electrode surface. Immobilization of thiolated ssDNA has also been done without the presence of surfactant as a control. After overnight immobilization, the electrodes were then thoroughly washed with MilliQ-water with gentle stirring until no more traces of surfactant that can be seen. Subsequently, the electrodes were exposed to a potential scan between -0.2 and -1 V in 0.05M KOH to facilitate reductive desorption of any immobilized thiol molecules [23]. The calculated probe density for each immobilization method has shown decreasing density when templated (Figure 5.2d-table). The values obtained were all in agreement to the reported typical surface coverage of probe DNA that can be immobilized in an electrode surface [24] confirming further the results obtained in reductive desorption (Figure 5.2c). Further confirmation has been done by immobilizing mercaptohexanol (1mM) instead of thiolated ssDNA. The obtained probe density in the absence of any templating was found to be 4.06 x 10^{-10} moles/cm^2 which is in agreement with previously reported data [25] (see Supplementary Information Figure 5.S2). The results clearly demonstrating that the templating with the different crystalline phases does result in a patterning of hydrophobic and hydrophilic domains. It also shows no significant difference in the ratio between available active area for each template used and the number of thiolated moles, i.e.

thiolated ssDNA and MCH, adsorbed using each template considering for the total area of the gold electrode giving a good degree of correlation as predicted in equation 1.

Equation 1

$$\frac{\text{Available active surface } A_{Hexagonal}}{\text{Available active surface } A_{Aqueous}} \approx \frac{\text{Total moles of MCH desorbed } A_{Hexagonal}}{\text{Total moles of MCH desorbed } A_{Aqueous}} \approx \frac{\text{Total moles of SDNA desorbed } A_{Hexagonal}}{\text{Total moles of SDNA desorbed } A_{Aqueous}}$$

The reductive desorption process further accounts how much thiolated probes could be immobilized in different immobilization condition.

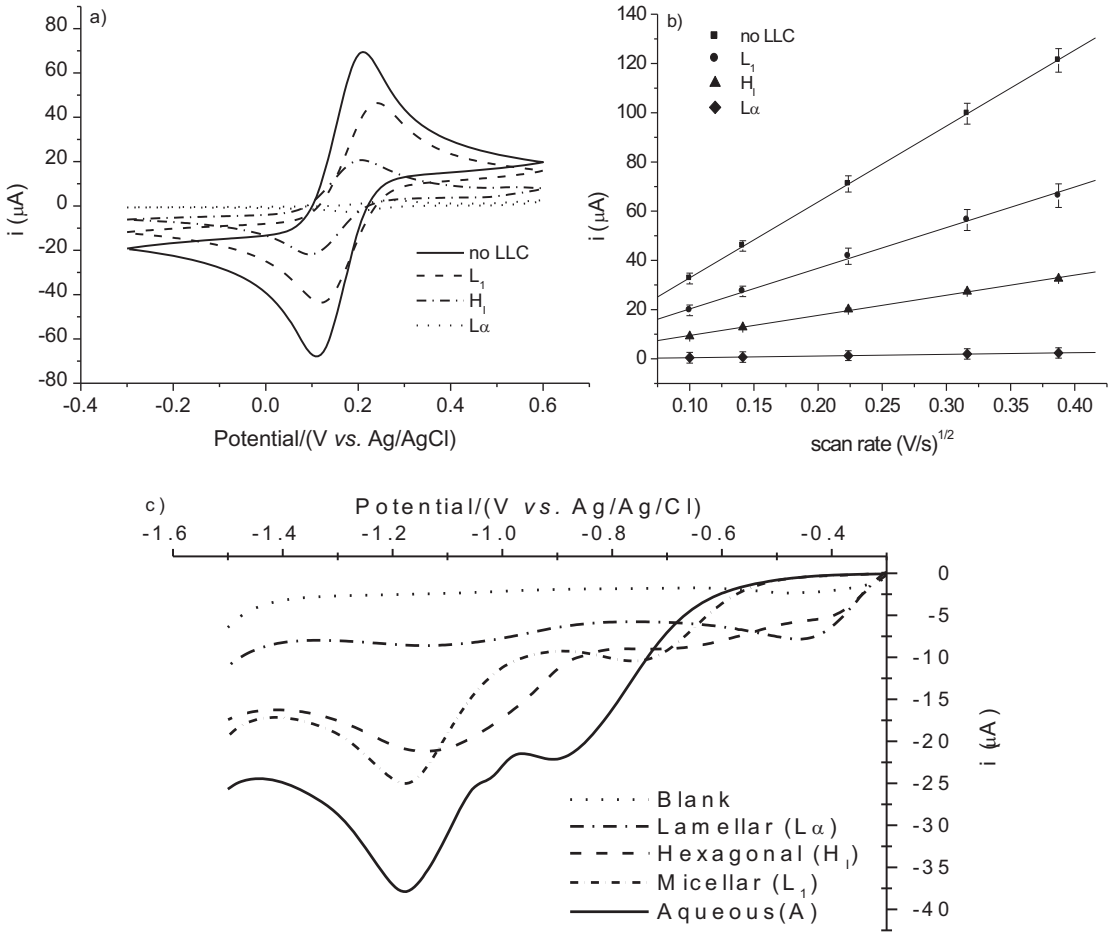

d) Immobilisation condition	Charge (C) 10^{-6}	moles (Q=mnF) 10^{-11}	available active surface area	% available active surface area	moles/cm² (total area=0.09) 10^{-10}	%moles/cm² (total area=0.09)	moles/cm² (available surface active area) 10^{-10}
Aqueous	1.96±0.30	2.03±0.30	0.090	100	2.26±0.40	100	3.11±0.40
Micellar	1.46±0.40	1.51±0.30	0.050	55.6	1.68±0.50	54.0	3.02±0.80
Hexagonal	0.78±0.23	0.81±0.20	0.023	25.6	0.89±0.30	28.6	3.50±0.10
Lamellar	0.07±0.03	0.08±0.03	0.002	2.22	0.08±0.10	2.50	3.76±0.40

Figure 5.2. a) Typical cyclic voltammograms of 5mM $Fe^{+3/+2}$ and their b) corresponding oxidation peak current in different mixture conditions, c) Cyclic voltammograms for the reductive desorption of immobilized thiolated DNA in different immobilization condition from the gold electrodes in 50mM of KOH at a scan rate of 0.05 V/s and d) summarized calculated available active area for a and surface coverage of thiols per area cm^2 for c.

5.3.1.2 Expanding the diameter of H_I template characterization

The swelling effect of hexane to H_I template further support the results obtained in the CV of $[Fe^{II}(CN)_6]^{4-}/[Fe^{III}(CN)_6]^{3}$ in different phases proving the existence of hydrophilic domains in which it can host the electroactive redox domains or thiolated molecules to pass through reaching the active surface area of the electrode. Figure 5.3 shows two possible orientation of $C_{16}EO_8$ cylinders formed in H_I phase with respect to their arrangement when in contact in electrode's surface by simply increasing the diameter of the cylinders. Hexane molecules at different mole fraction had been added to the H_I phase containing $[Fe^{II}(CN)_6]^{4-}/[Fe^{III}(CN)_6]^{3}$ and CV has been done to determine the electrochemically accessible active area(see Supplementary Information Figure 5.S3).

The mathematical model revealed the likeness of the cylinder orientation by comparing the relative electrochemically accessible surface area for each model systems to the actual experimental data. Figure 5.3c suggests that the experimental data values obtained is closer to the predicted values

based on the calculated theoretical data (Figure 5.3a) which signifies that the cylinders were oriented vertically to the electrodes' surface rather than horizontally positioned. Calculated and experimental values has been summarised in the Supplementary information table 5.S1.

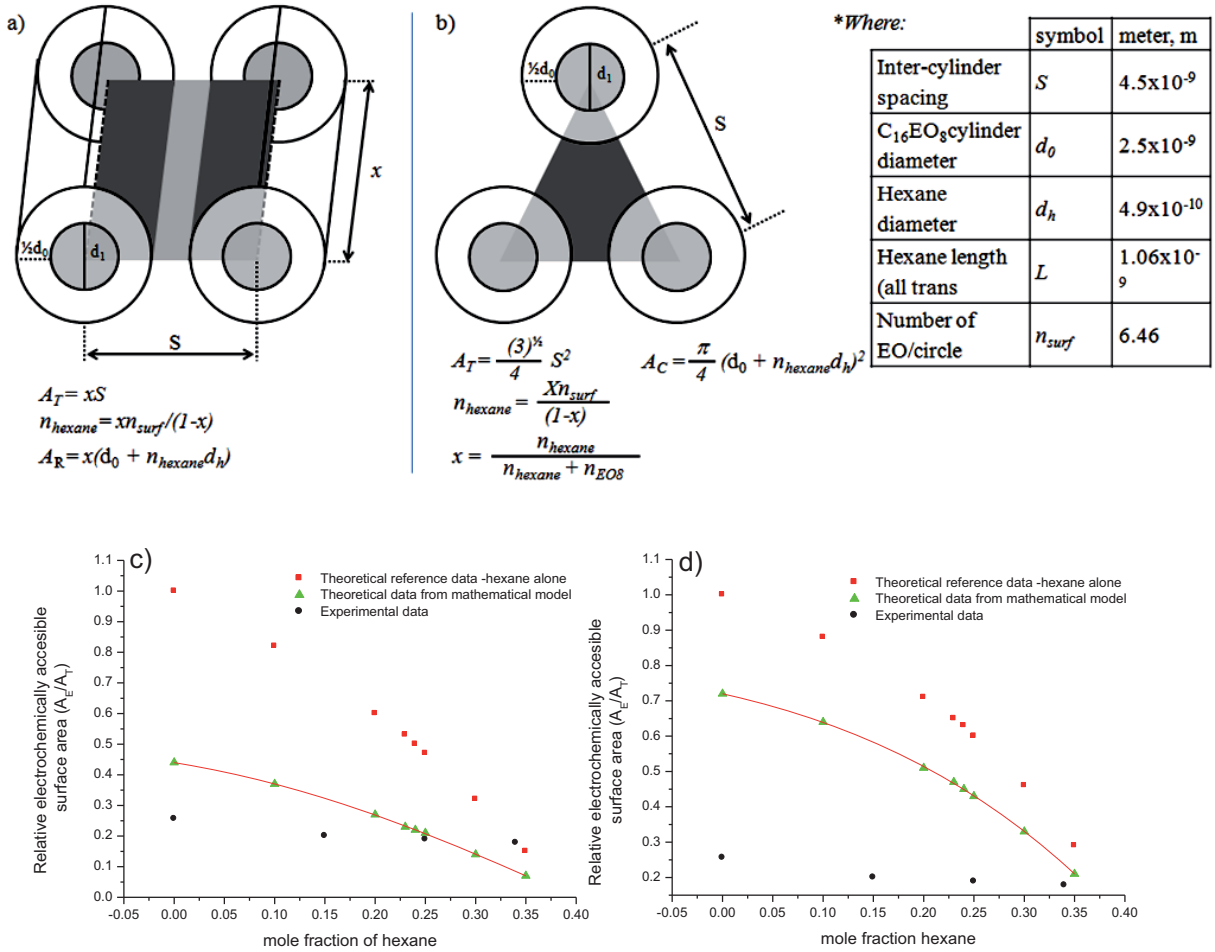

	symbol	meter, m
Inter-cylinder spacing	S	$4.5x10^{-9}$
$C_{16}EO_8$cylinder diameter	d_0	$2.5x10^{-9}$
Hexane diameter	d_h	$4.9x10^{-10}$
Hexane length (all trans	L	$1.06x10^{-9}$
Number of EO/circle	n_{surf}	6.46

Figure 5.3. Schematic model of possible orientation of H_I $C_{16}EO_8$ a) vertically and b) horizontally positioned to electrode's surface and obtained graphical representation of relative electrochemically accessible surface area of c) vertically and d) horizontally positioned H_I $C_{16}EO_8$ in the surface of electrode.*Values are based on previous studies [9, 26].

5.3.2 Electrochemical DNA detection

The assembly of whole assay was then explored in thiolated ssDNA probes immobilized in different phases of $C_{16}EO_8$ at fixed concentration of DNA target. The spacing concept of immobilized thiolated ssDNA probes through templating with LLC that led to the improved response of the biosensor has been confirmed. As can be seen in figure 5.4, the net amperometric response has improved after the thiolated ssDNA probes has been immobilized with a template especially the H_1 template and it can be observed that a value of ≥12 hours was enough to reach in all cases the maximum response before each sensor starts to saturate. It is apparent as well that even at <5 hours there was already an improved amperometric response. The diffusion of the thiolated ssDNA probes was still possible through the hydrophilic zones imposed by the LLC's and the electrochemical response has improved.

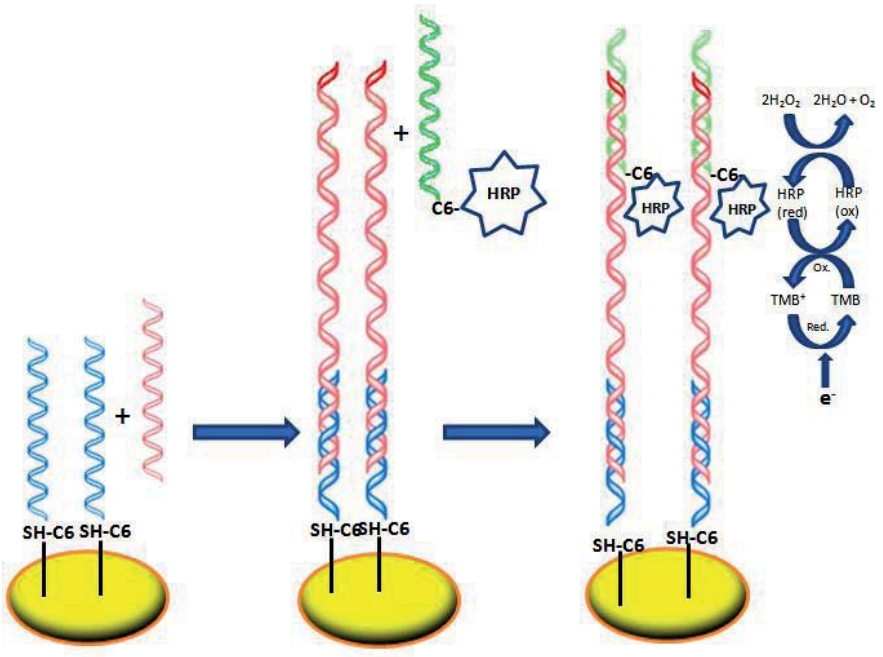

Figure 5.4. Amperometric detection of complementary target DNA hybridized at 5 nM to the immobilized thiolated ssDNA in templated and non templated system at different immobilization time.

After confirmation of the improved response, the assembly of whole assay was then repeatedly explored varying the concentration of DNA target to form a calibration curve. The best signal response was shown by the templated system most especially for the H_1 template which gave a huge increase in sensitivity of 4.5 $\mu A/cm^2.nM$ seven times fold higher compared to non templated immobilization of thiolated ssDNA probe and even better to the co-immobilization strategy that has been reported to be the optimum condition for thiolated SAM capture probes [4]. The immobilized thiolated ssDNA in H_1 template also gave the lowest limit of detection (LOD) which is 0.1 nM as compared to non templated system (Figure 5.5).

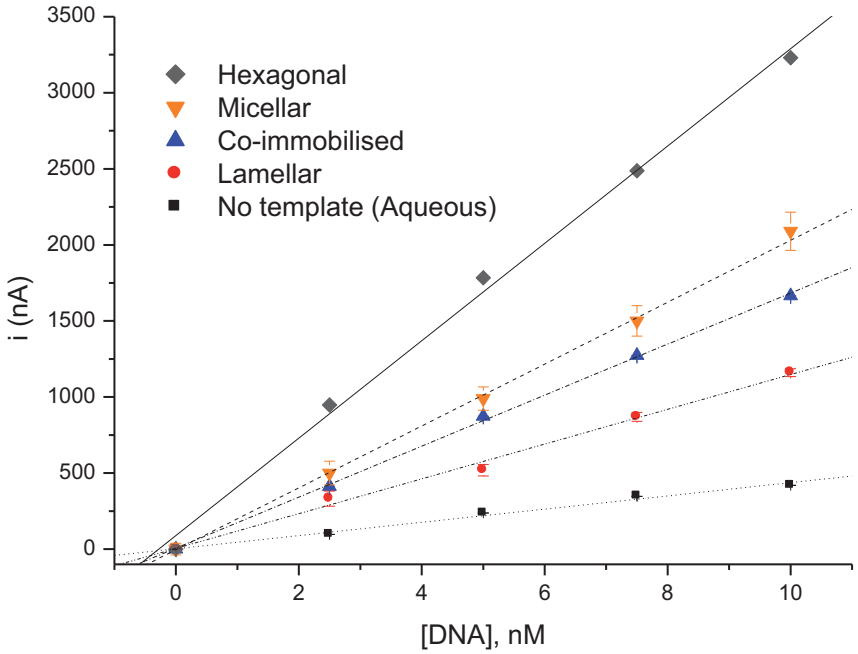

Immobilization Condition	LOD (nM)	Sensitivity (μA/nM.cm²)
Hexagonal	0.1	4.5
Micellar	0.3	3.7
Co-immobilized	0.4	2.4
Lamellar	1.3	1.6
No template (Aqueous)	2.6	0.6

Figure 5.5. Amperometric responses of the templated and non templated electrochemical DNA biosensor to different complementary target DNA concentrations. Each data point represents the average of three measurements on three separate sensors.

5.3.3 Imaging characterization

Thiolated DNA were immobilized overnight to ensure enough DNA's will be chemisorbed in Au surface in four different conditions to evaluate hybridization efficiency when exposed to the complementary ssDNA target modified with Cy3 fluorophore. Figure 5.6 shows the differences in the intensity of fluoresced light emitted by the target ssDNA with Cy3 fluorophore hybridized with its complementary thiolated capture. Co-immobilized thiolated ssDNA and MCH backfiller has shown the highest intensity in terms of integrated density of fluoresced light emitted. The integrated density of unhybridized surface as a control has been subtracted to the integrated density of the hybridized surface area to estimate the total number of immobilized molecules that has been hybridized in each condition. The non-templated immobilized thiolated ssDNA (figure 5.6 a and b), i.e. no backfiller and subsequent backfilling, has shown almost similar integrated density which is supposedly expected to give more hybridized capture probes than co-immobilization method since they contain more thiolated capture probes. This phenomena can be due to fully packed self assembled monolayers of thiolated DNA that results to strong intermolecular electrostatic repulsion [22, 24] between neighboring thiolated DNA as well as complementary targets that led to inefficiency of hybridization giving less target detection via fluoresced light emitted.

However, thiolated ssDNA molecules immobilized in aqueous media alone with sequential backfilling with mercaptohexanol (MCH) gave a little increase in the integrated density value signifying improvement in the hybridization efficiency (figure 5.6b). The purpose of MCH is not only to prevent nonspecifically adsorbed DNA off the surface but the net negative dipole of the alcohol terminus repelled the negatively charged DNA backbone, thus helping to project the probe strand out into solution being exposed better for hybridization[24]. Further increased in hybridization efficiency has been observed when co-immobilization of thiolated DNA with backfiller (mercaptohexanol) that accounts for better probe distribution giving a better hybridization efficiency of the target DNA [4]. Although co-immobilization process exhibited the most number of molecules hybridized per area than thiolated DNA's immobilized in the presence of H_I phase template, the efficiency in the detection of the target through amperometry via HRP-labeled DNA would still be dependent on the efficiency of hybridization between the target DNA molecule and HRP-labeled DNA in completing the sandwich assay for final measurement of analyte target in which a well spaced immobilized capture probes would favor more efficient hybridization due to less intermolecular electrostatic repulsion between neighboring probes for complementary target and the HRP-labeled DNA for sandwich assay format. This further confirms why sensitivity is far better for thiolated DNA immobilized in the presence of H_I phase template than the co-immobilized condition (Figure 5.5).

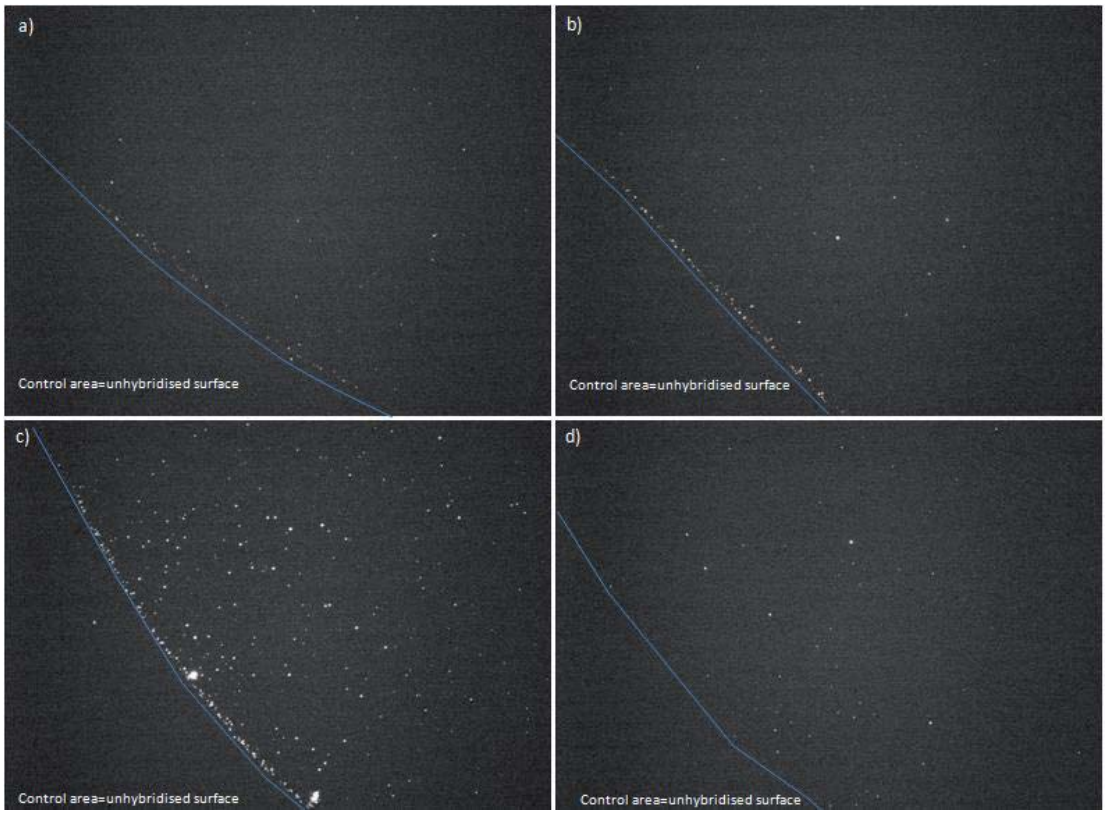

e) DNA Immobilization condition	*Total integrated density $2.5x10^{-5}$ cm^2 10^6	Fluorescence imaging total no. of molecules hybridized/total area image ($2.5x10^{-5}$ cm^2) 10^{10}
a) Aqueous only (no MCH)	1.95±0.05	7.8±0.3
b) Sequential backfilling	2.25±0.07	9.0±0.1
c)Co-immobilization (ssDNA:MCH)	3.80±0.09	15.2±0.5
d) H_I phase	2.22±0.05	8.89±0.02

Figure 5.6. Fluorescence microscopy imaging for immobilized thiolated DNA hybridized with its complementary target modified with Cy3 in a) aqueous media only (no MCH), b) Sequential backfilling with MCH, c) co-immobilization of SDNA and MCH (1:100 ratio), d) H_I phase of $C_{16}EO_8$ and e) summary table on the estimated total number of molecules hybridized in each

conditions.*The total integrated density was calculated by subtracting the integrated density of the unhybridized surface as control.

Further imaging characterization have been done through atomic force microscopy. Thiolated ssDNA were immobilised in mica surface in the presence and absence of a template. The cross sectional analysis further tells us the chemical information present in the surface of the substrate confirming the immobilization of ssDNA's in the presence of H_1 template. It can be visually observed as well how the ssDNA were immobilised creating spaces between probes when compared to non templated system where a fully packed surface can be observed. This further confirms why surfaces with uncontrolled full packing of probe density gave lower biosensor performance in terms of sensitivity and detection limit.

Through the images obtained, we were able to estimate how much thiolated molecules has been immobilised in each condition. In order to obtain a rough estimate on the amount of molecules immobilised, the integrated densities of the fluoresced light has been evaluated. The integrated density correlates the number of DNA molecules immobilised in different conditions and were compared to the obtained values in the reductive desorption. Although the total calculated amount of molecules per area absorbed obtained in the reductive desorption are higher than in the fluorescence imaging integrated density analysis, they are still in agreement in terms of typical surface coverage of probe DNA that can be immobilised in an electrode surface which is in the order of 10^{11}-10^{13} molecules/cm^2 [24] confirming further the results obtained in reductive desorption.

The 37 base ssDNAs in mica surface immobilised through non-templated and templated system (Figure 5.7 b and c) had globular conformations with mean measured diameters of 35-37 nm and 19-23 nm respectively. Although the obtained diameter of the immobilised 37 base ssDNAs is too big from its approximated actual length size (10 nm) [27], we have to take into account that short

ssDNAs tend to form aggregations and coiling leading to its larger mean measured diameter [28]. The results obtained is in agreement with the image that has been reported elsewhere for 25-50 base ssDNAs having a height of ~1 nm (figure 5.3e and 5.3f) [29, 30] that differs only in the diameter size of the globular formed ssDNAs. This could be due to longer incubation time of immobilisation allowing more ssDNAs to form conglomeration.

Immobilised ssDNAs without a template formed bigger aggregations than the templated system because ssDNAs in non-templated immobilisation were not confined or restricted in the solution unlike for the templated system where the ssDNAs were restricted within the hydrophilic zones formed in the H_I phase of $C_{16}EO_8$. Aggregation of ssDNAs in templated system could be formed after the surfactant has been washed off and dried with nitrogen gas.

Eventhough there is no eminent pattern obtained in the templated DNA, the presented AFM result gave us at least more information, which supports the fluorescence microscopy imaging results, about the ability of a template to have a controlled probe density avoiding a fully packed dense surface.

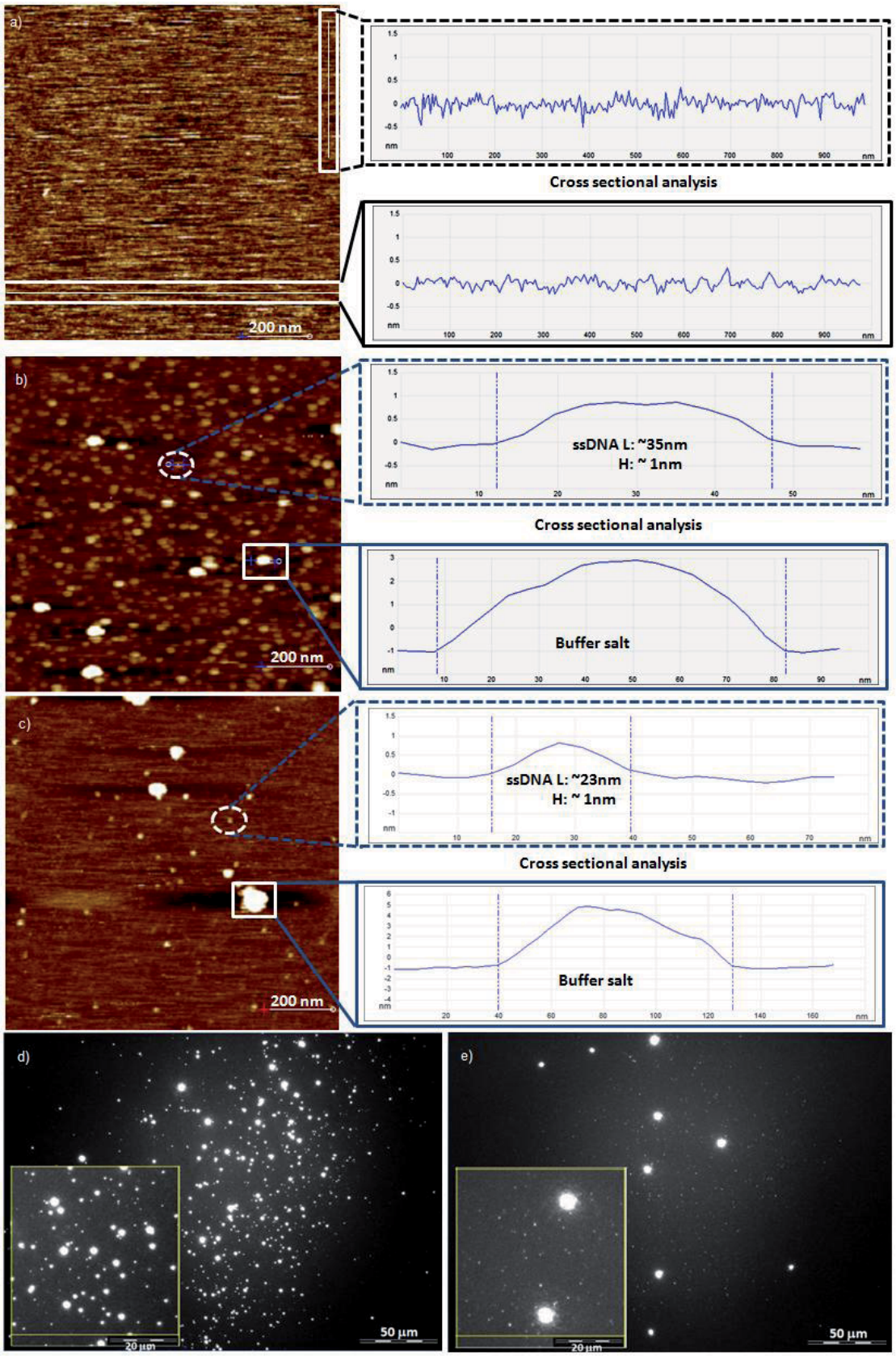
a)
200 nm
Cross sectional analysis
b)
200 nm
ssDNA L: ~35nm
H: ~ 1nm
Cross sectional analysis
Buffer salt
c)
200 nm
ssDNA L: ~23nm
H: ~ 1nm
Cross sectional analysis
Buffer salt
d)
50 µm
e)
50 µm

f) DNA Immobilization condition	Reductive desorption			Fluorescence imaging		AFM imaging	
	total no. of moles of ssDNA absorbed 10^{-11}	total no. of of ssDNA molecules absorbed 10^{13}	total no. Of thiol ssDNA molecules absorbed/total area (0.09cm^2) 10^{13}	*Integrated density 50x50 μm 10^5	total no. of molecules absorbed/total area image (2.5x10^{-5} cm^2) 10^{13}	Total counted dots (molecules) in 1x1μm	total no. of thiol ssDNA molecules absorbed/total area image (1x10^{-8} cm^2) 10^{13}
Aqueous only	2.03 ±0.30	1.22	13.6	28±1.0	0.012±0.001	435±36	0.00435±0.002
H_I phase	0.81 ±0.20	0.49	5.4	14.1±0.9	0.006±0.001	45±1	0.00045±0.0001

Figure 5.7. Atomic Force Microscopy (AFM) imaging for immobilised ssDNA in mica surface a) control, clean mica, b) in HEPES buffer with Ni+ salt only, c) HEPES buffer with Ni+ salt in the presence of H_I template (graph image: cross sectional surface analysis for each surfaces) and fluorescence microscopy imaging for immobilised thiolated DNA modified with Cy3 in: d) aqueous media only, e) H_I phase of $C_{16}EO_8$ (inset: enlarged area-50x50 μm) in Au electrode surface and f) calculated number of molecules for each immobilization method done. *The total integrated density was calculated by subtracting the integrated density of the unhybridized surface as control.

5.4. Conclusion

The improved performance of the biosensor when template has been used can be credited to better probe distribution which gives the following advantages: (i) less intermolecular electrostatic repulsion between immobilized probes and complementary targets for having enough spaces giving better hybridization efficiency and (ii) less steric hindrance in the electrode surface by having more electroactive spaces allowing electroactive species to freely diffuse in the electrode surface for a better current response and improved detection limit.

Acknowledgements

The research leading to these results has received funding from the European Community's Seventh Framework Programme "The lab-free CBRN detection device for the identification of biological pathogens on nucleic acid and immunological level as lab-on-a-chip system applying multisensor technologies", MultisenseChip [FP7/2007-2013]. Mr. Dulay would to thank Universitat Rovira I Virgili for the mobility grant given for him to have a short research stay at the University of Southampton, U.K.

References

1. Gooding, J.J., Lai, L. M. H., and Goon, I. Y., *Nanostructured electrodes with unique properties for biological and other applications.* Advances in electrochemical science and engineering, 2009. **11 Chemically modified electrodes**.
2. Tokuhisa, H., Liu, J., Omori, K., Kanesato, M., Hiratani, K., and Baker, L. A., *Efficient biosensor interfaces based on spaced-controlled self-assembled monolayers.* Langmuir, 2009. **25**: p. 1633-1637.
3. Oh, S.J., Ju, J., Kim, B. C., Ko, E., Hong, B. J., Park, J.-G., Park, J. W., and Choi, K. Y., *Isolation and identification of Streptomyces sp. producing substance inhibiting vancomycin-resistant Staphylococcus aureus.* Nucleic Acids Research, 2005. **33**(10): p. e90.
4. Henry, O., Y. F., Perez, J. G., Sanchez, J. L. A., and O'Sullivan, C. K, *Electrochemcial characterisation and hybridisation efficiency of co-assembled monolayers of PEGylated ssDNA and mercaptohexanol on planar gold electrodes* Biosensors and Bioelectronics, 2010. **25**(5): p. 978 - 983.
5. H.Nasef, V.B., V.C. Ozalp, C.K. O'Sullivan, Analytical and Bioanalytical Chemistry, 2010. **396**: p. 2565.
6. Beni, V., Gelaw, T. K., and O'Sullivan, C. K., *Study of the combination of the deposition/stripping of sacrificial metal nano-structures and alkanethiol as a route for genosensor surface preparation.* Electrochemistry Communications, 2011. **13**: p. 325-327.
7. Soreta, T.R., Henry, O. Y.F, and O'Sullivan, C. K., *Electrode surface nanostructuring via nanoparticle electronucleation for signal enhancement in electrochemical genosensors.* Biosensors and Bioelectronics, 2011. **26**: p. 3962 - 3966.
8. Smith, R.K., Reed, S. M., Lewis, P. A., Monnell, J. D., Clegg, R. S., Kelly, K. F., Bumm, L. A., Hutchison, J. E., and Weiss, P. S., *Phase Separation within a Binary Self-Assembled Monolayer on Au{111} Driven by an Amide-Containing Alkanethiol.* Journal of Physical Chemistry B, 2001. **105**(6): p. 1119–1122.
9. Attard, G.S., Bartlett, P. N., Coleman, N. R. B., Elliott, J. M., Owen, J. R., and Wang, J. H., *Mesoporous Platinum Films from Lyotropic Liquid Crystalline Phases.* Science 1997. **278**: p. 838 - 840.

10. Burducea, G., *Lyotropic Liquid crystals: Structural polymorphism.* Romanian reports in physics, 2004. **56**(1): p. 87 - 100.
11. Tiddy, G.J.T., *Surfactant-water liquid crystal phases.* Physics Reports, 1980. **57**(1): p. 1-46.
12. Wang, C., Chen, D., and Jiao, X., *Lyotropic liquid crystal directed synthesis of nanostructured materials.* Sci. Technol. Adv. Mater. , 2009. **10**: p. 023001.
13. Whitehead, A.H., Elliott, J. M, Owen, J. R., and Attard, G. S, *Electrodeposition of mesoporous tin films.* Chem. Commun., 1999: p. 331-332.
14. Gollas, B., Elliott, J. M., and Bartlett, P. N, *Electrodeposition and properties of nanostructured platinum films studied by quartz crystal impedance measurements at 10 MHz.* Electrochimica Acta 2000. **45** p. 3711-3724.
15. Zhao, J., Chen, X., Jiao, L., Chai, Y., and Wang, L., *Electrochemical deposition of lamellar platinum nanostructures from lyotropic liquid crystal template.* Scripta Materialia, 2004. **51**: p. 593-598.
16. Foyet, A., Hauser, A., and Schafer, W., *Template electrochemical deposition and characterization of zinc-nickel alloy nanomaterial.* Journal of electroanalytical chemistry, 2007. **604**: p. 137 - 143.
17. Guo, R., Zhang, B., and Liu, X., *Electrodeposition of nanostructured Pt films from lyotropic liquid crystalline phases on alpha-Al2O3 supported dense Pd membranes.* Applied surface science, 2007. **254**: p. 538 - 543.
18. Nandhakumar, I., Elliott, J. M., and Attard, G. S, *Electrodeposition of nanostructured mesoporous selenium films (HI-eSe).* Chem. Mater. , 2001. **13**: p. 3840-3842.
19. Elliott, J.M., Cabuche, L. M., , and Bartlett, P. N., *Electrochemical characterization of a templated insulating polymer-modified electrode.* Analytical Chemistry, 2001. **73**: p. 2855-2861.
20. Xu, Q., Zhu, JL., and Hu, XY., *Ordered mesoporous polyaniline filmm as a new matrix for enzyme immobilization and biosensor construction.* Analytica Chimica Acta, 2007. **597**: p. 151 - 156.
21. Fragoso, A., Latta, D., Laboria, N., von Germar, F., Hansen-Hagge, T. E, Kemmner, W, Gartner, C., Klemm, R., Dreseb, K. S., and O'Sullivan, C. K, *Integrated microfluidic platform for the electrochemical detection of breast cancer markers in patient serum samples.* Lab on a Chip, 2011. **11**: p. 625-631.
22. Herne, T.M., and Tarlov, M. J., *Characterization of DNA Probes Immobilized on Gold Surfaces.* J. Am. Chem. Soc. , 1997. **119**: p. 8916-8920.
23. Walczak, M.M., Popenoe, D. D., Deinhammer, R. S., Lamp, B. D., Chung, C., and Porter, M. D., *Reductive desorption of alkanethiolate monolayers at gold: A measure of surface coverage.* Langmuir, 1991. **7**: p. 2687 - 2693.
24. Gooding , J.J., *Electrochemical DNA Hybridization Biosensors.* Electroanalysis, 2002. **14**(17): p. 1149-1156.
25. Mizutani, F., sato, Y., Yabuki, S., Sawaguchi, T., and Iijima, S., *Enzyme electrodes based on self-assembled monolayers of thiol compounds on gold.* Electrochimica acta, 1999. **44**: p. 3833 - 3838.
26. Bartlett, P.N., *Electrodeposition of Nanostructured Films Using Self-Organizing Templates.* The Electrochemical Society Interface, 2004. **13**: p. 28-33.
27. Kotlyar, A., Borovok, N., Molotsky, T., Klinov, D., Dwir, B. and Kapon, E., *Synthesis of novel poly(dG)–poly(dG)–poly(dC) triplex structure by Klenow exo− fragment of DNA polymerase I.* Nucleic Acids Research, 2005. **33**(20): p. 6515–6521.

28. Venta, K., Shemer, G., Puster, M., Rodriguez-Manzo, J. A., Balan, A., Rosenstein, J. K., Shepard, K. and Drndi, M., *Differentiation of Short,Single-Stranded DNA Homopolymers in Solid-State Nanopores.* American Chemical Society Nano, 2013. **7**(5): p. 4629–4636.
29. Hansma, H.G., Revenko, I., Kim, K. and Laney, D. E, *Atomic force microscopy of long and short double-stranded, single-stranded and triple-stranded nucleic acids.* Nucleic Acids Research, 1996. **24**(4): p. 713–720.
30. Liu, Z., Li, Z., Zhou, H., Wei, G., Song, Y. and Wang, L., *Imaging DNA Molecules on Mica Surface by Atomic Force Microscopy in Air and in Liquid.* Microscopy research and technique, 2005. **66**(4): p. 179-185.

Chapter 5: Supplementary Information

Lyotropic liquid crystals as a template for DNA self-assembled monolayers

Samuel B. Dulay, Pablo Lozano-Sanchez, Iris S. Nandhakumar, George S. Attard*, and Ciara K. O'Sullivan*

*To whom correspondence should be addressed. E-mail: ciara.osullivan@urv.cat and gza@soton.ac.uk

This supplementary online material includes:

Materials and methods
Figures
References

MATERIALS AND METHODS

Materials

All the starting materials were obtained from commercial suppliers and used without further purification. Octaethylene glycol monohexadecyl ether, $C_{16}EO_8$, was purchased from Sigma-Aldrich. Oligonucleotides were purchased from ATDbio, England.HEPES buffer, Nickel Chloride, Mercaptohexanol, Potasium Hydroxide, Sulfuric acid, Potassium dihydrogen phosphate, Trizma buffer, and Phospate buffer saline (PBS) were all purchased from Sigma-Aldrich.

General Methods

Preparation of H_I phase mixture with thiolated ssDNA in HEPES buffer were prepared in 60:40 ratio of Aqueous ssDNA in HEPES buffer:$C_{16}EO_8$ % by weight. Aqueous solutions were prepared with Milli-Q water (Millipore).

DNA Sequences

Capture probe thiolated ssDNA: 5' modified with C3thiol and 3' modified with Cy3 fluorophore

5'-CTTAGTAATTGGGAAGCTTGTATCATGGCACTTAGAA-3'

Buffers

HEPES buffer in $NiCl_2$: 10 mM HEPES in 5mM NiC l_2 aqueous solution

Figures:

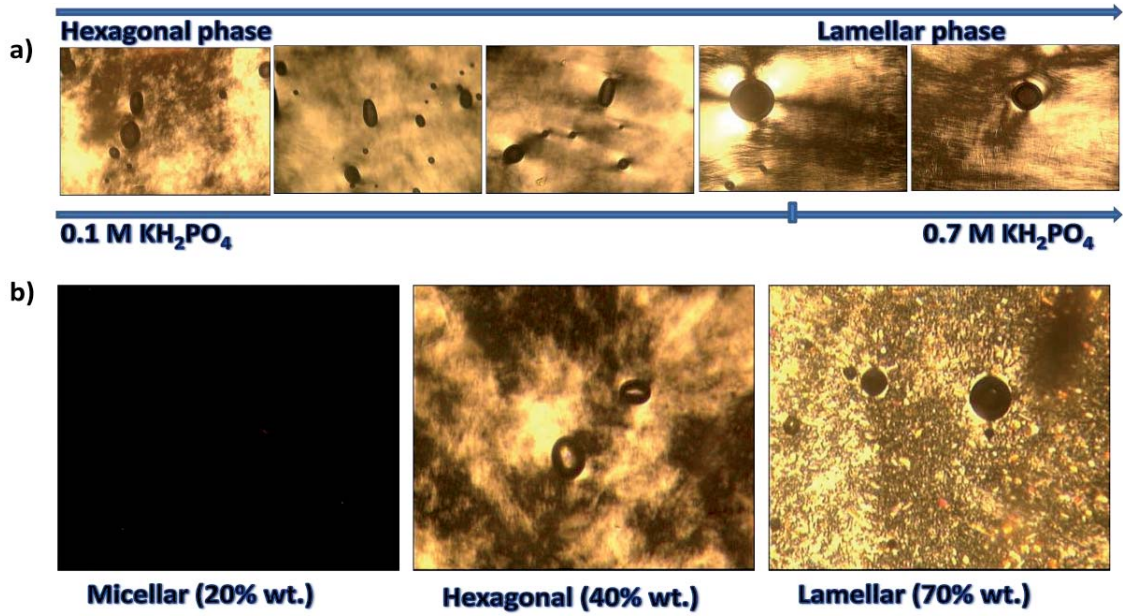

Figure 5.S1 Optical polarizing microscopy (OPM) Images of different phases of C16EO8 explored in a) different concentration of salt used at H_I $C_{16}EO_8$ b) increasing concentration of $C_{16}EO_8$ at fixed concentration of 0.4 M KH_2PO_4.

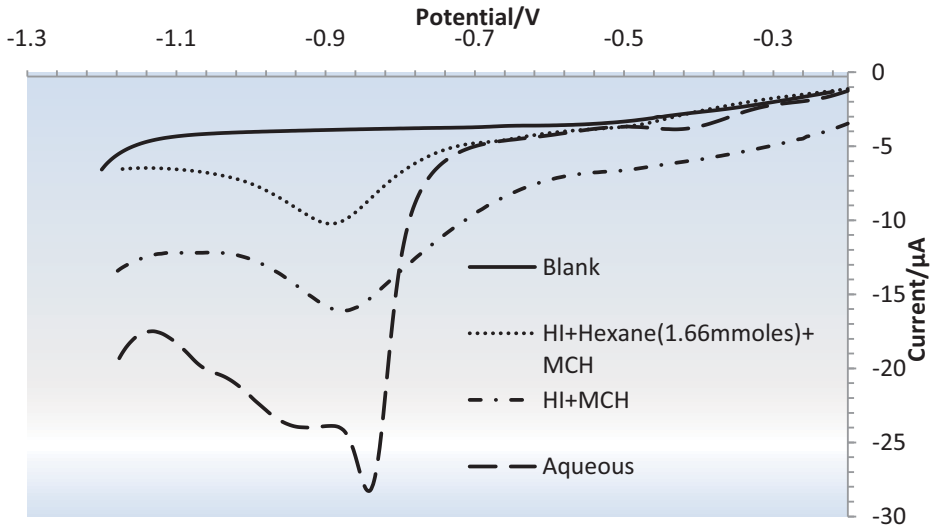

Immobilisation condition	Q (Coulombs) 10^{-6}	Moles 10^{-10}	moles/total surface area(0.090±0.002cm²) 10^{-10}	Available active surface area	Moles/available active surface area (cm²) 10^{-10}
Aqueous	3.52±2.37	0.365±0.246	4.06±2.73	0.090±0.002	6.59±2.73
H_I + MCH	1.40±0.38	0.146±0.039	1.62±0.44	0.023±0.002	6.33±1.71
H_I + 1.66mmoles Hexane + MCH	0.79±0.11	0.082±0.011	0.92±0.12	0.013±0.002	6.34±0.86

Figure 5.S2. Cyclic voltammograms for the reductive desorption of immobilised MCH monolayers from the gold electrodes in 50mM KOH and their calculated surface coverage (Q=mnF) of thiols per square cm.

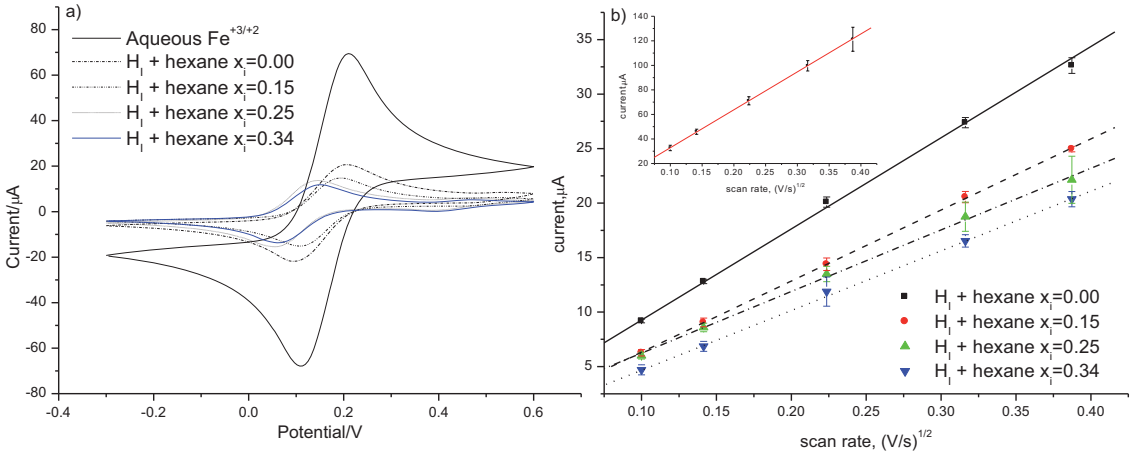

c) Electrode condition	Available surface active area (cm2)	% surface active area
5mM Fe^{+3}/Fe^{+2} aqueous solution only	0.090±0.002	100
5mM Fe^{+3}/Fe^{+2} + H_I	0.023±0.002	25.6
5mM Fe^{+3}/Fe^{+2} + H_I + hexane x_i=0.15	0.018±0.001	20.0
5mM Fe^{+3}/Fe^{+2} + H_I + hexane x_i=0.25	0.017±0.001	18.9
5mM Fe^{+3}/Fe^{+2} + H_I + hexane x_i=0.34	0.016±0.001	17.8

Figure 5.S3. a) Typical CV scans of the 5mM Fe^{+3}/Fe^{+2} in aqueous solution only and H_I of $C_{16}EO_8$ in different concentration of hexane added at 50mV/s scan rate and its b) Oxidation peak current Inset: oxidation peak current of aqueous 5mM Fe^{+3}/Fe^{+2} only. c) Calculated surface active area of the electrode in different conditions.

Table 5.S1. Summary of calculated values based on the mathematical model and the data based on actual experiment.

Theoretical data:

Area of total rectangular electrode (A_T): 4.77 x10 $^{-18}$ m^2

mole fraction of hexane	number of hexane molecules	Total area of rectangle/ m^2	Electrochemically accesible area/ m^2	Control (hexane only)	
x	n_{hexane}	A_R (10^{-18})	$A_E=A_T-A_R$ (10^{-18})	A_E/A_E	$*A_E/A_T$
0.00	0.00	2.65	2.12	1.00	0.72
0.10	0.72	3.02	1.75	0.82	0.64
0.20	1.62	3.49	1.28	0.60	0.51
0.23	1.93	3.65	1.12	0.53	0.47
0.24	2.04	3.71	1.06	0.50	0.45
0.25	2.15	3.77	1.00	0.47	0.43
0.30	2.77	4.09	0.68	0.32	0.33
0.35	3.48	4.46	0.31	0.15	0.21

Area of total triangular electrode(A_T): 8.77 x10 $^{-18}$ m^2

mole fraction of hexane	number of hexane molecules	Total area of circle/ m^2	Electrochemically accesible area/ m^2	Control (hexane only)	
x	n_{hexane}	A_C (10^{-18})	$A_E=A_T-A_C$ (10^{-18})	A_E/A_E	$*A_E/A_T$
0.00	0.00	2.45	6.31	1.00	0.72
0.10	0.72	3.19	5.57	0.88	0.64
0.20	1.62	4.25	4.51	0.71	0.51
0.23	1.93	4.66	4.11	0.65	0.47
0.24	2.04	4.81	3.96	0.63	0.45
0.25	2.15	4.96	3.80	0.60	0.43
0.30	2.77	5.84	2.93	0.46	0.33
0.35	3.48	6.94	1.82	0.29	0.21

Experimental data

Total active area of electrode(A_T): 0.090±0.002cm^2

	x_{hexane}	A_E,cm^2	$*A_E/A_T$
Control: no $C_{16}EO_8$	0.00	0.090±0.002	1.00
	0 .00	0.023±0.002	0.26
	0.15	0.018±0.001	0.20
	0.25	0.017±0.001	0.19
	0.34	0.016±0.001	0.18

Experimental data

Total active area of electrode(A_T): 0.090±0.002cm^2

	x_{hexane}	A_E,cm^2	$*A_E/A_T$
Control: no $C_{16}EO_8$	0.00	0.090±0.002	1.00
	0.00	0.023±0.002	0.26
	0.15	0.018±0.001	0.20
	0.25	0.017±0.001	0.19
	0.34	0.016±0.001	0.18

* Relative electrochemically accessible surface area

General conclusions

This thesis overviews the development of electrochemical immunosensor and DNA biosensors for the multiple detection of biowarfare agents, and nanostructuring probe distribution of thiolated ssDNA molecules based on nanotemplating strategies for improved biosensor performance. Fundamental aspects such as the surface chemistry for electrochemical platforms for the immunosensor and DNA biosensor were done such as evaluation of best assay format, preparation of fragment antibodies F(ab') for direct chemisorptions, antibody-enzyme or oligonucleotide-enzyme conjugates as labels and optimisation of DNA immobilisation. Complementary target ssDNA PCR products and bacterial cells were also prepared for its quantification and detection and the analytical performance of the electrochemical immunosensor and DNA biosensor were evaluated respectively. Finally, the use of a template to immobilise thiolated ssDNA molecules was explored. The nanotemplating strategies gave a better probe distribution that led to an increased sensitivity and lower limit of detection for the developed DNA biosensor.

In chapter 2, a comparative study on the use of whole antibodies immobilised via chemical cross-linking to a bipodal alkyl thiol self-assembled monolayer (SAM) and a SAM formed from the direct chemisorption of F(ab') antibody fragments for the detection of *Francisella tularensis* live vaccine strain (LVS) bacterial cells is presented. F(ab') fragments on Au surfaces gave better sensitivity compared to chemisorbed self-assembled monolayer cross-linked whole antibody. Antibody-enzyme conjugates were prepared in-house using whole antibody as well as antibody fragments, and similar results obtained in both cases. The immunosensor was used for the detection of the lipopolysaccharide antigen as well as *F. tularensis* LVS bacterial cells. The F(ab') fragments retained ~85% of antigen recognition ability after 45 days of storage at 4 °C. The developed

electrochemical immunosensor was then transferred to an automated microfluidic set-up housed within a tester set-up and the assay parameters were optimised. Microfluidics also highlights its role in improving the sensitivity of the biosensor as compared to the results obtained when detection were done outside fluidics. The specificity of the immunosensor has been clearly determined and no cross-reactivity has been found.

In Table C1, the developed immunosensor is compared to other techniques reported for the detection of *F. tularensis* LVS.

Table C1. Comparison with other techniques showing the detection limit obtained on the methods used

Techniques	Limit of detection (CFU/mL)	References
Fab - EC sensor in microfluidics	38	This work
Electrochemical biosensor	100	[1]
Piezoelectric immunosensor	105	[2]
Quartz crystal microbalance with dissipation monitoring	$4x10^3$	[3]
Fiber optic biosensor	$5x10^5$	[4]
ELISA	$6.9x10^6$	[5]

One of the advantages of our developed immunosensor is the facile integration of the biosensor in an electrochemical portable instrument which makes it very attractive for point-of-care applications.

Following this obtained result on the detection of *F. tularensis* bacterial cells, another immunosensor surface platform was developed for the detection of anti-*F. tularensis* antibodies present in the serum taken from an infected red fox (*Vulpes vulpes*) as presented in chapter 3. The sensor surface chemistry exploits gold-based self-assembled monolayers of a carboxylic group terminated bipodal

alkanethiol that is covalently linked to lipopolysaccharide (LPS) that can be found in the outer membrane of the bacteria *F. tularensis*. The presence of anti-*F. tularensis* antibodies was measured using HRP-Protein A from *Staphylococcus aureus* as a reporter molecule. The detection limit obtained is comparable to previously reported techniques in detecting antibodies against *F. tularensis* [6-9].

In the DNA sensing level, an electrochemical sensor array for the simultaneous recognition of PCR amplified gene segments of *Bacillus anthracis, Brucella melitensis, Bacteriophage lambda, Francisella tularensis, Burkholderia mallei, Coxiella burnetii, Yersinia pestis, and Bacillus thuringiensis var. Kurstaki* is discussed in chapter 4. These eight pathogens are among the biowarfare agents of the highest threat potential listed[10, 11]. In the developmental work, surface chemistry of the DNA biosensor was optimised such as immobilisation of thiolated ssDNA, the use of backfiller and incubation temperature. Oligonucleotide-enzyme conjugates were also prepared in-house using thiolated ssDNA and covalently linked to Maleimide activated HRP and similar results were obtained when compared to commercially obtained conjugates. The developed electrochemical multiplex DNA biosensor was then transferred to an automated microfluidic set-up housed within a tester set-up and the assay parameters were optimised. No cross-reactivity found and the specificity of the immunosensor has been clearly determined.

Finally, in chapter 5, the use of lyotropic liquid crystals (LLC) to act as a template to produce spaces between immobilized DNA probes was exploited. Thiolated ssDNA molecules were mixed in different phases of surfactant octaethylene glycol monohexadecyl ether (C16EO8) and were evaluated. The spacing concept of immobilized thiolated ssDNA probes through templating with LLC that led to the improved response of the biosensor was confirmed. The best signal response and lowest detection limit was shown by the templated system most especially for the H_I template which gave a huge increase in sensitivity of seven times fold higher compared to non templated immobilization of thiolated ssDNA probe and even better to the co-immobilization strategy that has

been previously reported to be the optimum condition for thiolated SAM capture probes [12]. To support the claim of improved biosensor performance especially using H_I template, several characterisation techniques was employed. Electrochemical characterisation such as cycling a redox specie in the presence of the templates revealed how much available active areas can be occupied by thiolated molecule DNA's. In the case of swollen H_I template where hexane was added, a mathematical model was derived and suggested how does the cylinders of H_I template is being orientated with respect to electrode's surface. It also further suggests that the presence of hydrophobic and hydrophilic domains imposed on the surface of the electrode by the amphiphilic nature of the surfactant molecules act as the driving force to achieve a homogenous, and even ordered distribution of probes on the surface. Imaging characterisation through fluorescence microscopy and atomic force microscopy further confirmed these claims. The non templated system have showed a fully packed immobilised probe whilst the H_I templated system showed a more spaced immobilised probe that favours better hybridisation with corresponding complementary targets which led to a much more improved sensitivity and better detection limit of the developed DNA biosensor.

References

1. Skladal, P., Symerska, Y., Pohanka, M., Safar, B., and Macela, A., *Electrochemical immunosensor for detection of Francisella tularensis*. Defense against Bioterror: Detection Technologies, Implementation Strategies and Commercial Opportunities, 2005: p. 221-232.
2. Pohanka, M.a.S., P., *Piezoelectric immunosensor for the direct and rapid detection of Francisella tularensis*. Folia microbiologica, 2007. **52**(4): p. 325-330.
3. Kleo, K., Schafer, D., Klar, S., Jacob, D., Grunow, R., and Lisdat, F., *Immunodetection of inactivated Francisella tularensis bacteria by using a quartz crystal microbalance with dissipation monitoring*. Anal Bioanal Chem, 2012. **404**: p. 843-851.
4. Anderson, G.P., King, K.D., Gaffney, K.L. and Johnson, L.H., *Multi-analyte interrogation using the fiber optic biosensor*. Biosensors and Bioelectronics, 2000. **14**: p. 771-777.
5. Pohanka, M., Pavlis, O., Kroca, M., *ELISA detection of Francisella tularensis using polyclonal and monoclonal antibodies*. DEFENCE SCIENCE JOURNAL, 2008. **58** (5): p. 698-702

6. Thirumalapura, N.R., Morton, R. J., Ramachandran, A. and Malayera, J. R., *Lipopolysaccharide microarrays for the detection of antibodies.* Journal of immunological methods, 2005. **298**(1-2): p. 73 – 81.
7. Skládal, P., Pohanka, M., Kupská, E., and Šafář, B., *Biosensors for Detection of Francisella tularensis and Diagnosis of Tularemia.* In: Biosensors, INTECH, Vienna, 2010: p. 115-126.
8. Dahouk, S.A., Nockler, K. N., Tomaso, H., Splettstoesser, W. D., Jungersen, G., Riber, U., Petry, T., Hoffmann, D., Scholz, H. C., Hensel, A., and Neubauer, H., *Seroprevalence of Brucellosis, Tularemia, and Yersiniosis in Wild Boars (Sus scrofa) from North-Eastern Germany.* Journal of veterinary medicine B. Infectious diseases and veterinary public health, 2005. **52**(10): p. 444-455.
9. Magnarelli, L., Levy, S., and Koski, R., *Detection of antibodies to Francisella tularensis in cats.* Research in vetenerary science, 2007. **82**: p. 22-26.
10. Klietmann, W.F., and Ruouff, K. L., *Bioterrorism: Implications for the Clinical Microbiologist.* Clinical Microbiology Reviews, 2001. **14**(2): p. 364–381.
11. Frischknecht, F., *The history of biological warfare.* EUROPEAN MOLECULAR BIOLOGY ORGANIZATION, 2003. **4**(Special issue): p. S47-S52.
12. Henry, O., Y. F., Perez, J. G., Sanchez, J. L. A., and O'Sullivan, C. K, *Electrochemcial characterisation and hybridisation efficiency of co-assembled monolayers of PEGylated ssDNA and mercaptohexanol on planar gold electrodes* Biosensors and Bioelectronics, 2010. **25**(5): p. 978 - 983.

Outlook

The presented results and conclusions from this thesis serve to guide future researches that would improve the present knowledge obtained in the field of electrochemical detection of pathogenic species based on immunosensing and genosensing level.

An immunosensor and DNA biosensor array for the detection of *F. tularensis* bacterial cells and eight different virulent species has been developed and an excellent analytical performance of these sensors was accomplished respectively.

The report on the development of immunosensor is the first stage of development of a platform for the multiplexed detection of a range of bioterrorism agents (i. e, *Bacillus anthracis, Brucella abortis and melitensis, Bacteriophage lambda, Burkholderia mallei and pseudomallei, Coxiella burnetii, Yersinia pestis, and Bacillus thuringiensis*) and the electrode arrays used in this work has been designed to allow incorporation of multiple antibodies immobilised on individual electrodes for the simultaneous detection of the listed bioterrorism agents and work is ongoing to achieve this goal. The applicability of the developed system to real situations such as an early detection of bioterrorism events is very promising as the obtained LOD was very low and the assay time quite short. This facilitates a rapid alarm based detection of *F. tularensis* when linked e.g. to an air-sampling system. Ongoing and future work will focus on attempting to further reduce the sampling time, to increase the stability of the Fab functionalised sensors using stabilising agents and to apply to the analysis of real samples within specialised regulatory laboratories.

Moreover, the developed multiplexed genosensor detection of a range of biowarfare agents has shown potential in its applicability to real situations such as an early detection of bioterrorism events as the developed system obtained very low detection limit and the assay time quite short when compared to conventional systems like ELONA or ELISA. Ongoing and future work will focus on attempting the use of a common reporter probes that would not only decrease the cost for

the use of different designed reporter probes but this would also eliminates the complex procedure of mixing all together the reporter probes for labelling the complementary targets, further reduce the incubation and sampling time, to increase the stability of the thiolated ssDNA functionalised sensors using stabilising agents.

Finally, the use of a template to immobilise sensing probes for the enhancement of biosensor performance will be explored as well in the developed multiplexed genosensor for real-time application.